# MODELLING DENSITY DEPENDENT *ESCHERICHIA COLI* IN WASTEWATER TREATMENT INCORPORATING RESISTANCE, OPTIMALITY AND NON-SINGULAR FRACTIONAL DERIVATIVES

**JULIA WANJIKU KARUNDITU**

A thesis submitted in partial fulfillment of the requirements for the award of the degree of Doctor of Philosophy in Applied and Computational Mathematics in the School of Pure and Applied Sciences, Kirinyaga University.

AUGUST 2026

# DECLARATION

This research project is my original work and has not been presented in any other form.

JULIA WANJIKU KARUNDITU
(PA300/S/15521/21)

Signature: Date:

This research project has been submitted for examination with our approval as university supervisors.

Signature: Date:

DR. CYRUS GITONGA NGARI, PhD
Department of Pure and Applied Sciences,
Kirinyaga University

Signature: Date:

DR. PETER NJORI WANJOHI, PhD
Department of Pure and Applied Sciences,
Kirinyaga University

©

2026 by JULIA WANJIKU KARUNDITU

All rights reserved. No part of this project may be reproduced, stored in any retrieval system or transmitted in any form or by any means, electronically, mechanically, by photocopying, or otherwise, without prior written permission of the author or Kirinyaga University on that behalf.

# Dedication

This thesis is dedicated to my beloved family for their unconditional love, patience, encouragement, and unwavering support throughout my academic journey. Their sacrifices, prayers, and belief in my abilities have been a constant source of strength and motivation. I also dedicate this work to all my mentors, colleagues, and friends whose guidance, inspiration, and encouragement contributed to the successful completion of this research. Above all, I dedicate this achievement to God Almighty for granting me wisdom, perseverance, strength, and the opportunity to accomplish this important milestone.

# Acknowledgement

I sincerely thank Almighty God for granting me the strength, wisdom, good health, and perseverance to successfully complete this thesis.

My deepest appreciation goes to my supervisor, [**DR. Cyrus Gitonga Ngari and DR. Peter Njori Wanjohi**], for the invaluable guidance, constructive feedback, patience, and encouragement throughout this research. I am equally grateful to the lecturers and staff of [**Kirinyaga University**] for their academic support and assistance.

I extend my sincere thanks to all the respondents who willingly participated in this study and provided valuable information that made this research possible.

Special appreciation goes to my family and friends for their unwavering support, prayers, encouragement, and understanding throughout my academic journey.

Finally, I acknowledge everyone who contributed, directly or indirectly, to the successful completion of this thesis. Your support has been invaluable, and I am truly grateful.

# ABSTRACT

The persistence of antibiotic-resistant *Escherichia coli* (*E. coli*) in wastewater poses a significant environmental and public health concern due to the increasing threat of antimicrobial resistance and its impact on water quality. Existing mathematical models often examine bacterial growth, antibiotic resistance, bacteriophage predation, treatment interventions, and biological memory effects separately, limiting understanding of their combined influence on bacterial persistence and control. This study develops a seven-compartment mathematical model integrating antibiotic-susceptible and antibiotic-resistant *E. coli*, Monod nutrient-dependent growth, bacteriophage predation, optimal control, and Caputo–Fabrizio fractional-order dynamics to provide a unified framework for analysing bacterial behaviour in wastewater environments. The model incorporates Monod kinetics to describe nutrient-limited bacterial growth, bacteriophage predation to represent biological suppression, optimal control to determine intervention strategies while balancing bacterial reduction and implementation costs, and fractional-order derivatives to capture memory effects in biological processes. The proposed model is analysed for positivity, boundedness, equilibria, stability, sensitivity, and optimal-control conditions using Pontryagin's Maximum Principle. Stability analysis is evaluated using the basic reproduction threshold $R_0$, which determines conditions associated with bacterial persistence or decline. Numerical simulations are performed using the fourth-order Runge–Kutta method (RK45) to investigate the influence of model parameters, fractional-order effects, and control strategies. Partial rank correlation coefficient analysis identifies $\beta_1$ as having the strongest negative association with bacterial persistence (PRCC $= -0.65831,\ p = 9.8345 \times 10^{-14}$). The parameters $\pi_1$ and $\gamma_1$ show significant positive associations, with PRCC values of 0.44660 ($p = 3.2021 \times 10^{-6}$) and 0.40187 ($p = 3.4085 \times 10^{-5}$), respectively. The parameter $\gamma_3$ demonstrates a significant negative association (PRCC $= -0.23424,\ p = 0.018992$), while the association of $\mu_1$ is negative but not statistically significant at the 5% level (PRCC $= -0.19124,\ p = 0.056648$). The findings demonstrate that nutrient availability, antibiotic resistance, bacteriophage interactions, intervention strategies, and memory effects jointly influence antibiotic-resistant *E. coli* dynamics. The developed fractional-order optimal control framework provides mathematical insights for designing effective and sustainable strategies for managing antibiotic-resistant *E. coli* contamination in wastewater.

**Keywords:** Antibiotic-resistant *Escherichia coli*; wastewater; Monod growth kinetics; bacteriophage predation; fractional-order modelling; Caputo–Fabrizio derivative; optimal control; sensitivity analysis.

# Abbreviation and Acronyms

| **Abbreviation** | **Meaning** |
|---|---|
| E. coli | *Escherichia coli* |
| CFU/mL | Colony-forming units per millilitre |
| CFU/100 mL | Colony-forming units per 100 millilitres |
| PFU/mL | Plaque-forming units per millilitre |
| PRCC | Partial Rank Correlation Coefficient |
| LHS | Latin Hypercube Sampling |
| Model A | Deterministic integer-order model |
| Model B | Caputo–Fabrizio fractional-order model |
| Model C | Optimal control model |

# List of Tables


2.1 Comparison of Existing Mathematical Models and the Present Study . . 32

3.1 Definition of Model A Parameters . . . . . 37
3.2 Definition of Model A Variables . . . . . 38

4.1 Parameters . . . . . 67
4.2 PRCC values and corresponding p-values . . . . . 90
4.3 Statistical summary for Figure 4.14 . . . . . 132
4.4 Statistical summary for Figure 4.15. . . . . 133
4.5 Statistical summary for Figure 4.16. . . . . 134
4.6 Statistical summary for Figure 4.17 . . . . . 135
4.7 Statistical summary for Figure 4.18. . . . . 136
4.8 Statistical summary for Figure 4.19. . . . . 137
4.9 Statistical summary for Figure 4.20. . . . . 138
4.10 Control Variables and Their Interpretations . . . . . 141

# List of Figures


3.1 Definition of Model A Parameters . . . . . 40

4.1 PRCC . . . . . 87
4.2 PRCC continues . . . . . 88
4.3 PRCC and p-values . . . . . 89
4.4 PRCC . . . . . 94
4.5 PRCC . . . . . 95
4.6 PRCC and p-values . . . . . 96
4.7 Concentration of E.coli with time incooporating algae . . . . . 99
4.8 Dynamics of E.coli with predation . . . . . 99
4.9 Concentration of E.coli in the secondary treatment dam . . . . . 100
4.10 Dynamics of E.coli in predation . . . . . 101
4.11 Dynamics of E.coli in preprimary dam with predation . . . . . 103
4.12 Dynamics of E.coli with and without predation . . . . . 104
4.13 Dynamics of E.coli concentration with competation of algae . . . . . 106
4.14 Dynamics of E.coli with predation and competation from algae . . . . . 107
4.15 Dynamics of concentration of E.coli with predation in the preprimary dam 109
4.16 Effect of Fractional Order on Pre-Primary Stage Dynamics . . . . . 132
4.17 Effects of Long-Term Growth and Memory in $W$ . . . . . 133
4.18 Secondary Stage Dynamics and Ordering Property . . . . . 134
4.19 Tertiary Stage Stability and Near-Linearity . . . . . 135
4.20 . . . . . 136
4.21 Bacteriophage Predator Dynamics and Stability . . . . . 137
4.22 Effect of Fractional Order on *E. coli* Concentration in Compartment $P$ . 138
4.23 Three-Dimensional Phase Portrait Interpretation . . . . . 139
4.24 Profile of $W(t)$ with time . . . . . 145
4.25 Profile of $X(t)$ with time . . . . . 146
4.26 Profile of $Y(t)$ with time . . . . . 146
4.27 Profile of $Z(t)$ with time . . . . . 147
4.28 Optimal Control Variables vs Time . . . . . 147

# Contents

**Declaration** ii

**Dedication** iv

**Acknowledgement** v

**Abstract** vi

**Abbreviation and Acronyms** viii

**List of Tables** ix

**List of Figures** x

**1 Introduction** 1

1.1 Background Information . . . . . 1

1.1.1 Wastewater Contamination and Environmental Health Challenges 1

1.1.2 Wastewater Management, Sustainable Development Goals and National Priorities . . . . . 2

1.1.3 Escherichia coli Dynamics in Wastewater Systems . . . . . 2

1.1.4 Antibiotic Resistance Dynamics in *E. coli* . . . . . 3

1.1.5 Density-Dependent Growth and Monod Kinetics . . . . . 3

1.1.6 Bacteriophage Predation as a Biological Control Mechanism . . . 4

1.1.7 Mathematical Modelling of Wastewater Bacterial Dynamics . . . 4

1.1.8 Optimal Control Strategies . . . . . 5

1.1.9 Fractional-Order Modelling and Memory Effects . . . . . 5

1.2 Statement of the Problem . . . . . 6

1.3 Justification of the Study . . . . . 7

1.4 Significance of the Study . . . . . 8

1.5 Scope of the Study . . . . . 9

1.6 Objectives of the Study . . . . . 10

1.6.1 General Objective . . . . . 10

1.6.2 Specific Objectives . . . . . 10

**2 LITERATURE REVIEW 11**

2.1 Introduction . . . . . 11

2.2 Deterministic Mathematical Modelling of Wastewater *Escherichia coli* Dynamics . . . . . 12

2.2.1 Classical Compartmental Models . . . . . 13

2.2.2 Mathematical Models of Antibiotic Resistance . . . . . 14

2.3 Density-Dependent Growth and Monod Kinetics . . . . . 15

2.3.1 Monod Growth Theory . . . . . 16

2.3.2 Applications of Monod Kinetics in Wastewater Modelling . . . . . 17

2.3.3 Relevance of Monod Kinetics to the Present Study . . . . . 18

2.4 Bacteriophage Predation and Biological Control . . . . . 18

2.4.1 Mathematical Phage–Bacteria Interaction Models . . . . . 19

2.4.2 Bacteriophage-Based Biological Control of Bacterial Populations . 19

2.4.3 Bacteriophage Predation and Antibiotic-Resistant *E. coli* . . . . . 20

2.4.4 Integration of Bacteriophage Predation with Monod Growth and Environmental Dynamics . . . . . 21

2.4.5 Critical Comparison with the Proposed Seven-Compartment Model 21

2.5 Optimal Control Theory and Biological Intervention Strategies . . . . . 22

2.5.1 Pontryagin's Maximum Principle . . . . . 22

2.5.2 Optimal Control Applications in Biological Systems . . . . . 23

2.5.3 Optimal Control in Wastewater Bacterial Management . . . . . 23

2.5.4 Objective Functional and Control Variables in the Present Study 24

2.5.5 Critical Comparison with Existing Approaches . . . . . 24

2.6 Fractional-Order Mathematical Modelling . . . . . 25

2.6.1 Riemann–Liouville Fractional Derivative . . . . . 25

2.6.2 Caputo Fractional Derivative . . . . . 26

2.6.3 Caputo–Fabrizio Fractional Derivative . . . . . 27

2.6.4 Memory Effects in Biological and Environmental Systems . . . . . 27

2.6.5 Justification for the Caputo–Fabrizio Operator in the Present Study 28

2.6.6 Critical Comparison with Existing Fractional Models . . . . . 28

2.7 Integrated Models of Antibiotic-Resistant *Escherichia coli* Dynamics . . 29

2.7.1 Existing Combined Mathematical Approaches . . . . . 30

2.7.2 Need for an Integrated Seven-Compartment Model . . . . . 31

2.8 Comparative Analysis of Existing Models . . . . . 31

2.9 Research Gap . . . . . 31

2.10 Chapter Summary . . . . . 33

**3 RESEARCH DESIGN AND METHODOLOGY** **34**
3.1 Introduction . . . 34
3.2 Deterministic Model A . . . 35
3.2.1 Model Formulation . . . 35
3.2.2 Model Variables and Parameters . . . 36
3.2.3 Model Assumptions . . . 38
3.2.4 Model Framework . . . 39
3.2.5 Biological Interpretation of Model Components . . . 41
3.2.6 Model Equations . . . 41
3.2.7 Justification of Monod Growth Kinetics . . . 43
3.2.8 Justification of Density-Dependent Growth Formulation . . . 44
3.2.9 Model A Analysis . . . 45
3.2.10 Model A Numerical Simulation . . . 52
3.3 Caputo–Fabrizio Fractional Model B . . . 52
3.3.1 Model Formulation . . . 52
3.3.2 Caputo–Fabrizio Model B Assumptions . . . 53
3.3.3 Caputo–Fabrizio Fractional Derivative . . . 54
3.3.4 Existence and Uniqueness Analysis . . . 56
3.3.5 Numerical Simulation of Model B . . . 56
3.4 Optimal Control Model C . . . 56
3.4.1 Controlled Model Formulation . . . 56
3.4.2 Optimal Control Model C Assumptions . . . 57
3.4.3 Optimal Control Variables . . . 58
3.4.4 Controlled Model Equations . . . 58
3.4.5 Objective Functional . . . 59
3.4.6 Hamiltonian Formulation . . . 60
3.4.7 Adjoint Equations . . . 61
3.4.8 Existence of Optimal Controls . . . 63
3.4.9 Numerical Solution of the Optimal Control System . . . 63
3.4.10 Numerical Simulation of Model C . . . 64
3.5 Chapter Summary . . . 65

**4 RESULTS AND DISCUSSIONS** **66**
4.1 Introduction . . . 66
4.2 Analysis of Deterministic Model A . . . 66
4.2.1 Model A formulation . . . 67
4.2.2 Model analysis methods . . . 68
4.2.3 Model simulation . . . 85
4.2.4 Model A Simulations . . . 93

4.2.5 Sensitivity Analysis Using PRCC . . . . . 94
4.3 Analysis of Caputo–Fabrizio fractional derivatives form model B . . . . 111
4.3.1 Caputo–Fabrizio fractional derivatives form model B . . . . . 112
4.3.2 Numerical simulations . . . . . 131
4.3.3 Effect of Fractional Order on Pre-Primary Stage Dynamics . . . . 132
4.3.4 Effects of Long-Term Growth and Memory in $W$ . . . . . 133
4.3.5 Secondary Stage Dynamics and Ordering Property . . . . . 134
4.3.6 Tertiary Stage Stability and Near-Linearity . . . . . 135
4.3.7 Tertiary Stage Dynamics of Resistant*E. coli* . . . . . 136
4.3.8 Bacteriophage Predator Dynamics and Stability . . . . . 137
4.3.9 Effect of Fractional Order on *E. coli* Concentration in Compartment $P$ . . . . . 138
4.3.10 Three-Dimensional Phase Portrait Interpretation . . . . . 139
4.3.11 Integrated System-Level Conclusion . . . . . 139
4.4 Optimal Control Model C . . . . . 140
4.4.1 Optimal Control of E. coli Dynamics in Wastewater Treatment Systems . . . . . 140
4.4.2 Optimal control model formulation . . . . . 141
4.4.3 Pontryagin's Maximum Principle . . . . . 142
4.4.4 Simulation Results . . . . . 145
4.4.5 Uncontrolled System . . . . . 148
4.4.6 Controlled System . . . . . 148
4.4.7 Control Profiles . . . . . 148
4.4.8 Sensitivity Analysis . . . . . 148

**5 DISCUSSION ,CONCLUSION AND RECOMMENDATIONS FOR FUTURE STUDY 150**
5.1 Summary and conclusion . . . . . 150
5.2 Limitations of the Study . . . . . 156
5.3 Reccommendation and scope for future study . . . . . 156
5.4 Conflict of interest . . . . . 157

**REFERENCES 158**

**A MATLAB Code for Deterministic Model A Simulation 165**

**B Publications 168**

# Chapter 1

# Introduction

## 1.1 Background Information

### 1.1.1 Wastewater Contamination and Environmental Health Challenges

Water is an essential natural resource that supports human survival, ecological processes, and socioeconomic development. It plays a critical role in maintaining environmental balance and sustaining life systems. However, increasing population growth, urbanisation, industrial activities, and inadequate wastewater management practices have placed significant pressure on global water resources. Effective management of water resources is therefore necessary to ensure availability, quality, and sustainability for present and future generations (Panwar *et al.*(2020)) .

Wastewater represents one of the major challenges affecting water quality because it contains organic matter, chemical pollutants, and microorganisms that may pose environmental and public health risks(Panwar *et al.*(2020)) . Poor wastewater management can contribute to contamination of aquatic systems, degradation of ecosystems, and increased exposure to waterborne diseases (Al-Mandhari *et al.*(2022)). Wastewater contamination has therefore become an important global concern requiring improved treatment approaches and effective monitoring strategies(Al-Mandhari *et al.*(2022))

Wastewater treatment systems are designed to reduce microbial contamination before discharge into the environment. However, bacterial populations may persist due to variations in environmental conditions, nutrient availability, microbial interactions, and adaptation mechanisms. Consequently, mathematical modelling has become an important approach for understanding bacterial behaviour, predicting contamination trends, and evaluating possible intervention strategies(Yezli *et al.*(2021)).

In this study, wastewater contamination is considered as a dynamic biological system in which bacterial populations change due to growth, removal processes, environmental

interactions, and control measures. Therefore, developing mathematical models that incorporate important biological mechanisms is essential for improving the understanding and management of bacterial persistence in wastewater systems.

### 1.1.2 Wastewater Management, Sustainable Development Goals and National Priorities

Access to safe water and effective wastewater management are fundamental components of sustainable development. The increasing pressure on water resources due to population growth, urban expansion, and industrial activities has created a need for improved approaches to water quality protection and wastewater treatment. Sustainable Development Goal (SDG) 6, which focuses on ensuring availability and sustainable management of water and sanitation for all, highlights the importance of improving water quality, reducing pollution, and strengthening wastewater treatment systems(Germann and Langergraber *et al.*(2022).

Wastewater treatment is therefore not only an environmental challenge but also a public health and development priority. Inadequately treated wastewater may contribute to the spread of pathogenic microorganisms and antibiotic-resistant bacteria, increasing risks associated with water reuse, environmental contamination, and community health. Mathematical approaches that improve understanding of bacterial persistence and treatment efficiency can contribute to evidence-based decision-making in wastewater management(Rodriguez *et al* (2022)).

In the Kenyan context, improving water security, sanitation infrastructure, and environmental protection forms part of national development priorities. Sustainable management of water resources requires scientific approaches capable of supporting efficient treatment strategies and improved resource allocation. The development of mathematical models for predicting bacterial dynamics and evaluating control interventions can therefore provide valuable insights for wastewater management planning.

This study contributes to these objectives by developing a mathematical framework for analysing antibiotic-resistant *Escherichia coli* dynamics in wastewater systems. By integrating nutrient-dependent growth, bacteriophage interactions, fractional-order memory effects, and optimal control strategies, the proposed model provides a theoretical basis for understanding bacterial persistence and evaluating possible intervention approaches.

### 1.1.3 Escherichia coli Dynamics in Wastewater Systems

*Escherichia coli* (*E. coli*) is a Gram-negative bacterium belonging to the Enterobacteriaceae family. It commonly exists as part of the intestinal microbiota of humans and animals; however, when introduced into unsuitable environments, certain strains can be-

come pathogenic and cause disease. Due to its association with faecal contamination, *E. coli* is widely used as an indicator organism for assessing water quality and microbial contamination Jang*et al.* ((2017).

Although many *E. coli* strains are harmless, pathogenic strains can cause gastrointestinal infections and other serious health complications when transmitted through contaminated food or water sources Jang*et al.* ((2017). The ability of *E. coli* to survive under different environmental conditions makes it an important organism for wastewater research and mathematical modelling.

Wastewater environments provide complex conditions that influence bacterial survival and persistence. Factors such as nutrient availability, competition, environmental stress, treatment processes, and biological interactions determine bacterial population dynamicsPetersen and Hubbart *et al.* ((2020)). Therefore, mathematical models describing *E. coli* behaviour should account for the mechanisms that regulate bacterial growth and persistenceYang *et al.*((2017).

The present study incorporates susceptible and antibiotic-resistant *E. coli* populations to represent differences in bacterial behaviour under environmental and treatment pressures. This approach provides a more realistic representation of wastewater bacterial dynamics compared with models that consider only a single bacterial population.

### 1.1.4 Antibiotic Resistance Dynamics in *E. coli*

Antibiotic resistance has become an important global challenge because resistant microorganisms can survive antimicrobial exposure and contribute to treatment difficulties. Environmental systems, including wastewater treatment facilities, provide conditions where resistant bacteria and resistance determinants may persist and spread Petersen and Hubbart *et al.* ((2020)).

The presence of antibiotic-resistant *E. coli* in wastewater represents a significant concern because resistant populations may remain viable despite conventional treatment processes. Mathematical models that consider only total bacterial populations may fail to capture differences between susceptible and resistant strains.

Therefore, incorporating separate antibiotic-susceptible and antibiotic-resistant compartments is necessary for understanding how resistance influences bacterial persistence and control. In this study, resistance dynamics are included as a fundamental component of the mathematical framework to investigate interactions between bacterial growth, predation, and intervention strategies.

### 1.1.5 Density-Dependent Growth and Monod Kinetics

Microbial populations are strongly influenced by environmental resources, particularly nutrient availability. Population growth is therefore not unlimited but depends on eco-

logical factors such as available substrates, competition, and environmental carrying capacity. This relationship represents density-dependent population dynamics (Ghosh *et al.*(2021)).

The Monod equation provides a mathematical description of microbial growth under nutrient limitation by relating bacterial growth rate to substrate concentration @articleMonod1949 . Unlike simple exponential growth assumptions, Monod kinetics provide a biologically realistic representation of bacterial growth because microorganisms require available nutrients to reproduce @articleMonod1949 .

In wastewater environments, nutrient availability directly influences bacterial persistence and growth. Therefore, the present study uses Monod kinetics as the mathematical functional response describing nutrient-dependent density regulation of *E. coli*. The incorporation of Monod growth allows the model to represent how environmental resources influence bacterial population changes.

### 1.1.6 Bacteriophage Predation as a Biological Control Mechanism

Bacteriophages are viruses that infect specific bacterial hosts and contribute naturally to bacterial population regulation. Their ability to reduce bacterial populations makes them an important biological mechanism for controlling bacterial contamination.

In wastewater environments, bacteriophage interactions influence bacterial survival, population size, and ecological balance. However, the effectiveness of phage-based control depends on bacterial growth characteristics, environmental conditions, and interactions with resistant populations.

Therefore, incorporating bacteriophage predation into mathematical models provides a framework for investigating biological control mechanisms and their contribution to reducing antibiotic-resistant *E. coli* persistence.

### 1.1.7 Mathematical Modelling of Wastewater Bacterial Dynamics

Mathematical modelling provides a framework for representing complex biological systems through mathematical relationships. Differential equation models are particularly useful for describing population interactions, environmental processes, and intervention strategies(Nieto *et al.*(2023)).

Previous mathematical studies have demonstrated the importance of modelling microbial contamination and environmental pollution dynamics ). However, many existing models consider only selected mechanisms and do not simultaneously incorporate bacterial resistance, nutrient-dependent growth, bacteriophage predation, fractional memory

effects, and optimal interventions (Nieto *et al.*(2023)).

This study addresses this limitation by developing three linked mathematical models: a deterministic compartmental model, a Caputo–Fabrizio fractional-order extension, and an optimal control model(Prakasha and Veresha (2020)).

### 1.1.8 Optimal Control Strategies

Wastewater management requires effective intervention strategies while considering economic and operational limitations. Optimal control theory provides mathematical tools for determining strategies that minimise undesirable outcomes while balancing associated costs (Seidu *et al.*(2014)).

Pontryagin's Maximum Principle provides a fundamental framework for solving optimal control problems by determining control functions that optimise a defined objective function In this study, optimal control is incorporated to evaluate intervention strategies for reducing antibiotic-resistant *E. coli* populations while considering implementation costs (Seidu *et al.*(2014)).

### 1.1.9 Fractional-Order Modelling and Memory Effects

Biological systems often exhibit memory effects where previous states influence current behaviour. Classical integer-order differential equations may not fully capture these characteristics because they primarily describe instantaneous changes( Ali *et al.* (2020)).

Fractional-order derivatives provide an alternative mathematical approach for representing non-local dynamics and memory effects(Prakasha and Veresha (2020)). The Caputo–Fabrizio fractional derivative introduces a non-singular kernel, allowing biological processes with memory characteristics to be represented without the singularity associated with some traditional fractional operators (Ur Rahman *et al.*(2021))(Ahmad, Jan, Razak, Khan, & Abdeljawad, 2025) .

Fractional modelling has been applied in environmental and biological systems to describe processes where historical states influence present dynamics ( Ali *et al.* (2020)). Antibiotic-resistant *Escherichia coli* in wastewater presents a complex modelling problem because its persistence is influenced by several biological and environmental mechanisms acting simultaneously. Nutrient availability affects bacterial growth, antibiotic resistance alters bacterial response to treatment, bacteriophages reduce bacterial populations through predation, and intervention strategies must be applied efficiently to achieve effective control while minimising associated costs. Furthermore, biological processes in wastewater may exhibit memory effects, where current bacterial dynamics depend partly on previous environmental conditions, resistance pressures, and treatment exposure. Existing mathematical models frequently investigate these processes separately or in limited

combinations, restricting their ability to explain how their interactions influence the persistence and control of antibiotic-resistant *E. coli*.

This study is therefore justified by the need for an integrated mathematical framework that simultaneously incorporates nutrient-dependent bacterial growth, antibiotic resistance, bacteriophage predation, optimal control, and fractional-order dynamics. Monod kinetics are employed to describe bacterial growth under nutrient limitation, while the bacterial population is divided into antibiotic-susceptible and antibiotic-resistant classes to capture differences in persistence and response to interventions. Bacteriophage predation is included as a biological mechanism for reducing bacterial populations, whereas optimal control theory is applied to determine intervention strategies that balance bacterial reduction with implementation costs. The Caputo–Fabrizio fractional derivative is incorporated to represent memory effects that may influence bacterial growth, resistance development, phage–bacteria interactions, and treatment responses. By integrating these mechanisms, this study addresses the central scientific question of how nutrient limitation, antibiotic resistance, bacteriophage predation, intervention strategies, and memory effects jointly determine the persistence and effective control of antibiotic-resistant *E. coli* in wastewater.

## 1.2 Statement of the Problem

The increasing occurrence of antibiotic-resistant *Escherichia coli* in wastewater represents a significant environmental and public health challenge due to the potential spread of antimicrobial resistance through aquatic ecosystems. Wastewater environments provide favourable conditions for bacterial survival and proliferation because they contain nutrients, antibiotic residues, and diverse microbial communities that may promote the persistence and dissemination of resistant bacteria. Consequently, understanding the mechanisms governing the survival, transmission, and control of antibiotic-resistant *E. coli* is essential for developing effective wastewater management strategies.

Mathematical modelling has become an important approach for investigating bacterial dynamics and evaluating possible intervention strategies. Existing models have provided valuable insights into individual processes such as bacterial growth, antibiotic resistance development, bacteriophage predation, treatment interventions, and memory effects. However, many of these models consider these mechanisms independently or incorporate only partial interactions among them. Such simplified approaches may not adequately represent wastewater environments, where nutrient availability, resistance characteristics, biological control through bacteriophages, intervention strategies, and historical effects interact simultaneously to determine bacterial persistence and elimination.

In particular, existing models often lack an integrated framework that simultaneously considers antibiotic-susceptible and antibiotic-resistant *E. coli* populations, nutrient-

dependent growth, bacteriophage predation, optimal control, and fractional-order dynamics. Models based only on classical integer-order derivatives may also fail to capture memory effects inherent in biological systems, where previous environmental conditions and treatment exposure can influence present bacterial behaviour. Furthermore, without incorporating optimal control, it remains difficult to determine effective intervention strategies that reduce bacterial populations while considering the costs associated with implementing control measures.

Therefore, there is a need for a comprehensive mathematical framework that combines these interacting mechanisms to provide a more realistic representation of antibiotic-resistant *E. coli* dynamics in wastewater. This study addresses this gap by developing a seven-compartment mathematical model incorporating antibiotic resistance, Monod nutrient-dependent growth, bacteriophage predation, optimal control, and Caputo–Fabrizio fractional-order dynamics.

The central scientific question addressed in this study is:

> *How do nutrient limitation, antibiotic resistance, bacteriophage predation, intervention strategies, and memory effects interact to influence the persistence and effective control of antibiotic-resistant Escherichia coli in wastewater?*

By addressing this question, the study aims to provide deeper insight into the factors controlling antibiotic-resistant *E. coli* persistence and contribute to the development of biologically effective and economically sustainable control strategies.

## 1.3 Justification of the Study

The persistence of antibiotic-resistant *Escherichia coli* in wastewater is governed by multiple interacting biological and environmental processes that cannot be fully understood when considered independently. Wastewater environments contain variable nutrient levels, antibiotic residues, and microbial interactions that influence bacterial growth, survival, resistance development, and response to control measures. Therefore, a comprehensive mathematical framework that integrates these mechanisms is necessary to provide a realistic representation of antibiotic-resistant *E. coli* dynamics.

Monod nutrient-dependent growth is incorporated because bacterial proliferation in wastewater is strongly influenced by the availability of limiting nutrients. The use of Monod kinetics enables the model to represent how environmental resources regulate bacterial growth rather than assuming unrestricted exponential growth. The inclusion of antibiotic-susceptible and antibiotic-resistant *E. coli* populations is essential because resistant bacteria may persist under conditions where susceptible populations decline, creating a major challenge for wastewater treatment and antimicrobial resistance control.

Bacteriophage predation is included because bacteriophages represent a natural biological mechanism capable of reducing bacterial populations. However, the effectiveness of phage-based control depends on interactions between bacterial populations, environmental conditions, and bacterial growth dynamics. Optimal control is incorporated because reducing antibiotic-resistant *E. coli* requires not only understanding bacterial behaviour but also determining how control measures should be applied over time while balancing bacterial reduction and implementation costs. Without an optimal-control framework, it is difficult to identify efficient intervention strategies.

Furthermore, conventional mathematical models based on integer-order derivatives may not adequately describe biological systems where previous conditions influence current behaviour. The incorporation of the Caputo–Fabrizio fractional-order derivative allows the model to capture memory effects associated with previous nutrient availability, resistance pressures, bacteriophage interactions, and treatment exposure. This provides a more flexible representation of bacterial dynamics in wastewater environments.

Although previous studies have investigated bacterial growth, antibiotic resistance, bacteriophage predation, control strategies, and memory effects, many have examined these mechanisms separately or through simplified combinations. Consequently, they do not fully explain how these processes interact simultaneously to determine the persistence and control of antibiotic-resistant *E. coli*. This study is therefore justified by the need for an integrated seven-compartment mathematical model that combines these mechanisms within a unified framework.

The proposed model addresses the scientific question of how nutrient limitation, antibiotic resistance, bacteriophage predation, intervention strategies, and memory effects interact to influence the persistence and effective control of antibiotic-resistant *E. coli* in wastewater. By integrating these processes, the study provides a more comprehensive understanding of bacterial dynamics and establishes a mathematical basis for developing biologically effective and economically sustainable control strategies.

## 1.4 Significance of the Study

This study contributes to mathematical modelling, environmental microbiology, and wastewater management by providing an integrated framework for analysing the persistence and control of antibiotic-resistant *E. coli*. The main theoretical contribution is the development of a seven-compartment mathematical model that combines antibiotic resistance, Monod nutrient-dependent growth, bacteriophage predation, optimal control, and fractional-order dynamics within a unified system. This integrated approach provides a more comprehensive representation of bacterial behaviour compared with models that analyse these mechanisms independently.

The study is also significant because it identifies important parameters influencing bac-

terial persistence and control. Sensitivity analysis demonstrates that $\beta_1$ has the strongest negative association with bacterial persistence, with a partial rank correlation coefficient of PRCC $= -0.65831$ and $p = 9.8345 \times 10^{-14}$. The parameters $\pi_1$ and $\gamma_1$ exhibit significant positive associations, with PRCC values of 0.44660 ($p = 3.2021 \times 10^{-6}$) and 0.40187 ($p = 3.4085 \times 10^{-5}$), respectively. These findings identify key processes that influence bacterial dynamics and provide insight into parameters that may be prioritised in control strategies.

The optimal-control component provides a mathematical basis for determining effective intervention strategies that reduce susceptible and antibiotic-resistant *E. coli* while considering the cost associated with implementing control measures. The incorporation of bacteriophage predation evaluates the potential contribution of biological control, while the fractional-order formulation extends classical models by considering memory effects in bacterial systems. Collectively, the findings may support improved understanding of antimicrobial resistance dynamics and contribute to the development of efficient and sustainable approaches for controlling antibiotic-resistant bacteria in wastewater environments.

## 1.5 Scope of the Study

This study focuses on the mathematical modelling and analysis of antibiotic-susceptible and antibiotic-resistant *Escherichia coli* dynamics in a wastewater environment. The proposed model consists of seven interacting compartments and incorporates Monod nutrient-dependent bacterial growth, antibiotic resistance, bacteriophage predation, optimal control interventions, and fractional-order dynamics. The study investigates the mechanisms governing bacterial persistence, decline, and response to control measures.

The mathematical analysis includes the establishment of positivity and boundedness of model solutions, determination of equilibrium points, stability analysis, sensitivity analysis, and formulation of optimal-control strategies using Pontryagin's Maximum Principle. Numerical simulations are conducted to examine the influence of important parameters and compare bacterial behaviour under different control scenarios. In addition, the Caputo–Fabrizio fractional-order extension is analysed to evaluate the influence of memory effects on system dynamics compared with the classical integer-order model.

The study does not aim to represent every physical, chemical, and microbiological process occurring in wastewater treatment systems. Factors such as temperature variation, pH changes, complex microbial community interactions, multiple resistance genes, horizontal gene transfer mechanisms, and detailed wastewater hydraulic processes are outside the current modelling framework unless indirectly represented through model parameters. Therefore, the study provides a theoretical and computational framework for understanding major factors affecting antibiotic-resistant *E. coli* persistence and control

rather than a complete representation of all wastewater treatment processes.

## 1.6 Objectives of the Study

### 1.6.1 General Objective

The general objective of this study is to develop and analyse a mathematical model for the dynamics and optimal control of antibiotic-resistant *Escherichia coli* in wastewater by incorporating antibiotic resistance, Monod nutrient-dependent growth, bacteriophage predation, and fractional-order dynamics.

### 1.6.2 Specific Objectives

The specific objectives of this study are to:

1. To formulate a seven-compartment mathematical model describing the dynamics of antibiotic-susceptible and antibiotic-resistant *Escherichia coli* in wastewater.

2. To analyse the mathematical properties of the proposed model, including positivity, boundedness, and equilibrium solutions.

3. To determine the stability conditions of the equilibrium points of the proposed model.

4. To extend the proposed integer-order model to a fractional-order model using the Caputo–Fabrizio derivative and analyse the influence of memory effects on bacterial dynamics.

5. To perform sensitivity analysis to determine the parameters that significantly influence the persistence and control of antibiotic-resistant *Escherichia coli*.

6. To formulate and analyse an optimal-control problem using Pontryagin's Maximum Principle for reducing antibiotic-resistant *Escherichia coli* populations while considering control costs.

7. To perform numerical simulations to investigate the effects of model parameters and evaluate the effectiveness of optimal control strategies.

# Chapter 2

# LITERATURE REVIEW

## 2.1 Introduction

The increasing emergence and persistence of antibiotic-resistant *Escherichia coli* in wastewater environments has become a significant scientific and public health concern. Wastewater systems receive diverse biological and chemical inputs, including antibiotic residues, resistant microorganisms, and mobile genetic elements associated with antimicrobial resistance. These conditions create an environment where resistant bacteria may survive, multiply, and contribute to the wider dissemination of antibiotic resistance. Therefore, understanding the mechanisms controlling antibiotic-resistant *E. coli* dynamics requires mathematical frameworks capable of describing the interaction between biological processes, environmental conditions, and control interventions.

Mathematical modelling provides an effective approach for investigating complex microbial systems because it enables biological mechanisms to be represented using quantitative relationships. Experimental studies often focus on specific mechanisms under controlled conditions; however, bacterial persistence in wastewater results from the simultaneous interaction of several processes, including microbial growth, nutrient availability, antibiotic selection pressure, biological predation, and environmental variability. Mathematical models provide a means of integrating these processes and evaluating their combined effects on bacterial populations.

Several mathematical approaches have been developed to study bacterial and environmental dynamics. Deterministic compartmental models have traditionally been used to describe bacterial populations through systems of ordinary differential equations. These models have provided valuable information regarding bacterial growth, decay, and interaction processes. However, classical models often assume homogeneous populations and may not adequately represent differences between antibiotic- susceptible and antibiotic-resistant bacteria.

To overcome these limitations, subsequent studies have incorporated additional bio-

logical mechanisms. Density-dependent growth models have been developed to account for nutrient limitations affecting microbial proliferation, while bacteriophage predation models have examined biological control of bacterial populations. Optimal control theory has further extended mathematical modelling by providing strategies for determining effective interventions under resource constraints. More recently, fractional-order models have been introduced to capture memory effects associated with biological and environmental processes.

Although these approaches have significantly contributed to the understanding of individual mechanisms, many existing models investigate antibiotic resistance, bacterial growth, bacteriophage predation, optimal control, and memory effects separately or through limited combinations. Consequently, they may not fully represent wastewater environments where these mechanisms operate simultaneously. For example, the persistence of antibiotic-resistant bacteria depends not only on resistance characteristics but also on nutrient availability, environmental conditions, microbial interactions, and biological control pressure.

This chapter presents a critical review of mathematical models relevant to antibiotic-resistant *Escherichia coli* dynamics in wastewater. The literature is organised according to the major components incorporated into the proposed model, including deterministic modelling, antibiotic resistance, density-dependent growth through Monod kinetics, bacteriophage predation, optimal control, and fractional-order dynamics. Each section evaluates previous contributions, mathematical approaches, limitations, and their relevance to the development of the proposed seven-compartment model.

## 2.2 Deterministic Mathematical Modelling of Wastewater *Escherichia coli* Dynamics

Deterministic mathematical models have been extensively applied in biological and environmental systems to describe population changes and interactions between different system components. These models are commonly formulated using ordinary differential equations, where each equation represents the rate of change of a particular compartment. In microbial systems, compartments may represent bacterial populations, environmental reservoirs, treatment stages, or different biological states Hurdoganoglu *et al.* ((2022)) .

A major strength of deterministic models is their ability to provide analytical insights into system behaviour. Through equilibrium analysis, stability analysis, and numerical simulations, these models allow researchers to investigate conditions under which bacterial populations persist or decline. Furthermore, deterministic models provide a foundation for sensitivity analysis, enabling identification of parameters that have the greatest influence on bacterial dynamics (nevzerka *et al* (2022).

In wastewater applications, early deterministic models focused mainly on pollutant removal processes and microbial activity within treatment systems. These approaches improved understanding of wastewater treatment performance; however, many models treated microbial populations as a single homogeneous group. Such assumptions may be inadequate when analysing antibiotic-resistant bacteria because resistant and susceptible populations may exhibit different survival characteristics and responses to environmental pressuresHurdoganoglu *et al.* ((2022)) .

The increasing importance of antimicrobial resistance has therefore encouraged the development of models that explicitly distinguish between bacterial states. These models allow researchers to investigate resistance emergence, persistence, and control strategies. However, resistance alone does not determine bacterial survival in wastewater systems. Environmental factors such as nutrient availability, microbial competition, predation, and intervention strategies must also be considered to develop a realistic representation of bacterial dynamics.

### 2.2.1 Classical Compartmental Models

Compartmental modelling provides a mathematical representation of biological systems by dividing complex populations into interacting components. The transitions between compartments represent biological processes such as bacterial growth, death, conversion, infection, or removal. This approach has been widely applied because it provides a relatively simple but powerful framework for analysing dynamic biological systems.

In wastewater microbial modelling, compartmental approaches have been used to represent bacterial concentrations, contaminant movement, and treatment processes. These models have demonstrated that mathematical frameworks can successfully describe environmental processes and provide insights into factors influencing system behaviour. However, classical compartmental models often simplify microbial communities by assuming similar behaviour among bacterial populations.

Such simplification becomes problematic when modelling antibiotic-resistant *E. coli*. Resistant bacteria may survive under conditions where susceptible bacteria decline, and therefore the two populations should not always be represented as a single compartment. A more realistic model requires separate compartments for antibiotic-susceptible and antibiotic-resistant bacteria.

(Prakasha and Veresha (2020)) developed a fractional mathematical model for environmental pollution dynamics. Their work demonstrated that environmental systems may exhibit memory-dependent behaviour and that fractional-order approaches can provide additional flexibility compared with classical integer-order models. The study was important because it highlighted that the current state of an environmental system may depend on previous conditions.

However, the model mainly focused on pollution dynamics rather than microbial population interactions. It did not incorporate antibiotic-resistant bacterial populations, nutrient-dependent growth, bacteriophage predation, or control strategies. Therefore, although the study provided valuable insight into advanced environmental modelling, it does not fully represent the biological complexity of antibiotic-resistant *E. coli* persistence in wastewater.

Bonyaha *et al.* ((2021)) applied mathematical modelling and sensitivity analysis to investigate environmental pollution processes. Their study demonstrated the importance of mathematical approaches in identifying influential parameters and understanding environmental system behaviour. The application of sensitivity analysis was particularly valuable because it allowed evaluation of parameter importance within the proposed model.

Nevertheless, the study concentrated on general pollution dynamics rather than microbial population interactions. It did not distinguish antibiotic-resistant and antibiotic-susceptible bacteria and did not consider biological control mechanisms such as bacteriophage predation Bonyaha *et al.* ((2021)). Consequently, while the study contributes to environmental modelling, additional biological mechanisms are required for accurate representation of resistant bacterial persistence.

Ghosh *et al.* ((2021))investigated nonlinear mathematical approaches for biological population systems and demonstrated the importance of interaction terms in describing complex biological behaviour. Their work contributed to understanding how population interactions influence system dynamics. However, the model did not combine antibiotic resistance, nutrient limitation, biological predation, and intervention strategies within a unified wastewater framework.

The limitations identified in previous deterministic models demonstrate the need for an integrated approach. The present study extends classical compartmental modelling by incorporating antibiotic-susceptible and antibiotic-resistant *E. coli* populations together with Monod nutrient-dependent growth, bacteriophage predation, optimal control, and fractional-order dynamics.

### 2.2.2 Mathematical Models of Antibiotic Resistance

Antibiotic resistance introduces additional complexity into bacterial modelling because resistant populations may persist despite environmental conditions that reduce susceptible bacteria. Mathematical models of antibiotic resistance have therefore been developed to investigate resistance emergence, transmission, maintenance, and response to antibiotic pressure (Liui*et al* (2021) ).

A fundamental consideration in antibiotic resistance modelling is the representation of bacterial populations. Models that treat bacteria as a single population may fail to

capture the survival advantage associated with resistance. Consequently, many modern approaches divide bacterial populations into susceptible and resistant compartments, allowing transitions between these states to be represented mathematically.

Hurdoganoglu *et al.* ((2022)) investigated antibiotic resistance dynamics in *Escherichia coli* and demonstrated the importance of explicitly representing resistant bacterial populations. Their study showed that resistant bacteria possess distinct characteristics that influence their persistence under selective pressure. This contribution is important because it confirms that antibiotic resistance should be treated as a biological state rather than merely as a modification of bacterial growth parameters.

However, the framework primarily focused on resistance dynamics and did not integrate important ecological factors influencing bacterial persistence. In wastewater systems, antibiotic-resistant bacteria are affected by nutrient availability, environmental conditions, microbial interactions, and biological control mechanisms. Therefore, resistance models alone provide an incomplete description of wastewater bacterial dynamics.

The present study addresses this limitation by incorporating antibiotic resistance within a broader ecological framework. The proposed seven-compartment model combines resistant and susceptible bacterial populations with nutrient-dependent growth, bacteriophage predation, optimal control, and fractional-order memory effects to provide a more comprehensive representation of antibiotic-resistant *E. coli* dynamics.

## 2.3 Density-Dependent Growth and Monod Kinetics

Bacterial growth is a fundamental process determining the persistence and abundance of microbial populations in wastewater environments. Unlike ideal laboratory conditions where nutrients may be continuously supplied, wastewater systems are characterised by limited and variable nutrient availability. Consequently, bacterial populations cannot increase indefinitely and their growth becomes dependent on environmental resources. This relationship between population growth and available resources is commonly referred to as density-dependent growth(Savini*et al.*(2017)).

Density-dependent growth describes the phenomenon where the growth rate of a population changes as a consequence of population size or environmental limitations. In microbial systems, nutrient availability is one of the most important factors regulating bacterial proliferation. As bacterial density increases, available substrates are consumed, resulting in reduced growth rates. Therefore, mathematical models that incorporate density dependence provide a more realistic representation of bacterial dynamics compared with models assuming unrestricted exponential growth(Savini*et al.*(2017)).

Several mathematical approaches have been developed to represent microbial growth. The exponential growth model assumes unlimited resources and constant growth rates; however, this assumption is rarely appropriate for wastewater environments. Logistic

growth models introduced environmental carrying capacity, representing the maximum population size supported by available resources. Although logistic models provide an improvement over exponential growth, they do not explicitly describe the relationship between microbial growth and substrate concentration(Savini*et al.*(2017)).

For wastewater microbial systems, Monod kinetics provide a more biologically realistic representation because they directly relate bacterial growth rate to available substrate concentration. The incorporation of Monod kinetics into the present study is therefore essential because it provides the mathematical basis for representing density-dependent growth of antibiotic-resistant and antibiotic- susceptible *E. coli* populations.

### 2.3.1 Monod Growth Theory

Monod et al 1949 introduced one of the most influential mathematical descriptions of microbial growth by establishing a relationship between bacterial growth rate and limiting substrate concentration. The model was developed from experimental observations of bacterial cultures and demonstrated that microbial growth is controlled by the availability of essential nutrients.

The Monod growth equation is expressed as:

$$\mu(S) = \frac{\mu_{\max} S}{K_s + S} \tag{2.1}$$

where $\mu(S)$ represents the specific growth rate of microorganisms, $\mu_{\max}$ represents the maximum specific growth rate, $S$ denotes the limiting substrate concentration, and $K_s$ represents the half-saturation constant at which the growth rate reaches half of its maximum value.

The biological interpretation of the Monod equation is important for wastewater systems. When substrate concentration is low, bacterial growth is limited because microorganisms cannot obtain sufficient resources for reproduction. As substrate availability increases, growth accelerates until the maximum growth rate is reached. Beyond this point, additional increases in substrate concentration produce limited effects because other biological constraints become dominant(Savini*et al.*(2017)).

Unlike exponential growth models, Monod kinetics incorporate environmental limitations directly into the growth function. This makes the model particularly suitable for wastewater systems, where bacterial populations experience fluctuations in nutrient availability. In such environments, bacterial persistence depends not only on biological characteristics such as antibiotic resistance but also on access to resources required for survival and reproduction(2017)),(Savini*et al.*(2017)).

The use of Monod kinetics in mathematical models has been widely adopted in wastewater treatment studies because it provides a realistic representation of microbial activity. Activated sludge models, biological wastewater treatment models, and micro-

bial population models frequently incorporate Monod-type relationships to describe the interaction between microorganisms and substrates.

However, although Monod kinetics successfully describe nutrient-dependent growth, many existing models apply them to general microbial populations without considering antibiotic resistance. In wastewater environments, antibiotic-resistant and antibiotic-susceptible bacteria may have different survival characteristics, and therefore nutrient-dependent growth should be investigated together with resistance dynamics.

The present study addresses this limitation by incorporating Monod kinetics within a model that distinguishes between antibiotic-susceptible and antibiotic-resistant *E. coli*. This approach allows the influence of nutrient availability on both populations to be examined while considering additional biological mechanisms such as bacteriophage predation and control interventions.

### 2.3.2 Applications of Monod Kinetics in Wastewater Modelling

The application of Monod kinetics in wastewater modelling has significantly improved the understanding of microbial growth and treatment processes. Biological wastewater treatment depends largely on microbial communities that transform organic matter and remove pollutants. Mathematical models incorporating Monod relationships have been used to describe microbial substrate utilisation, biomass production, and treatment efficiency.

The activated sludge modelling framework developed by Henze et al.2000 demonstrated the importance of representing microbial growth according to substrate availability. Their work provided a foundation for modern wastewater process models by describing the relationship between microbial activity and environmental conditions. However, these models were primarily designed for treatment process optimisation and did not focus on antibiotic-resistant bacterial populations.

Similarly, Grady et al.2011 highlighted the importance of microbial kinetics in biological wastewater treatment systems. Their work showed that microbial growth models must consider environmental limitations to accurately predict system behaviour. Nevertheless, the models mainly addressed general microbial communities and did not incorporate antibiotic resistance, bacteriophage predation, or optimal control.

More recent environmental models have extended microbial growth frameworks by including additional ecological interactions. However, many studies continue to consider growth, resistance, and biological control as separate modelling components. This separation limits the ability of models to explain the combined influence of nutrient availability, antibiotic pressure, and biological interactions on resistant bacterial persistence.

The incorporation of Monod kinetics into the present study provides an important advancement because it connects environmental conditions with antibiotic-resistant bac-

terial dynamics. By including nutrient-dependent growth within the seven- compartment model, the study recognises that resistance alone does not determine bacterial survival; instead, resistant populations must also compete for resources within a changing wastewater environment.

### 2.3.3 Relevance of Monod Kinetics to the Present Study

The inclusion of Monod kinetics in this study is motivated by the need to represent realistic bacterial growth behaviour in wastewater systems. The term "density-dependent" in the context of this research refers to the limitation of bacterial growth by available environmental resources. Therefore, the growth rate of *E. coli* populations is not assumed to remain constant but varies according to substrate availability.

This assumption improves the biological realism of the proposed model because wastewater environments rarely provide unlimited nutrients. Antibiotic-resistant bacteria must survive within ecological constraints where growth, competition, and control mechanisms interact. Consequently, incorporating Monod kinetics allows the model to investigate how nutrient availability influences the persistence of antibiotic-resistant bacteria.

Furthermore, combining Monod growth with antibiotic resistance provides a more comprehensive framework than resistance models alone. A resistant population may possess survival advantages under antibiotic pressure; however, its persistence also depends on its ability to grow successfully under environmental limitations. The integration of Monod kinetics, resistance dynamics, bacteriophage predation, optimal control, and fractional-order effects therefore provides a more realistic representation of antibiotic-resistant *E. coli* behaviour in wastewater

## 2.4 Bacteriophage Predation and Biological Control

Bacteriophage predation represents an important biological mechanism influencing bacterial population dynamics in natural and engineered environments. Bacteriophages, commonly referred to as phages, are viruses that specifically infect bacterial cells and can regulate bacterial abundance through infection, replication, and host cell lysis. Due to their ability to selectively target bacteria, bacteriophages have received increasing attention as potential biological control agents, particularly against antibiotic-resistant bacterial populations.

The interaction between bacteriophages and bacteria introduces an additional ecological process that must be considered when modelling bacterial persistence. Unlike chemical antimicrobial interventions, bacteriophage predation is a biological interaction that depends on bacterial density, phage availability, infection efficiency, and environmental conditions. Therefore, mathematical models describing phage-bacteria interactions pro-

vide an important framework for understanding the potential role of bacteriophages in controlling antibiotic-resistant *Escherichia coli* populations.

### 2.4.1 Mathematical Phage–Bacteria Interaction Models

Mathematical modelling of predator-prey interactions has a long history in ecology. The classical predator-prey framework introduced through the Lotka–Volterra model provided the foundation for describing interactions between biological populations where one population depends on another for survival. In bacterial systems, bacteriophages can be considered biological predators because their reproduction depends on infecting and replicating within bacterial hosts Hurdoganoglu *et al.* ((2022)) .

The general predator-prey concept has been adapted to describe phage-bacteria interactions by introducing bacterial populations, phage populations, infection rates, and bacterial removal due to lysis. These models have demonstrated that bacteriophages can significantly influence bacterial population dynamics by reducing host abundance and altering bacterial growth patternsHurdoganoglu *et al.* ((2022)) .

A typical phage-bacteria model can be represented by coupled differential equations where bacterial growth is reduced by phage infection:

$$\frac{dB}{dt} = G(B) - \phi BP \tag{2.2}$$

where $B$ represents bacterial population, $P$ represents bacteriophage population, $G(B)$ represents bacterial growth, and $\phi$ represents the phage infection rate.

Although simplified, such models provide valuable insight into the biological mechanisms controlling bacterial populations. However, many traditional phage-bacteria models assume a single homogeneous bacterial population and do not distinguish between antibiotic-susceptible and antibiotic-resistant bacteria.

This assumption may limit their application to wastewater systems because bacterial communities contain diverse populations with different survival characteristics. Antibiotic-resistant bacteria may respond differently to environmental stress, antibiotic exposure, and biological predation. Therefore, phage predation models must be extended to incorporate bacterial population structure when analysing antibiotic-resistant *E. coli* dynamics.

### 2.4.2 Bacteriophage-Based Biological Control of Bacterial Populations

The application of bacteriophages as biological control agents has gained attention because of the increasing limitations associated with antibiotic treatment. The selective

nature of phages provides an opportunity to target specific bacterial populations while reducing dependence on chemical antimicrobial agents.

Several studies have investigated bacteriophage applications in bacterial control systems. These studies demonstrate that phages can reduce bacterial populations and may contribute to the management of antibiotic-resistant bacteria. However, the success of phage-based control depends on several factors, including bacterial density, phage-host specificity, environmental conditions, and the development of bacterial defence mechanisms.

From a mathematical perspective, phage-based control introduces additional nonlinear interactions into bacterial population models. The effect of predation is not simply a constant removal process but depends on the interaction between bacterial and phage populations. Consequently, models incorporating bacteriophage predation require appropriate interaction terms to capture the biological relationship between host availability and phage activity.

### 2.4.3 Bacteriophage Predation and Antibiotic-Resistant *E. coli*

The integration of bacteriophage predation with antibiotic resistance modelling is particularly important because resistant bacteria represent a major challenge in wastewater environments. While antibiotic resistance provides bacteria with protection against antimicrobial compounds, bacteriophages may offer an alternative mechanism for reducing resistant populations.

However, the relationship between antibiotic resistance and bacteriophage susceptibility is complex. Some resistant bacteria may experience biological trade-offs, such as reduced growth efficiency or altered surface structures, which may influence their interaction with bacteriophages. Conversely, some bacteria may develop phage resistance through mechanisms that affect antibiotic susceptibility. These interactions demonstrate that resistance and predation should not be studied independently.

Existing mathematical models have contributed to understanding phage-bacteria interactions; however, many models focus on bacterial populations without considering antibiotic resistance states. Similarly, antibiotic resistance models often neglect biological predation processes. This separation limits understanding of how bacteriophages may influence the persistence of antibiotic-resistant bacteria in wastewater ecosystems.

The present study addresses this limitation by incorporating bacteriophage predation within a model containing both antibiotic-susceptible and antibiotic-resistant *E. coli* compartments. This approach allows investigation of how phage activity influences resistant and susceptible populations under different environmental conditions.

### 2.4.4 Integration of Bacteriophage Predation with Monod Growth and Environmental Dynamics

Wastewater bacterial dynamics are influenced by multiple interacting processes. Although bacteriophage predation can reduce bacterial populations, its effectiveness depends on bacterial growth and availability of resources. A rapidly growing population supported by sufficient nutrients may respond differently to phage pressure compared with a nutrient-limited population.

Therefore, integrating bacteriophage predation with Monod nutrient-dependent growth provides a more realistic representation of wastewater systems. The growth rate of bacteria determines the availability of host cells for phage replication, while phage predation influences bacterial population size and competition for resources(Dokuyucu & Dutta, 2020).

This interaction demonstrates the importance of developing integrated models rather than analysing individual mechanisms separately. In the proposed seven-compartment model, bacteriophage predation is incorporated alongside antibiotic resistance and Monod growth kinetics to capture the combined effects of environmental limitation and biological control.

### 2.4.5 Critical Comparison with the Proposed Seven-Compartment Model

Previous bacteriophage models have provided valuable understanding of biological control mechanisms; however, several limitations remain. First, many existing models represent bacterial populations as a single compartment and therefore do not distinguish between antibiotic-susceptible and antibiotic-resistant bacteria. Second, nutrient limitation is often simplified or excluded, despite its importance in wastewater environments. Third, optimisation of intervention strategies is rarely included.

The proposed model extends previous approaches by incorporating bacteriophage predation together with antibiotic resistance, Monod nutrient-dependent growth, optimal control, and fractional-order dynamics. This integrated framework allows investigation of how biological control interacts with bacterial resistance, environmental limitations, and intervention strategies.

Consequently, bacteriophage predation is not treated as an isolated removal mechanism but as part of a broader ecological system influencing the persistence and control of antibiotic-resistant *E. coli* in wastewater.

## 2.5 Optimal Control Theory and Biological Intervention Strategies

Mathematical models describing bacterial dynamics provide important information regarding population behaviour; however, prediction alone is insufficient when the objective is to reduce bacterial persistence or optimise intervention strategies. In wastewater systems, control measures must consider not only the effectiveness of an intervention but also the associated costs, resource limitations, and long-term impact. Optimal control theory provides a mathematical framework for determining the most effective control strategy by balancing system objectives with intervention efforts.

Optimal control theory has been widely applied in biological, epidemiological, and environmental systems where decision variables influence the evolution of dynamic processes. In microbial systems, optimal control approaches allow researchers to determine how biological interventions, treatment processes, or management strategies can be applied efficiently to reduce undesirable populations.

For antibiotic-resistant *Escherichia coli* in wastewater, optimal control is particularly relevant because bacterial reduction cannot depend solely on one mechanism. Effective management may require combining biological control through bacteriophages, environmental interventions, and treatment strategies. Therefore, incorporating optimal control into bacterial models provides a means of identifying strategies that achieve population reduction while minimising intervention costs.

### 2.5.1 Pontryagin's Maximum Principle

The theoretical foundation of optimal control was established by Pontryagin et al 1962 , who developed the Maximum Principle for determining optimal solutions in controlled dynamic systems. The principle provides a systematic approach for transforming an optimisation problem into a set of differential equations involving state variables, control variables, and adjoint variables (2014)).

A general optimal control problem considers a dynamic system represented as:

$$\frac{dx(t)}{dt} = f(x(t), u(t), t) \tag{2.3}$$

where $x(t)$ represents the state variables describing the biological system and $u(t)$ represents the control variables applied to influence system behaviour.

The objective of the control problem is commonly expressed through an objective functional(2014)):

$$J(u) = \int_0^T L(x(t), u(t), t)dt \tag{2.4}$$

where $L(x(t), u(t), t)$ represents the cost function associated with the system state and applied controls over the time interval $[0, T]$.

The Hamiltonian formulation is then introduced as:

$$H(x, u, \lambda, t) = L(x, u, t) + \lambda f(x, u, t) \tag{2.5}$$

where $\lambda$ represents the adjoint variables associated with the system states.

The optimal control is obtained by minimising the Hamiltonian subject to the state and adjoint equations. This mathematical framework enables researchers to determine control strategies that achieve desired biological outcomes while considering practical limitations.

### 2.5.2 Optimal Control Applications in Biological Systems

Optimal control theory has been widely applied in biological systems where interventions influence population dynamics. In epidemiological models, optimal control has been used to determine effective vaccination strategies, treatment schedules, and prevention programmes. Similarly, in ecological systems, control theory has been applied to manage interacting populations and optimise resource allocation (Boltyanskiy *et al.*(1962)).

In microbial systems, optimal control provides a useful framework for investigating strategies aimed at reducing harmful bacterial populations.Unlike models that only simulate bacterial behaviour under fixed conditions, optimal control models consider how interventions can actively influence system dynamics.

Previous biological control studies have demonstrated that optimal strategies depend on the interaction between biological processes and intervention costs. For example, a control strategy that produces rapid bacterial reduction may require excessive resources, while a less intensive strategy may be more sustainable over longer periods. Therefore, optimal control provides a balance between effectiveness and practical feasibility.

### 2.5.3 Optimal Control in Wastewater Bacterial Management

Wastewater environments present unique challenges for bacterial control because microbial populations are influenced by continuous environmental changes. Antibiotic- resistant bacteria may persist despite conventional treatment approaches due to their survival advantages and ability to adapt to selective pressures(Xu and Gao(2020)).

Mathematical optimisation provides a means of evaluating different intervention strategies before implementation. For example, control variables may represent the application of bacteriophages, treatment intensity, removal processes, or other management interventions. The optimal strategy is then determined by minimising bacterial populations while controlling the associated intervention cost(Xu and Gao(2020)).

However, many existing wastewater bacterial models focus mainly on describing population dynamics and do not incorporate optimisation. Similarly, optimal control models frequently focus on epidemiological systems rather than environmental bacterial communities. This creates a gap in the application of optimal control to antibiotic-resistant bacteria in wastewater environments.

### 2.5.4 Objective Functional and Control Variables in the Present Study

The formulation of an appropriate objective functional is essential because it defines the goal of the optimal control problem. In the context of antibiotic- resistant *E. coli* dynamics, the objective should reflect both bacterial reduction and the cost associated with implementing control measures Seidu and Makinde ((2014)).

A suitable objective functional may therefore include two components: the reduction of bacterial populations and the cost of applying control interventions. This approach ensures that the optimal solution does not simply maximise bacterial elimination but also considers the practical limitations associated with control implementationSeidu and Makinde ((2014)).

The control variables in the proposed model represent interventions capable of influencing bacterial dynamics. These controls may include biological control through bacteriophage application and other management strategies represented within the mathematical framework. The inclusion of control variables allows investigation of how interventions influence antibiotic-resistant and antibiotic-susceptible bacterial populationsSeidu and Makinde ((2014)).

The incorporation of optimal control into the present study is therefore justified because understanding bacterial dynamics alone does not provide information about the most effective management strategy. By combining optimal control with antibiotic resistance, Monod nutrient-dependent growth, bacteriophage predation, and fractional- order dynamics, the proposed model provides a more comprehensive framework for analysing the control of antibiotic-resistant *E. coli* in wastewater.

### 2.5.5 Critical Comparison with Existing Approaches

Previous mathematical models have contributed significantly to understanding biological population dynamics and intervention strategies. However, several limitations remain. Many bacterial models describe growth and persistence without considering optimisation, while many optimal control studies focus on disease transmission rather than environmental bacterial systems.

Furthermore, existing control models often simplify bacterial populations by ignoring

antibiotic resistance states or environmental limitations affecting growth. Such simplifications may reduce their applicability to wastewater systems where resistant bacteria interact with nutrients, predators, and environmental conditions.

The present study addresses these limitations by integrating optimal control into a seven-compartment wastewater model. The proposed framework considers resistant and susceptible bacterial populations, nutrient-dependent growth through Monod kinetics, bacteriophage predation, and fractional-order memory effects. This integration allows the identification of effective control strategies while maintaining a realistic representation of antibiotic-resistant *E. coli* dynamics.

## 2.6 Fractional-Order Mathematical Modelling

Classical mathematical models based on integer-order derivatives have been widely used to describe biological and environmental systems. These models assume that the rate of change of a system depends primarily on its current state. Although this assumption is appropriate for many applications, biological systems frequently exhibit memory effects, where previous conditions influence present behaviour Ali *et al.* (2020).

In wastewater microbial systems, historical environmental conditions may affect bacterial growth, adaptation, persistence, and response to control measures. Antibiotic-resistant *Escherichia coli* populations, for example, may be influenced by previous exposure to antibiotics, previous nutrient conditions, and earlier interactions with biological control agents. Such processes cannot always be fully represented using classical integer-order models Ali *et al.* (2020).

Fractional-order mathematical models provide an alternative framework by introducing derivatives of non-integer order. Unlike classical derivatives that describe instantaneous rates of change, fractional derivatives incorporate information from previous states of the system. This property makes fractional-order models suitable for representing systems with memory, hereditary characteristics, and long-term dependencies.

The application of fractional calculus has expanded considerably in biological, environmental, and epidemiological modelling. However, the choice of fractional operator is important because different operators provide different mathematical representations of memory effects. Therefore, understanding the properties of different fractional derivatives is necessary when selecting an appropriate operator for modelling antibiotic-resistant bacterial dynamics.

### 2.6.1 Riemann–Liouville Fractional Derivative

The Riemann–Liouville fractional derivative is one of the earliest and most widely studied definitions in fractional calculus. It extends classical differentiation by allowing

derivatives of non-integer order and introduces a mathematical representation of memory through an integral formulation (Ahmad et al., 2025) Ali *et al.*, (2020).

The Riemann–Liouville fractional derivative of order $\alpha$ is generally defined as:

$$D^{\alpha}_{RL} f(t) = \frac{1}{\Gamma(n-\alpha)} \frac{d^n}{dt^n} \int_0^t (t-\tau)^{n-\alpha-1} f(\tau) d\tau \tag{2.6}$$

where $\Gamma(.)$ represents the Gamma function, $n-1 < \alpha < n$, and $\alpha$ denotes the fractional order(Ahmad et al., 2025).

The main advantage of the Riemann–Liouville operator is its strong mathematical foundation and ability to represent long-range memory effects. However, one limitation is that the derivative of a constant is not necessarily zero, which may create difficulties when applying the operator to physical and biological models. Furthermore, the initial conditions required for Riemann–Liouville models may not always have direct biological interpretations (Ahmad et al., 2025)..

Because biological systems are generally described using measurable initial conditions, researchers have increasingly considered alternative fractional operators that provide more practical interpretations Ali *et al.* (2020).

### 2.6.2 Caputo Fractional Derivative

The Caputo fractional derivative was introduced to overcome some limitations associated with the Riemann–Liouville formulation. A major advantage of the Caputo operator is that it allows the use of classical initial conditions, making it more suitable for applications in physics, engineering, and biological systems (Ahmad et al., 2025), Ali *et al.* (2020).

The Caputo derivative is defined as:

$$D^{\alpha}_{C} f(t) = \frac{1}{\Gamma(n-\alpha)} \int_0^t (t-\tau)^{n-\alpha-1} f^{(n)}(\tau) d\tau \tag{2.7}$$

where $0 < \alpha < 1$ represents the fractional order.

The Caputo derivative has been widely applied in biological modelling because its initial conditions have direct physical meaning. In microbial systems, it allows previous population states to influence current dynamics while maintaining a biologically interpretable starting condition(Ahmad et al., 2025).

Despite these advantages, the Caputo derivative contains a singular power-law kernel. This singularity means that the influence of past states decreases according to a power-law relationship, which may not always accurately represent biological memory processes where past influences decay smoothly over time.

### 2.6.3 Caputo–Fabrizio Fractional Derivative

To address limitations associated with singular kernels, Caputo and Fabrizio introduced a new fractional derivative with a non-singular exponential kernel. The Caputo–Fabrizio (C–F) derivative provides an alternative representation of memory effects where the influence of previous states decreases gradually rather than following a singular power-law decay(Ahmad et al., 2025), Ali *et al.* (2020).

The Caputo–Fabrizio derivative of order $\alpha$ is defined as:

$$ {}^{CF}D^{\alpha} f(t) = \frac{M(\alpha)}{1-\alpha} \int_0^t f'(\tau) \exp\left(-\frac{\alpha(t-\tau)}{1-\alpha}\right) d\tau \tag{2.8} $$

where $M(\alpha)$ is a normalisation function and $0 < \alpha < 1$ represents the fractional order(Ahmad et al., 2025).

The main advantage of the Caputo–Fabrizio operator is the absence of a singular kernel. This characteristic provides a smoother representation of memory effects and avoids unrealistic mathematical behaviour near the initial time. For biological systems, where changes often occur gradually, a non-singular kernel may provide a more realistic description of historical dependence(Ahmad et al., 2025) .

The C–F derivative has been applied in several biological and environmental models because of its ability to represent systems where previous conditions influence current dynamics(Ahmad et al., 2025). In microbial systems, memory effects may arise from bacterial adaptation, environmental persistence, delayed responses to treatment, and previous exposure to antimicrobial agents (Dokuyucu & Dutta, 2020)(Dokuyucu & Dutta, 2020).

### 2.6.4 Memory Effects in Biological and Environmental Systems

Biological systems frequently exhibit memory behaviour because current states are influenced by previous interactions and environmental conditions. In wastewater systems, bacterial populations are not determined only by current nutrient concentration or treatment conditions but also by historical exposure to antibiotics, previous growth conditions, and earlier ecological interactions Ali *et al.* (2020).

For antibiotic-resistant *E. coli*, memory effects may represent several biological processes. These include persistence after antibiotic exposure, delayed changes in population structure, gradual adaptation to environmental stress, and long-term effects of biological control mechanisms Ali *et al.* (2020).

Integer-order models assume that the system response depends primarily on the current state variables. While useful, this assumption may simplify biological processes by ignoring historical dependence. Fractional-order models provide additional flexibility by allowing previous states to influence current behaviour through the fractional operatorAli

*et al.* (2020).

The incorporation of memory effects is therefore particularly relevant for the present study because antibiotic-resistant bacterial populations exist within complex environments where previous biological and environmental conditions influence future dynamics (ur Rahman *et al* (2021)).

### 2.6.5 Justification for the Caputo–Fabrizio Operator in the Present Study

The selection of the Caputo–Fabrizio derivative in this study is motivated by its ability to represent biological memory using a non-singular exponential kernel. The choice is particularly relevant for wastewater bacterial systems because biological responses typically occur through gradual adaptation rather than abrupt changes(Dokuyucu & Dutta, 2020) (ur Rahman *et al* (2021)).

Compared with the Riemann–Liouville derivative, the Caputo–Fabrizio operator avoids singular behaviour. Compared with the classical Caputo derivative, it provides a different memory representation where previous states lose influence smoothly over time. This characteristic makes it suitable for modelling biological processes where historical effects gradually diminish(Dokuyucu & Dutta, 2020).

Furthermore, the integration of the Caputo–Fabrizio derivative with antibiotic resistance, Monod nutrient-dependent growth, bacteriophage predation, and optimal control provides a more comprehensive representation of wastewater bacterial dynamics. The fractional formulation allows the proposed model to capture not only population changes but also the influence of previous environmental and biological conditions on current bacterial behaviour Ali *et al.* (2020).

### 2.6.6 Critical Comparison with Existing Fractional Models

Previous fractional-order models have demonstrated the importance of memory effects in environmental and biological systems. (Prakasha and Veresha (2020)), for example, showed that fractional operators can improve the representation of environmental processes by incorporating historical dependence(Dokuyucu & Dutta, 2020).

However, many existing fractional models focus on general pollution dynamics or disease systems rather than antibiotic-resistant bacterial populations in wastewater Ali *et al.* (2020). Additionally, fractional models often exclude biological interactions such as bacteriophage predation, nutrient limitation, and intervention optimisation (Dokuyucu & Dutta, 2020).

The present study extends previous fractional modelling approaches by integrating the Caputo–Fabrizio operator into a seven-compartment wastewater model Ali *et al.*

(2020). This approach combines fractional memory effects with antibiotic resistance, Monod growth kinetics, bacteriophage predation, and optimal control, thereby providing a more complete mathematical representation of antibiotic-resistant *E. coli* dynamics.

## 2.7 Integrated Models of Antibiotic-Resistant *Escherichia coli* Dynamics

The previous sections have demonstrated that bacterial persistence in wastewater is controlled by multiple interacting mechanisms rather than by a single biological process. Antibiotic resistance influences bacterial survival under antimicrobial pressure, Monod kinetics describes the dependence of bacterial growth on available resources, bacteriophage predation provides a biological control mechanism, optimal control determines effective intervention strategies, and fractional-order operators describe memory effects associated with biological processes.

Although each modelling approach provides valuable insights into specific aspects of bacterial dynamics, wastewater ecosystems involve simultaneous interactions among these mechanisms. Therefore, integrated mathematical models are required to provide a more realistic representation of antibiotic-resistant *E. coli* persistence and control.

Existing mathematical studies have progressively incorporated multiple mechanisms into bacterial models. Some studies have combined bacterial growth with environmental factors, while others have integrated predator-prey interactions or resistance dynamics. However, most existing models consider only a subset of the processes involved in wastewater bacterial persistence.

For example, antibiotic resistance models have successfully represented transitions between susceptible and resistant bacterial states but often neglect environmental growth limitations and biological control mechanisms. These models provide important information about resistance evolution but may not fully explain bacterial survival within wastewater ecosystems where nutrient availability and ecological interactions play significant roles.

Similarly, bacteriophage models have demonstrated the potential of biological control in reducing bacterial populations. However, many phage-bacteria models assume a single bacterial population and do not distinguish between antibiotic-susceptible and antibiotic-resistant strains. This limitation reduces their ability to describe the selective pressures affecting resistant bacterial populations Hurdoganoglu *et al.* ((2022)).

Environmental microbial models incorporating Monod kinetics provide improved descriptions of bacterial growth because they consider substrate limitation. Nevertheless, many growth models focus on general microbial populations and do not include resistance mechanisms, biological predation, or intervention optimisationHurdoganoglu *et al.*

((2022)).

Fractional-order models have further improved mathematical descriptions by incorporating memory effects. However, many fractional models are developed for general environmental processes rather than antibiotic-resistant bacterial systems. Consequently, the combined influence of resistance, nutrient limitation, biological control, optimisation, and memory effects remains insufficiently explored.

### 2.7.1 Existing Combined Mathematical Approaches

Several researchers have attempted to integrate multiple biological mechanisms into mathematical models. These studies demonstrate that combining biological processes can improve model realism; however, complete integration remains challenging due to the complexity of wastewater microbial systems (ur Rahman *et al* (2021)).

Models combining bacterial growth and environmental limitations have demonstrated that microbial populations are strongly influenced by resource availability. However, these models commonly assume that bacterial populations are homogeneous and therefore do not represent differences between antibiotic-resistant and antibiotic-susceptible populations.

Resistance models have addressed this limitation by introducing separate bacterial compartments. The distinction between susceptible and resistant populations allows analysis of selective pressure and resistance persistence. Nevertheless, resistance models often simplify environmental conditions by assuming constant growth rates or excluding ecological interactions Hurdoganoglu *et al.* ((2022)).

Predator-prey models involving bacteriophages have provided insight into biological control mechanisms. These models demonstrate that phage activity can reduce bacterial populations and influence ecological balance. However, their application to antibiotic-resistant wastewater bacteria remains limited because bacterial resistance states and environmental growth limitations are often excluded.

Optimal control models have expanded biological modelling by introducing intervention strategies. These models determine how controls can be applied efficiently while considering system objectives and intervention costs. However, optimal control has rarely been integrated with antibiotic resistance, bacteriophage predation, and fractional memory effects in wastewater systems.

The limitations of previous approaches indicate that a comprehensive model must consider the interaction between bacterial population structure, environmental constraints, biological control, optimisation, and memory effects.

### 2.7.2 Need for an Integrated Seven-Compartment Model

The proposed seven-compartment model is developed to address the limitations identified in previous mathematical frameworks. Rather than analysing individual mechanisms independently, the model integrates multiple biological and mathematical components within a single system.

The inclusion of antibiotic-susceptible and antibiotic-resistant *E. coli* compartments allows the model to distinguish between bacterial populations with different responses to antimicrobial pressure. This representation is essential because resistant bacteria may persist even when susceptible bacteria are reduced Hurdoganoglu *et al.* ((2022)).

The incorporation of Monod kinetics introduces density-dependent growth by linking bacterial proliferation to nutrient availability. This improves biological realism because wastewater environments contain limited resources that influence bacterial growth and survival.

Bacteriophage predation is incorporated to represent biological control mechanisms. This allows investigation of how phage interactions influence both susceptible and resistant bacterial populations. The inclusion of optimal control provides a framework for identifying effective intervention strategies while considering control effort.

Finally, the use of the Caputo–Fabrizio fractional derivative introduces memory effects into the system. This enables the model to represent situations where past environmental conditions, antibiotic exposure, and biological interactions influence current bacterial dynamics Ali *et al.* (2020).

The integration of these components provides a comprehensive framework for analysing antibiotic-resistant *E. coli* dynamics in wastewater environments.

## 2.8 Comparative Analysis of Existing Models

A comparison of previous mathematical approaches demonstrates the limitations of existing models and highlights the contribution of the present study. Table 2.1 summarises the major components considered in previous approaches and the contribution of the proposed model.

## 2.9 Research Gap

The reviewed literature demonstrates significant progress in mathematical modelling of bacterial growth, antibiotic resistance, environmental processes, biological control, optimal interventions, and fractional dynamics. However, existing studies generally examine these mechanisms independently or through limited combinations.

Table 2.1: Comparison of Existing Mathematical Models and the Present Study

| **Component** | **Existing Contributions** | **Main Limitation** | **Contribution of Present Study** |
|---|---|---|---|
| **Antibiotic resistance** | Models representing resistant and susceptible bacterial populations | Often analysed separately from environmental growth processes and ecological interactions | Integrates antibiotic-resistant and antibiotic-susceptible *E. coli* populations within a wastewater ecosystem |
| **Monod growth kinetics** | Describes nutrient-dependent microbial growth and substrate limitation | Rarely combined with antibiotic resistance and biological control mechanisms | Introduces density-dependent bacterial growth through nutrient availability |
| **Bacteriophage predation** | Provides biological control through phage–bacteria interactions | Many models assume homogeneous bacterial populations and exclude resistance states | Incorporates phage interactions with resistant and susceptible bacterial populations |
| **Optimal control** | Provides mathematical optimisation of intervention strategies | Limited application in wastewater antibiotic-resistant bacterial systems | Determines effective control strategies while considering intervention costs |
| **Fractional dynamics** | Represents memory effects in biological and environmental systems | Few applications combine fractional dynamics with antibiotic-resistant wastewater bacteria | Applies the Caputo–Fabrizio operator to capture historical dependence in bacterial dynamics |

Antibiotic resistance models provide important insights into resistant bacterial persistence but frequently neglect environmental growth limitations and biological interactions. Growth models incorporating Monod kinetics describe nutrient dependence but commonly ignore bacterial resistance. Bacteriophage models explain biological suppression of bacterial populations but often do not consider resistant and susceptible bacterial states simultaneously. Optimal control models provide intervention strategies but have limited application to antibiotic-resistant wastewater bacteria. Fractional models capture memory effects but are rarely combined with antimicrobial resistance and biological control mechanisms.

Therefore, an important research gap remains in developing an integrated wastewater model that simultaneously incorporates antibiotic-susceptible and antibiotic-resistant *Escherichia coli*, Monod nutrient-dependent growth, bacteriophage predation, optimal control, and Caputo–Fabrizio fractional dynamics Ali *et al.* (2020).

The present study addresses this gap through the development of a seven-compartment mathematical framework that combines these mechanisms into a unified model. This approach provides a more comprehensive representation of antibiotic-resistant *E. coli* persistence, interaction, and control within wastewater systems.

## 2.10 Chapter Summary

This chapter reviewed mathematical approaches relevant to the modelling of antibiotic-resistant *Escherichia coli* dynamics in wastewater environments. Deterministic models provide the foundation for representing bacterial population changes, while antibiotic resistance models demonstrate the importance of separating susceptible and resistant bacterial states.

Monod kinetics provides a biologically realistic representation of density-dependent growth by incorporating nutrient limitations. Bacteriophage predation introduces a biological control mechanism capable of influencing bacterial populations, while optimal control theory provides a framework for determining effective intervention strategies. Fractional-order modelling extends classical approaches by incorporating memory effects associated with biological and environmental processes.

Although previous studies have advanced understanding of these individual mechanisms, a comprehensive framework integrating all components remains limited(Prakasha and Veresha (2020)),(Ahmad et al., 2025), Hurdoganoglu *et al.* ((2022))n-compartment model addresses this limitation by combining antibiotic resistance, Monod growth kinetics, bacteriophage predation, optimal control, and Caputo–Fabrizio fractional dynamics to provide an integrated mathematical description of antibiotic-resistant *E. coli* dynamics in wastewater.

# Chapter 3

# RESEARCH DESIGN AND METHODOLOGY

## 3.1 Introduction

This chapter presents the mathematical modelling framework and analytical procedures used in this study to investigate the dynamics of antibiotic-resistant *Escherichia coli* in wastewater treatment systems. The methodology was developed through three interconnected mathematical approaches: a deterministic compartmental model (Model A), a Caputo–Fabrizio fractional-order model (Model B), and an optimal control model (Model C).

The deterministic model provides the foundation for describing the movement, growth, removal, and interaction of *E. coli* populations and bacteriophages within different wastewater treatment stages. The model incorporates antibiotic resistance explicitly through the resistant *E. coli* compartment $T(t)$, density-dependent microbial growth through Monod kinetics, and bacteriophage predation mechanisms.

Although deterministic models provide important information regarding bacterial population dynamics, they assume that the present state depends only on current conditions. However, wastewater microbial systems may exhibit memory effects due to previous environmental conditions, antibiotic exposure history, and biological adaptation. Therefore, the deterministic framework is extended using the Caputo–Fabrizio fractional derivative to capture such historical dependence.

Furthermore, prediction of bacterial dynamics alone does not determine the most effective intervention strategy. Therefore, an optimal control framework is developed to identify intervention strategies that minimise antibiotic-resistant *E. coli* concentration while considering the cost associated with control implementation.

The three models are therefore connected as follows:

Deterministic dynamics ⟶ Fractional memory extension ⟶ Optimal intervention strategy

The three modelling approaches developed in this study are interconnected and collectively address the objectives of investigating antibiotic-resistant *Escherichia coli* dynamics in wastewater treatment systems. The deterministic compartmental model (Model A) provides the foundational framework for describing the population dynamics, transfer processes, microbial growth, bacteriophage interactions, and persistence of antibiotic-resistant *E. coli* within different treatment stages. However, biological systems may exhibit historical dependence due to previous environmental conditions and microbial adaptation. Therefore, the deterministic framework is extended through the Caputo–Fabrizio fractional-order model (Model B) to incorporate memory effects and provide a more flexible representation of microbial dynamics. Finally, the optimal control model (Model C) builds upon the deterministic framework by introducing intervention strategies and applying optimal control theory to determine effective approaches for reducing antibiotic-resistant *E. coli* concentrations while considering intervention costs.

Therefore, Model A addresses the fundamental dynamics of the bacterial system, Model B investigates the influence of biological memory effects, and Model C determines optimal intervention strategies for controlling antibiotic-resistant *E. coli* in wastewater treatment environments. The following sections present the formulation, analysis, and numerical procedures applied to each mathematical framework .

## 3.2 Deterministic Model A

### 3.2.1 Model Formulation

A deterministic compartmental model was developed to describe the dynamics of *Escherichia coli* and bacteriophage populations throughout different wastewater treatment stages. The compartmental modelling approach was adopted because wastewater treatment systems consist of sequential biological and physical processes in which microbial populations undergo recruitment, growth, transfer between treatment stages, predation, and removal (nevzerka *et al* (2022)).

The model consists of seven state variables representing bacterial and bacteriophage populations within the wastewater treatment system. The bacterial population is separated into antibiotic-susceptible and antibiotic-resistant populations to explicitly represent resistance dynamics. The antibiotic-resistant *E. coli* population is represented by the compartment $T(t)$.

The compartment $T(t)$ describes the persistence of antibiotic-resistant *E. coli* un-

der treatment pressure within the wastewater environment. Unlike susceptible bacterial populations that may be reduced through treatment processes, resistant bacteria may survive due to selective pressure, environmental adaptation, and reduced treatment susceptibility. Therefore, including $T(t)$ as an independent state variable allows the model to investigate resistant bacterial survival, transfer, and removal mechanisms separately from the total bacterial population.

The explicit representation of the resistant compartment strengthens the ability of the proposed model to evaluate antibiotic resistance persistence within wastewater treatment systems and supports the main objective of understanding the dynamics of antibiotic-resistant *E. coli*.

$$(W(t), X(t), Y(t), Z(t), T(t), V(t), P(t))$$

where:

- $W(t)$ represents the *E. coli* concentration in the pre-primary treatment stage.
- $X(t)$ represents the *E. coli* concentration in the primary treatment stage.
- $Y(t)$ represents the *E. coli* concentration in the secondary treatment stage.
- $Z(t)$ represents the *E. coli* concentration in the tertiary treatment stage.
- $T(t)$ represents the antibiotic-resistant *E. coli* population.
- $V(t)$ represents the bacteriophage population in the pre-primary treatment stage.
- $P(t)$ represents the bacteriophage population in the primary treatment stage.

The interactions among bacterial populations, resistant bacteria, and bacteriophages are represented using a system of ordinary differential equations. Each equation describes the rate of change of a population with respect to time by incorporating microbial growth, movement between treatment stages, bacteriophage predation, treatment effects, and natural removal processes.

### 3.2.2 Model Variables and Parameters

The parameters of the deterministic model describe bacterial recruitment, growth, transfer, removal, bacteriophage interaction, and treatment processes within the wastewater system. The definitions of the parameters are presented in Table (5.1)

The state variables of Model A are defined as Table (5.2):

Table 3.1: Definition of Model A Parameters

| Parameter | Description |
|---|---|
| $\pi_1$ | Recruitment rate of *E. coli* into the wastewater system through stormwater inflow |
| $\pi_2$ | Additional recruitment rate of *E. coli* into the treatment system |
| $\pi_3$ | Recruitment rate of bacteriophages into the wastewater treatment system |
| $\pi_4$ | Additional recruitment rate of *E. coli* into the tertiary treatment stage |
| $\pi_m$ | Maximum microbial growth rate used in the Monod growth function |
| $K_2$ | Monod half-saturation constant representing nutrient limitation |
| $\mu_1$ | Natural removal rate of *E. coli* and bacteriophage populations |
| $\mu_2$ | Additional bacterial removal rate due to environmental effects |
| $\beta_1$ | Bacteriophage-induced removal rate of *E. coli* in the pre-primary stage |
| $\beta_2$ | Bacteriophage growth rate resulting from interaction with bacterial hosts |
| $\omega_1$ | Bacteriophage-induced bacterial removal rate in the primary stage |
| $\omega_2$ | Bacteriophage amplification rate due to bacterial interaction |
| $\gamma_1$ | Transfer rate of *E. coli* from pre-primary to primary stage |
| $\gamma_2$ | Transfer rate of *E. coli* from primary to secondary stage |
| $\gamma_3$ | Transfer rate of *E. coli* from secondary to tertiary stage |
| $\gamma_4$ | Treatment/removal rate of *E. coli* from tertiary stage |
| $\Omega$ | Treatment efficiency parameter associated with bacterial reduction |
| $\Phi$ | Effluent removal rate of antibiotic-resistant *E. coli* |
| $K_E$ | Carrying capacity of the *E. coli* population |
| $K_P$ | Carrying capacity of the bacteriophage population |
| $M$ | Limiting nutrient concentration influencing bacterial growth |

Table 3.2: Definition of Model A Variables

| Variable | Description |
|---|---|
| $W(t)$ | *E. coli* concentration in the pre-primary treatment stage |
| $X(t)$ | *E. coli* concentration in the primary treatment stage |
| $Y(t)$ | *E. coli* concentration in the secondary treatment stage |
| $Z(t)$ | *E. coli* concentration in the tertiary treatment stage |
| $T(t)$ | Antibiotic-resistant *E. coli* concentration |
| $V(t)$ | Bacteriophage concentration in the pre-primary treatment stage |
| $P(t)$ | Bacteriophage concentration in the primary treatment stage |

### 3.2.3 Model Assumptions

The deterministic model was developed under the following assumptions:

1. The concentrations of *E. coli* and bacteriophages can be quantified per unit volume of wastewater.

2. The wastewater treatment system is considered sufficiently mixed; hence, microbial populations within each compartment are represented by average concentrations.

3. The antibiotic-resistant *E. coli* population is represented explicitly through the resistant compartment $T(t)$.

4. Bacterial growth follows Monod kinetics due to nutrient limitation within the wastewater environment.

5. All state variables remain non-negative for all time $t \geq 0$.

6. Bacteriophage predation contributes to bacterial reduction in treatment stages where bacteriophage populations are significant.

7. Water evaporation and spatial diffusion effects are assumed negligible.

8. Model parameters are assumed to be non-negative constants during the simulation period.

9. Initial conditions are biologically feasible and belong to the non-negative solution domain.

10. All initial conditions are non-negative, such that

$$W(0), X(0), Y(0), Z(0), T(0), V(0), P(0) \geq 0.$$

This ensures that all state variables begin within the biologically feasible non-negative region.

11. All model parameters are assumed to be non-negative constants throughout the simulation period unless otherwise stated. This assumption ensures that recruitment, transfer, mortality, treatment, and interaction rates remain mathematically and biologically meaningful.

12. The solutions of the model are assumed to remain within a positively invariant feasible region, so that bacterial and bacteriophage populations remain non-negative and bounded for all $t \geq 0$.

13. The total bacterial and bacteriophage populations are bounded by the environmental carrying capacities of their respective treatment compartments,

### 3.2.4 Model Framework

The deterministic model framework describes the movement and interaction of *E. coli*, antibiotic-resistant bacteria, and bacteriophage populations through different wastewater treatment stages.

The framework incorporates bacterial recruitment, microbial growth, stage-to-stage transfer, bacteriophage predation, treatment removal, and resistance persistence mechanisms. The arrows in the framework represent the direction of population movement and interaction among the compartments.

A schematic representation of the deterministic model framework is presented in Figure.

**Model Framework**

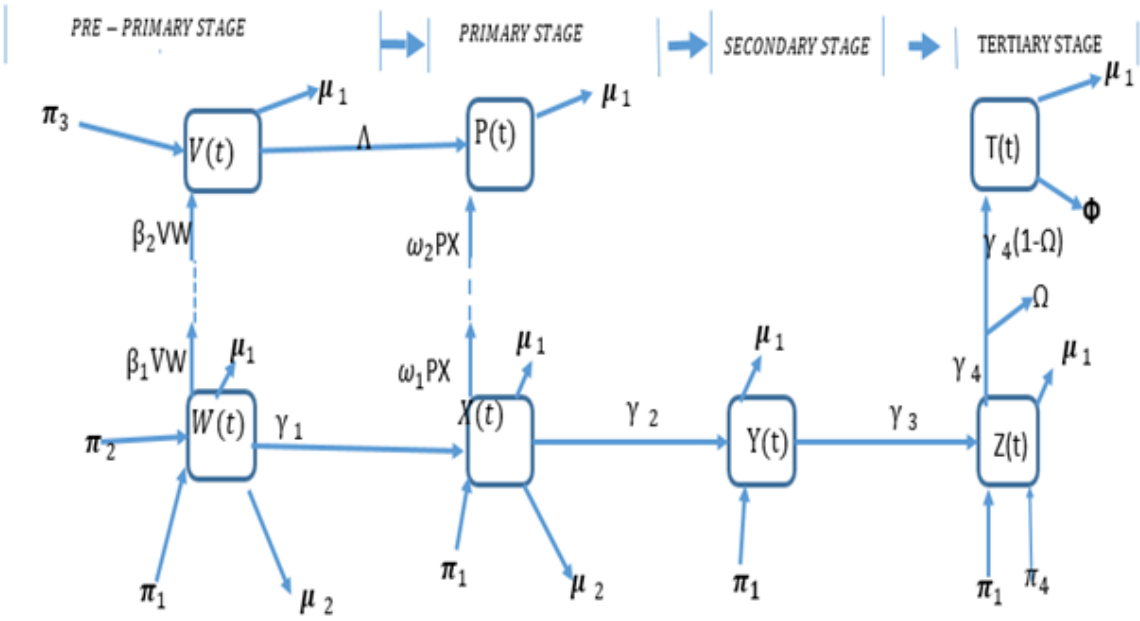


Figure 3.1: Definition of Model A Parameters

### 3.2.5 Biological Interpretation of Model Components

The deterministic framework integrates environmental processes responsible for the persistence and reduction of antibiotic-resistant *E. coli* in wastewater systems.

The compartments $W(t)$, $X(t)$, $Y(t)$, and $Z(t)$ represent the progression of bacterial populations through sequential wastewater treatment stages. The resistant compartment $T(t)$ captures the survival of antibiotic-resistant bacteria following treatment pressure. The bacteriophage compartments $V(t)$ and $P(t)$ represent biological control through predator-prey interactions between bacteriophages and bacterial populations.

Therefore, the model provides an integrated representation of microbial growth, environmental limitation, resistance persistence, and biological control within wastewater treatment systems.

### 3.2.6 Model Equations

The deterministic model was formulated as a system of seven ordinary differential equations representing the temporal changes of the state variables $W(t), X(t), Y(t), Z(t), T(t), V(t), P(t)$. The equations were derived from the model framework by considering the biological processes affecting each compartment, including microbial recruitment, density-dependent growth, wastewater treatment removal, bacteriophage interaction, and antibiotic resistance persistence.

The density-dependent growth component is incorporated through the combination of environmental limitation and nutrient-dependent microbial growth. The carrying capacity term limits population expansion within each treatment compartment, while the Monod formulation represents the influence of available nutrients on microbial growth.

The deterministic model is expressed as:

$$\begin{aligned}
\frac{dW}{dt} &= \left(\pi_1 + \pi_2 - \mu_1 W - \mu_2 W - \beta_1 WV + \frac{\pi_m WS}{K_2 + S} - \gamma_1 W\right)\left(1 - \frac{N}{A}\right), \\
\frac{dX}{dt} &= \left(\gamma_1 W + \pi_1 - \mu_1 X - \mu_2 X - \omega_1 XP + \frac{\pi_m XS}{K_2 + S} - \gamma_2 X\right)\left(1 - \frac{N}{A}\right), \\
\frac{dY}{dt} &= \left(\gamma_2 X + \pi_1 - \mu_1 Y + \frac{\pi_m YS}{K_2 + S} - \gamma_3 Y\right)\left(1 - \frac{N}{A}\right), \\
\frac{dZ}{dt} &= \left(\gamma_3 Y + \pi_1 + \pi_4 - \mu_1 Z + \frac{\pi_m ZS}{K_2 + S} - \gamma_4 Z\right)\left(1 - \frac{N}{A}\right), \\
\frac{dT}{dt} &= \left(\gamma_4 Z(1 - \Omega) - \mu_1 T + \frac{\pi_m TS}{K_2 + S} - \Phi T\right)\left(1 - \frac{N}{A}\right), \\
\frac{dV}{dt} &= \left(\beta_2 WV + \pi_3 - \mu_1 V + \frac{\pi_m VS}{K_2 + S} - \Lambda V\right)\left(1 - \frac{B}{A}\right), \\
\frac{dP}{dt} &= \left(\Lambda V + \omega_2 XP - \mu_1 P + \frac{\pi_m PS}{K_2 + S}\right)\left(1 - \frac{B}{A}\right).
\end{aligned} \tag{3.1}$$

Where
$0 \leq \omega_1 \leq 1$, $0 \leq \omega_2 \leq 1$, $0 \leq \beta_1 \leq 1$,$0 \leq \beta_2 \leq 1$
$A \geq W$,$B \geq X$,$C \geq Y D \geq Z$,$E \geq SA \geq V$,$B \geq P$.

represents the available nutrient concentration within the wastewater environment, $K_2$ represents the half-saturation constant associated with Monod growth, and $A, B, C, D, E$ represent the environmental carrying capacities of the corresponding compartments.

The parameter restrictions are given by:

$$0 \leq \beta_1, \beta_2, \omega_1, \omega_2 \leq 1$$

and all biological parameters satisfy:

$$\pi_i, \pi_m, \mu_i, \gamma_i, \Phi, \Omega, \Lambda_V \geq 0.$$

The initial conditions satisfy:

$$W(0), X(0), Y(0), Z(0), T(0), V(0), P(0) \geq 0. \tag{3.2}$$

The model equations describe the following biological processes:

- The terms $\pi_1$ and $\pi_2$ represent bacterial recruitment into the wastewater treatment system.
- The terms involving $\frac{\pi_m XM}{K_2+M}$ represent nutrient-dependent microbial growth described

by Monod kinetics.

- The terms involving $\beta_1 WV$ and $\omega_1 XP$ represent bacterial reduction caused by bacteriophage predation.
- The parameters $\gamma_1, \gamma_2, \gamma_3, \gamma_4$ represent movement of bacterial populations between sequential treatment stages.
- The compartment $T(t)$ describes the persistence of antibiotic-resistant *E. coli* after treatment pressure.
- The parameters $\Phi$ and $\Omega$ represent resistant bacterial removal and treatment efficiency, respectively.

The system provides the mathematical foundation for subsequent analysis of positivity, boundedness, equilibrium behaviour, stability properties, sensitivity analysis, and numerical simulations. :

### 3.2.7 Justification of Monod Growth Kinetics

Microbial growth within wastewater treatment systems is strongly influenced by the availability of nutrients and organic substrates. Since bacterial populations cannot increase indefinitely in an environment with limited resources, the growth rate of *E. coli* is dependent on the concentration of available nutrients. Therefore, Monod kinetics was incorporated into the proposed model to describe nutrient-dependent microbial growth.

The Monod growth function is represented as:

$$\frac{\pi_m M T(t)}{K_2 + T(t)} \tag{3.3}$$

where $\pi_m$ represents the maximum microbial growth rate, $M$ represents the available nutrient concentration within the wastewater environment, $T(t)$ represents the antibiotic-resistant *E. coli* population, and $K_2$ represents the Monod half-saturation constant. .

Biologically, when nutrient availability is low, the value of the Monod term remains small, representing restricted bacterial growth due to nutrient limitation. As nutrient availability increases, bacterial growth increases until it approaches the maximum growth rate $\pi_m$. This relationship provides a realistic representation of microbial behaviour in wastewater environments where organic matter and nutrients regulate bacterial population expansion.

The Monod formulation is appropriate for modelling wastewater bacterial dynamics because wastewater treatment systems contain complex microbial communities where growth is controlled by substrate availability rather than unlimited exponential expansion. Compared with simple growth assumptions, Monod kinetics captures the saturation effect

that occurs when bacteria approach the maximum growth capacity supported by the wastewater environment.

Therefore, incorporating Monod kinetics enables the proposed model to represent the biological mechanisms governing *E. coli* growth, persistence, and interaction with treatment processes more realistically.

### 3.2.8 Justification of Density-Dependent Growth Formulation

The term density-dependent growth is incorporated in the deterministic model to represent the limitation imposed by environmental capacity and nutrient availability on microbial population growth within wastewater treatment systems. In natural and engineered aquatic environments, bacterial growth does not increase indefinitely because available resources, space, and environmental conditions restrict population expansion.

In the proposed model, density dependence is represented through two biological mechanisms. The first mechanism is the environmental carrying-capacity limitation represented by the logistic growth component:

$$\left(1 - \frac{N}{K}\right) \tag{3.4}$$

where $N$ represents the total microbial concentration within a compartment and $K$ represents the maximum carrying capacity supported by the wastewater environment. This term reduces population growth as the microbial concentration approaches the environmental limit, thereby preventing unrealistic unlimited population increase.

The second mechanism is nutrient-dependent microbial growth represented through the Monod kinetic formulation:

$$\frac{\pi_m X M}{K_2 + M} \tag{3.5}$$

where $\pi_m$ represents the maximum microbial growth rate, $M$ represents the available nutrient concentration, and $K_2$ represents the half-saturation constant. The Monod function describes the relationship between microbial growth and limiting nutrient availability, where growth increases with nutrient availability but approaches a maximum value when sufficient nutrients are available.

The incorporation of Monod kinetics is appropriate for wastewater microbial systems because bacterial populations are strongly influenced by organic substrates and nutrient concentrations present in wastewater. Unlike simple exponential growth assumptions, Monod kinetics provides a biologically realistic description of microbial growth under resource-limited conditions.

Therefore, the proposed formulation combines nutrient-dependent growth and population-density limitation to describe the complex environmental conditions experienced by *E. coli*

populations during wastewater treatment. This approach enables the model to capture both microbial competition for available resources and restriction of population expansion due to environmental capacity.

The density-dependent formulation is particularly important for modelling antibiotic-resistant *E. coli* because resistant populations may persist even after treatment interventions. By incorporating growth limitation, treatment removal, and bacteriophage predation simultaneously, the model provides a more realistic representation of resistant bacterial dynamics within wastewater treatment systems.

### 3.2.9 Model A Analysis

The deterministic Model A was analysed using mathematical techniques including positivity analysis, boundedness analysis, equilibrium determination, stability analysis, and sensitivity analysis. These analyses were performed to determine the behaviour of the bacterial and bacteriophage populations under different environmental conditions.

#### Feasible Region

The feasible region ensures that all biological variables remain physically meaningful. Since bacterial and bacteriophage concentrations cannot be negative, the model solutions are restricted to the non-negative region.

The feasible region is defined as:

$$\Omega = \left\{(W, X, Y, Z, T, V, P) \in \mathbb{R}^7_+ : N \leq K_E,\ B \leq K_P\right\}. \tag{3.6}$$

**Theorem 1:Positivity**

Let the initial conditions satisfy:

$$W(0), X(0), Y(0), Z(0), T(0), V(0), P(0) \geq 0. \tag{3.7}$$

Then the solutions of Model A remain non-negative for all $t \geq 0$.

**Proof.**

The bacterial and bacteriophage equations contain only non-negative recruitment terms and removal terms proportional to the state variables. Therefore, a solution cannot cross the boundary of the positive orthant. Hence,

$$(W, X, Y, Z, T, V, P) \in \mathbb{R}^7_+ \tag{3.8}$$

for all $t \geq 0$.

The positivity of the solutions has an important biological interpretation in the proposed wastewater treatment model. Since the state variables represent microbial con-

centrations, including *E. coli*, antibiotic-resistant *E. coli*, and bacterophage populations, negative values have no physical meaning. The non-negative initial conditions together with the structure of the model ensure that recruitment, growth, transfer, predation, and removal processes maintain all populations within the biologically feasible region for all $t \geq 0$. Therefore, the model preserves the biological requirement that microbial concentrations cannot become negative during wastewater treatment processes.

**Theorem 2: Boundedness**

Let

$$N(t) = W(t) + X(t) + Y(t) + Z(t) + T(t) \tag{3.9}$$

represent the total bacterial population, and let

$$B(t) = V(t) + P(t) \tag{3.10}$$

represent the total bacteriophage population. Assume that all initial conditions are non-negative and that the model parameters remain non-negative. Then the solutions of Model A remain bounded for all $t \geq 0$.

**Proof.**

From the model equations, the total bacterial population satisfies

$$\frac{dN}{dt} = \frac{dW}{dt} + \frac{dX}{dt} + \frac{dY}{dt} + \frac{dZ}{dt} + \frac{dT}{dt}. \tag{3.11}$$

By combining the bacterial equations and applying the carrying-capacity restrictions, the total bacterial population can be bounded above by a positive constant. Hence,

$$0 \leq N(t) \leq K_E, \tag{3.12}$$

where $K_E$ represents the effective bacterial carrying capacity of the wastewater treatment environment.

Similarly, the total bacteriophage population satisfies

$$\frac{dB}{dt} = \frac{dV}{dt} + \frac{dP}{dt}, \tag{3.13}$$

and the corresponding carrying-capacity restriction gives

$$0 \leq B(t) \leq K_P, \tag{3.13}$$

where $K_P$ represents the effective carrying capacity of the bacteriophage population.

Therefore, all state variables remain bounded within the biologically feasible region for all $t \geq 0$.

**Biological Interpretation of Boundedness**

The boundedness of the model solutions reflects the physical and biological limitations of microbial populations within wastewater treatment systems. Bacterial and bacteriophage populations cannot increase indefinitely because their growth is constrained by finite nutrient availability, environmental conditions, treatment processes, and carrying capacities of the respective treatment compartments.

Therefore, the boundedness property ensures that the predicted concentrations of *E. coli*, antibiotic-resistant *E. coli*, and bacteriophages remain within biologically realistic limits. This prevents the model from producing unrealistic unlimited population growth and supports the biological feasibility of the proposed wastewater treatment model.

**Equilibrium Points**

The equilibrium points represent states where the bacterial and bacteriophage populations remain constant over time. They are obtained by setting the right hand sides of Equations in 3.1equal to zero.

Therefore,

$$\frac{dW}{dt} = \frac{dX}{dt} = \frac{dY}{dt} = \frac{dZ}{dt} = \frac{dT}{dt} = \frac{dV}{dt} = \frac{dP}{dt} = 0. \tag{3.14}$$

The model produces five biologically meaningful equilibrium cases:

$$E_0 = (0, 0, 0, 0, 0, 0, 0)$$

representing complete elimination of bacterial and bacteriophage populations.

$$E^1 = (0, 0, 0, 0, 0, V^*, P^*)$$

representing bacteriophage persistence without bacterial populations.

$$E^2 = (W^*, X^*, Y^*, Z^*, T^*, 0, 0)$$

representing bacterial persistence without bacteriophage populations.

$$E^3 = (W^*, X^*, Y^*, Z^*, T^*, V^*, 0)$$

representing coexistence of bacterial and partial bacteriophage populations.

$$E^4 = (W^*, X^*, Y^*, Z^*, T^*, V^*, P^*)$$

representing complete coexistence equilibrium.

**Biological interpretation of equilibrium points**

The equilibrium points represent different possible long-term states of the wastewater treatment system.

The equilibrium point

$$E^0 = \{0, 0, 0, 0, 0, 0, 0\} \tag{3.15}$$

represents the complete elimination state where both bacterial and bacteriophage populations are absent. Biologically, this corresponds to a theoretical condition where wastewater treatment has completely removed all microbial populations.

The equilibrium point

$$E^1 = \{0, 0, 0, 0, V^1, P^1\} \tag{3.16}$$

represents a bacteriophage-only equilibrium. At this state, bacterial populations are absent while bacteriophage populations persist within the treatment system.

The equilibrium point

$$E^2 = \{W^2, X^2, Y^2, Z^2, T^2, 0, 0\} \tag{3.17}$$

represents a predator-free equilibrium where bacterial populations persist in the absence of bacteriophages. This condition describes a wastewater system where biological control through bacteriophage predation is unavailable.

The equilibrium point

$$E^3 = \{W^3, X^3, Y^3, Z^3, T^3, V^3, P^3\} \tag{3.18}$$

represents the coexistence equilibrium where bacterial populations and bacteriophage populations are simultaneously present. This equilibrium describes continuous interaction between bacteria and their biological predators.

The equilibrium point

$$E^4 = \{W^4, X^4, Y^4, Z^4, T^4, V^4, P^4\} \tag{3.19}$$

represents the interior coexistence equilibrium involving susceptible bacteria, antibiotic-resistant *E. coli*, and bacteriophage populations. This is the most biologically relevant equilibrium because it represents the long-term behaviour of the wastewater treatment system under continuous microbial interaction and treatment pressure.

### Local Stability Analysis

The local stability of the equilibrium points of Model A was analysed using the Jacobian matrix approach. The Jacobian matrix describes the behaviour of the system near an equilibrium point and determines whether small disturbances increase or decay with time.

Let the system of equations represented by Equation 3.1 be expressed as:

$$\frac{dX}{dt} = F(X), \tag{3.20}$$

where

$$X = (W, X, Y, Z, T, V, P)^T.$$

The Jacobian matrix of the system is given by:

$$J = \begin{bmatrix} \frac{\partial f_1}{\partial W} & \frac{\partial f_1}{\partial X} & \frac{\partial f_1}{\partial Y} & \frac{\partial f_1}{\partial Z} & \frac{\partial f_1}{\partial T} & \frac{\partial f_1}{\partial V} & \frac{\partial f_1}{\partial P} \\ \frac{\partial f_2}{\partial W} & \frac{\partial f_2}{\partial X} & \frac{\partial f_2}{\partial Y} & \frac{\partial f_2}{\partial Z} & \frac{\partial f_2}{\partial T} & \frac{\partial f_2}{\partial V} & \frac{\partial f_2}{\partial P} \\ \vdots & \vdots & \vdots & \vdots & \vdots & \vdots & \vdots \\ \frac{\partial f_7}{\partial W} & \frac{\partial f_7}{\partial X} & \frac{\partial f_7}{\partial Y} & \frac{\partial f_7}{\partial Z} & \frac{\partial f_7}{\partial T} & \frac{\partial f_7}{\partial V} & \frac{\partial f_7}{\partial P} \end{bmatrix}. \tag{3.21}$$

or

$$\begin{bmatrix} A_1 & A_2 & A_3 & A_4 & A_5 & A_6 & A_7 \\ B_1 & B_2 & B_3 & B_4 & B_5 & B_6 & B_7 \\ C_1 & C_2 & C_3 & C_4 & C_5 & C_6 & C_7 \\ D_1 & D_2 & D_3 & D_4 & D_5 & D_6 & D_7 \\ E_1 & E_2 & E_3 & E_4 & E_5 & E_6 & E_7 \\ F_1 & F_2 & F_3 & F_4 & F_5 & F_6 & F_7 \\ G_1 & G_2 & G_3 & G_4 & G_5 & G_6 & G_7 \end{bmatrix} \tag{3.22}$$

The eigenvalues of the Jacobian matrix evaluated at each equilibrium point were used to determine local stability. An equilibrium point is locally asymptotically stable when all eigenvalues possess negative real parts.

The characteristic equation associated with the Jacobian matrix is expressed as:

$$a_7\lambda^7 + a_6\lambda^6 + a_5\lambda^5 + a_4\lambda^4 + a_3\lambda^3 + a_2\lambda^2 + a_1\lambda + a_0 = 0. \tag{3.23}$$

The Routh–Hurwitz stability criterion was applied to determine the conditions under which all eigenvalues have negative real parts. The criterion provides necessary and sufficient conditions for stability based on the signs of the coefficients of the characteristic polynomial. For the equilibrium point to be locally asymptotically stable, all roots of the characteristic equation must have negative real parts. According to the Routh–Hurwitz stability criterion, this condition is satisfied when all Hurwitz determinants are positive:

$$\Delta_i > 0, \qquad i = 1, 2, \ldots, 7.$$

Therefore, the equilibrium point is locally asymptotically stable when the Routh–Hurwitz conditions are satisfied. If any Hurwitz determinant becomes negative, the system loses stability and perturbations around the equilibrium may increase with time.

**Global Stability Analysis**

Local stability only describes the behaviour of the system near equilibrium points. Therefore, global stability analysis was performed to determine whether the system converges to an equilibrium state from a wider range of initial conditions (Odhiambo, 2023).

The Lyapunov stability method was used to establish global asymptotic stability. A suitable Lyapunov function was constructed as:

$$V = \frac{1}{2}(W-W^*)^2+\frac{\delta_1}{2}(X-X^*)^2+\frac{\delta_2}{2}(Y-Y^*)^2+\frac{\delta_3}{2}(Z-Z^*)^2+\frac{\delta_4}{2}(T-T^*)^2+\frac{\delta_5}{2}(V-V^*)^2+\frac{\delta_6}{2}(P-P^*)^2. \tag{3.24}$$

where:

$$\delta_i > 0, \qquad i = 1, 2, \ldots, 6$$

are positive constants.

The derivative of the Lyapunov function along the solutions of the system is given by:

$$\frac{dV}{dt} \leq 0. \tag{3.25}$$

Therefore, according to Lyapunov's stability theorem, the equilibrium point is globally asymptotically stable when the derivative of the Lyapunov function is negative semi-definite and the only invariant set satisfying

$$\frac{dV}{dt} = 0$$

is the equilibrium point. The Lyapunov stability condition demonstrates that the proposed function decreases along the trajectories of the system. Since

$$\dot{V} \leq 0,$$

the distance between the system solution and the equilibrium point does not increase with time. This indicates that the system energy or deviation from the equilibrium state continuously decreases, allowing the solution to converge towards the equilibrium point (Odhiambo, 2023).

Therefore, according to Lyapunov's stability theorem, the equilibrium point is globally asymptotically stable when the Lyapunov function is positive definite and its derivative is negative semi-definite. Biologically, this implies that the wastewater microbial system will eventually return to the stable equilibrium state after small or large disturbances in bacterial or bacteriophage populations.

**Sensitivity Analysis**

Sensitivity analysis was conducted to determine the influence of model parameters on antibiotic-resistant *E. coli* dynamics. Understanding parameter importance is essential because wastewater microbial systems contain uncertainties associated with environmental conditions and biological processes.

The study employed Latin Hypercube Sampling (LHS) combined with Partial Rank Correlation Coefficient (PRCC) analysis.

A total of [insert actual number] Latin Hypercube samples were generated to explore the uncertainty space of the model parameters. The sampled parameter sets were analysed using PRCC to determine the influence of each parameter on the antibiotic-resistant *E. coli* concentration represented by $T(t)$. The sensitivity coefficient was calculated to identify parameters that contribute significantly to variation in the predicted bacterial concentration.

Parameters with high positive PRCC values indicate parameters that increase antibiotic-resistant *E. coli* concentration, while negative PRCC values indicate parameters that contribute to bacterial reduction. The sensitivity analysis was performed using Latin Hypercube Sampling (LHS) to generate a representative sample of the model parameter space. The sampled parameters were subsequently analysed using Partial Rank Correlation Coefficient (PRCC) to determine the strength and direction of their influence on the model output.

The analysis considered the uncertainty associated with the biological parameters governing bacterial growth, removal, transfer, and bacteriophage interaction. The concentration of antibiotic-resistant *E. coli*, represented by the state variable $T(t)$, was selected as the primary output variable because it represents the main public health concern investigated in this study.

The PRCC values were calculated to identify parameters with the greatest contribution to the uncertainty of resistant bacterial dynamics. Parameters with large absolute PRCC values were considered the most influential, while parameters with values close to zero indicated limited influence on the model output. The sensitivity results provide biological insight into the mechanisms controlling antibiotic-resistant *E. coli* persistence within the wastewater treatment system.

Parameters associated with bacterial recruitment, growth, transfer between treatment stages, and removal processes strongly influence the resistant bacterial population because they directly affect the rate at which bacteria enter, survive, and leave the treatment system.

A positive PRCC value indicates that an increase in the parameter value results in an increase in antibiotic-resistant *E. coli* concentration, whereas a negative PRCC value indicates that increasing the parameter reduces the resistant bacterial population.

Therefore, highly sensitive parameters represent potential targets for management and intervention strategies because small changes in these parameters can produce significant changes in resistant bacterial dynamics. This information supports the development of the optimal control framework presented in Model C.

### 3.2.10 Model A Numerical Simulation

Numerical simulations were performed to investigate the behaviour of the deterministic model under different parameter conditions.

The system of ordinary differential equations was solved numerically using MATLAB. The solver [ode45 ] was used to obtain the numerical solutions of the system. The parameter values and initial conditions were maintained within the biologically feasible region, and the resulting trajectories of $W(t), X(t), Y(t), Z(t), T(t), V(t)$, and $P(t)$ were analysed graphically.. The simulations were used to illustrate bacterial growth patterns, bacteriophage interactions, treatment effects, and persistence of antibiotic-resistant *E. coli* populations.

The numerical results were presented graphically to demonstrate the influence of model parameters on bacterial dynamics and to support the analytical results obtained from stability and sensitivity analyses. The numerical simulations of Model A were implemented using MATLAB and Mathematica. The parameter values used in the simulations were obtained from the parameter values specified in the model formulation and the corresponding secondary literature sources. The initial conditions were selected within the biologically feasible region.

The system of ordinary differential equations was then solved numerically over the specified simulation interval, and the resulting trajectories of $W(t), X(t), Y(t), Z(t), T(t), V(t)$, and $P(t)$ were examined graphically. The same parameter definitions and initial conditions were maintained throughout the numerical experiments to ensure consistency between the analytical and numerical analyses.

## 3.3 Caputo–Fabrizio Fractional Model B

### 3.3.1 Model Formulation

Although the deterministic model provides important information about the dynamics of antibiotic-resistant *E. coli* in wastewater systems, classical integer-order models assume that the present state of the system depends only on current conditions. However, biological wastewater systems may exhibit memory effects due to previous nutrient availability, antibiotic exposure, bacterial adaptation, and environmental changes.

To incorporate these historical effects, Model B extends the deterministic Model A

by introducing the Caputo–Fabrizio fractional derivative. Fractional-order modelling provides additional flexibility by allowing the system dynamics to depend on both current and previous states (Dokuyucu & Dutta, 2020).

The fractional model maintains the same biological compartments as Model A:

$$(W(t), X(t), Y(t), Z(t), T(t), V(t), P(t)).$$

The only modification is the replacement of the classical first-order derivative with the Caputo–Fabrizio fractional operator of order

$$0 < \alpha \leq 1.$$

When

$$\alpha = 1,$$

the fractional model reduces to the deterministic Model A.

### 3.3.2 Caputo–Fabrizio Model B Assumptions

The Caputo–Fabrizio fractional model is based on the following assumptions:

1. The biological compartments considered in the deterministic Model A remain unchanged in the fractional extension. The fractional model only modifies the time derivative to incorporate memory effects.

2. The growth of *E. coli* populations remains dependent on nutrient availability and follows the Monod growth function.

3. Antibiotic-resistant *E. coli* is represented separately through the compartment $T(t)$ because resistant populations may exhibit different persistence characteristics compared with susceptible populations.

4. The wastewater treatment compartments are considered well mixed, and spatial variation of bacterial concentration is not explicitly included.

5. The influence of previous environmental conditions, treatment processes, and bacterial adaptation is represented through the fractional order parameter $\alpha$.

6. The Caputo–Fabrizio fractional derivative provides a fading memory effect through its non-singular exponential kernel.

7. Bacteriophage activity remains significant mainly in the pre-primary and primary treatment stages.

8. All biological populations remain non-negative under non-negative initial conditions.

9. The fractional order satisfies:

$$0 < \alpha \leq 1$$

where $\alpha = 1$ corresponds to the classical deterministic model.

### 3.3.3 Caputo–Fabrizio Fractional Derivative

The Caputo–Fabrizio fractional model (Model B) is formulated as an extension of the deterministic Model A rather than as an independent model. The same seven state variables,

$$(W(t), X(t), Y(t), Z(t), T(t), V(t), P(t)),$$

and the same biological parameters are retained from Model A. The only modification is the replacement of the classical first-order derivatives with Caputo–Fabrizio fractional derivatives of order $\alpha$. This extension allows the model to incorporate memory effects associated with biological and environmental processes while maintaining the original biological structure of the wastewater treatment system (Dokuyucu & Dutta, 2020).
The Caputo–Fabrizio fractional derivative was introduced to overcome some limitations associated with traditional fractional operators that contain singular kernels. The operator uses a non-singular exponential kernel, allowing memory effects to decay smoothly over time(Ahmed, Akgül, Jarad, Kumam, & Nonlaopon, 2023). he fractional order parameter $\alpha$ represents the degree of memory within the system and satisfies

$$0 < \alpha \leq 1. \tag{3.26}$$

When $\alpha = 1$, the fractional derivative reduces to the classical integer-order derivative, and Model B becomes equivalent to the deterministic Model A (Ahmed et al., 2023).
When $0 < \alpha < 1$, the model incorporates memory effects, indicating that previous states of the microbial population influence current system behaviour. Therefore, varying $\alpha$ allows investigation of how historical environmental conditions affect antibiotic-resistant *E. coli* dynamics. For a differentiable function $f(t)$, the Caputo–Fabrizio derivative of order $0 < \alpha < 1$ is defined as:

$${}^{CF}D_t^{\alpha} f(t) = \frac{M(\alpha)}{1-\alpha} \int_0^t f'(\tau) \exp\left(-\frac{\alpha}{1-\alpha}(t-\tau)\right) d\tau, \tag{3.27}$$

where:

- $\alpha$ is the fractional order,
- $M(\alpha)$ is the normalization function satisfying

$$M(0) = M(1) = 1,$$

- the exponential kernel represents the fading memory effect(ur Rahman *et al* (2021)) ,Ali *et al.* ((2020)).

The non-singular kernel provides a smooth representation of biological memory(Ahmed et al., 2023). This property makes the Caputo–Fabrizio derivative suitable for wastewater microbial systems where previous environmental conditions influence present bacterial behaviour.(Ahmed et al., 2023). The Caputo–Fabrizio fractional derivative of order $0 < \alpha < 1$ is defined as

$$^{CF}D_t^{\alpha} f(t) = \frac{M(\alpha)}{1-\alpha} \int_0^t f'(\tau) \exp\left(-\frac{\alpha(t-\tau)}{1-\alpha}\right) d\tau, \tag{3.28}$$

where $M(\alpha)$ is a normalization function satisfying $M(0) = M(1) = 1$. Unlike classical fractional operators with singular kernels, the Caputo–Fabrizio derivative employs a non-singular exponential kernel that represents fading memory effects Ali *et al.* (2020).

The non-singular kernel is advantageous for biological systems because environmental and microbial processes often exhibit memory behaviour without requiring infinite weighting of past states. In wastewater treatment systems, previous microbial conditions, environmental exposure, and treatment history may influence current bacterial dynamics. Therefore, the Caputo–Fabrizio operator provides an appropriate mathematical framework for describing the memory-dependent behaviour of resistant *E. coli*.

$$\begin{aligned}
^{CF}W_t^q &= \left(\pi_1 + \pi_2 - \mu_1 W - \mu_2 W - \beta_1 WV + \frac{\pi_m WS}{K_2 + S} - \gamma_1 W\right)\left(1 - \frac{N}{A}\right), \\
^{CF}X_t^q &= \left(\gamma_1 W + \pi_1 - \mu_1 X - \mu_2 X - \omega_1 XP + \frac{\pi_m XS}{K_2 + S} - \gamma_2 X\right)\left(1 - \frac{N}{A}\right), \\
^{CF}Y_t^q &= \left(\gamma_2 X + \pi_1 - \mu_1 Y + \frac{\pi_m YS}{K_2 + S} - \gamma_3 Y\right)\left(1 - \frac{N}{A}\right), \\
^{CF}Z_t^q &= \left(\gamma_3 Y + \pi_1 + \pi_4 - \mu_1 Z + \frac{\pi_m ZS}{K_2 + S} - \gamma_4 Z\right)\left(1 - \frac{N}{A}\right), \\
^{CF}T_t^q &= \left(\gamma_4 Z(1-\Omega) - \mu_1 T + \frac{\pi_m TS}{K_2 + S} - \Phi T\right)\left(1 - \frac{N}{A}\right), \\
^{CF}V_t^q &= \left(\beta_2 WV + \pi_3 - \mu_1 V + \frac{\pi_m VS}{K_2 + S} - \Lambda V\right)\left(1 - \frac{B}{A}\right), \\
^{CF}P_t^q &= \left(\Lambda V + \omega_2 XP - \mu_1 P + \frac{\pi_m PS}{K_2 + S}\right)\left(1 - \frac{B}{A}\right).
\end{aligned} \tag{3.29}$$

### 3.3.4 Existence and Uniqueness Analysis

The existence and uniqueness of solutions for the Caputo–Fabrizio fractional system were investigated using fixed point theory (ur Rahman *et al* (2021)).

The fractional model can be represented in integral form as:

$$X(t) = X(0) + \frac{1-\alpha}{M(\alpha)}F(X,t) + \frac{\alpha}{M(\alpha)}\int_0^t F(X,\tau)d\tau. \tag{3.30}$$

A suitable operator is defined and analysed using Banach's fixed point theorem.

If the operator satisfies the contraction condition, then the fractional system has a unique solution (Ahmed et al., 2023).

The existence and uniqueness analysis ensures that the proposed fractional model is mathematically well-defined and suitable for numerical investigation (ur Rahman *et al* (2021)),(Edessa, 2022).

### 3.3.5 Numerical Simulation of Model B

Numerical simulations were conducted to investigate the influence of fractional order $\alpha$ on antibiotic-resistant *E. coli* dynamics.

The simulations were performed using MATLAB with appropriate numerical methods for fractional differential equations. Different fractional orders were evaluated to determine how memory effects influence bacterial persistence and treatment outcomes.

The results were compared with the deterministic model to demonstrate the effect of introducing memory into the wastewater bacterial dynamics.

The fractional simulations provide insight into how historical environmental conditions may influence future bacterial behaviour.

The numerical simulations of Model B were implemented in MATLAB using the specified parameter values and initial conditions adopted from Model A and the corresponding secondary literature sources. Different fractional orders $0 < \alpha \leq 1$ were considered to examine the influence of memory effects on the model dynamics. The resulting trajectories were compared across fractional orders to determine how the incorporation of memory modifies the behaviour of antibiotic-resistant *E. coli*. The numerical procedure was applied consistently to the seven state variables of the fractional model.

## 3.4 Optimal Control Model C

### 3.4.1 Controlled Model Formulation

The deterministic Model A describes the dynamics of antibiotic-resistant *E. coli* populations and bacteriophage interactions within wastewater treatment systems. However,

prediction of bacterial behaviour alone does not provide information on the most effective intervention strategies.

Therefore, Model C extends the deterministic framework by incorporating optimal control theory. The purpose of the optimal control model is to determine intervention strategies that minimise antibiotic-resistant *E. coli* concentration while considering the cost associated with implementing control measures.

The controlled system maintains the same biological compartments:

$$(W(t), X(t), Y(t), Z(t), T(t), V(t), P(t)).$$

The control vector is defined as:

$$U(t) = (u_1(t), u_2(t), u_3(t), u_4(t)). \tag{3.1}$$

where each control variable represents an intervention strategy applied over the time interval $[0, t_f]$. The control variables represent biological intervention strategies introduced to reduce antibiotic-resistant *E. coli* concentrations within the wastewater treatment system.

The control $u_1(t)$ represents the effort associated with bacteriophage application for biological reduction of bacterial populations.

The control $u_2(t)$ represents treatment intervention, such as enhanced wastewater disinfection processes, aimed at increasing bacterial removal.

The control $u_3(t)$ represents intervention affecting bacterial recruitment and exposure pathways, thereby reducing the introduction and persistence of bacterial populations.

The control $u_4(t)$ represents environmental management strategies that modify conditions influencing bacterial growth.

These controls allow the model to evaluate how different intervention strategies influence the long-term behaviour of antibiotic-resistant *E. coli* populations.

### 3.4.2 Optimal Control Model C Assumptions

The optimal control model is formulated under the following assumptions:

1. The biological interactions described in the deterministic model remain valid after introducing intervention strategies.

2. The antibiotic-resistant *E. coli* population is represented by the compartment $T(t)$ and remains affected by bacterial growth, treatment, and environmental conditions.

3. Control variables are measurable time-dependent functions representing realistic intervention strategies.

4. Each intervention has a bounded effect and satisfies the admissible control condition:

$$0 \leq u_i(t) \leq 1, \qquad i = 1, 2, 3, 4.$$

5. The implementation cost of each intervention increases with increasing control effort.

6. The objective of the control strategy is to reduce bacterial concentration while avoiding excessive intervention costs.

7. The wastewater treatment system remains biologically feasible under the applied interventions.

### 3.4.3 Optimal Control Variables

The four control variables incorporated into Model C are defined as follows:

1. $u_1(t)$ represents bacteriophage-based biological control aimed at reducing *E. coli* populations through predator-prey interaction.

2. $u_2(t)$ represents wastewater treatment intervention, including enhanced disinfection processes aimed at increasing bacterial removal.

3. $u_3(t)$ represents environmental management intervention aimed at reducing external recruitment of *E. coli* into the wastewater treatment system.

4. $u_4(t)$ represents an ecological intervention aimed at reducing bacterial growth by modifying environmental conditions influencing microbial productivity.

The admissible control set is therefore defined as:

$$\mathcal{U} = \{(u_1, u_2, u_3, u_4) : 0 \leq u_i(t) \leq 1, i = 1, 2, 3, 4\}. \tag{3.31}$$

### 3.4.4 Controlled Model Equations

After incorporating the four control variables into the deterministic framework, the optimal control Model C is formulated as follows:

$$
\begin{aligned}
\frac{dW}{dt} &= \left(u_3\pi_1 + (1-u_1)\pi_2 - \mu_1 W - \mu_2 W - \beta_1 WV + u_3u_4\frac{\pi_m WS}{K_2+S} - \gamma_1 W\right)\left(1-\frac{W}{A}\right),\\
\frac{dX}{dt} &= \left((1-u_1)\gamma_1 W + u_3\pi_1 - \mu_1 X - \mu_2 X - \omega_1 XP + u_3u_4\frac{\pi_m XS}{K_2+S} - \gamma_2 X\right)\left(1-\frac{X}{B}\right),\\
\frac{dY}{dt} &= \left(\gamma_2 X + u_3\pi_1 - \mu_1 Y + u_3u_4\frac{\pi_m YS}{K_2+S} - \gamma_3 Y\right)\left(1-\frac{Y}{C}\right),\\
\frac{dZ}{dt} &= \left((1-u_2)\gamma_3 Y + u_3\pi_1 - \mu_1 Z + u_3u_4\frac{\pi_m ZS}{K_2+S} - \gamma_4 Z\right)\left(1-\frac{Z}{D}\right),\\
\frac{dS}{dt} &= \left(\gamma_4 Z(1-\Omega) - \mu_1 S + u_3u_4\frac{\pi_m S_S}{K_2+S} - \Phi_S\right)\left(1-\frac{S}{E}\right),\\
\frac{dV}{dt} &= \left(\beta_2 WV + (1-u_1)\pi_3 - \mu_1 V + u_3u_4\frac{\pi_m V_S}{K_2+S} - (1-u_1)\Lambda_V\right)\left(1-\frac{V}{A}\right),\\
\frac{dP}{dt} &= \left((1-u_1)\Lambda_V + \omega_2 XP - \mu_1 P + u_3u_4\frac{\pi_m PS}{K_2+S}\right)\left(1-\frac{P}{B}\right)
\end{aligned}
\tag{3.32}
$$

Where

$$0 \le u_1 < 1, 0 \le u_2 < 1, 0 \le u_3 < 1, 0 \le u_4 < 1, \tag{3.33}$$

To study optimal control levels,the control set U lesbegue measurable and will be defined as $U = u_1(t), u_2(t), u_3(t), u_4(t)$.

### 3.4.5 Objective Functional

The objective functional was formulated to determine the optimal intervention strategy that minimizes the concentration of antibiotic-resistant *E. coli* while controlling the cost associated with implementing the interventions.

The functional consists of two components:

1. The bacterial burden associated with the presence of antibiotic-resistant *E. coli*.
2. The cost associated with applying the control measures.

Therefore, the objective functional is defined as:

$$J(U) = \int_0^{t_f} \left[A_1 W + A_2 X + A_3 Y + A_4 Z + A_5 T + \frac{1}{2}\left(B_1 u_1^2 + B_2 u_2^2 + B_3 u_3^2 + B_4 u_4^2\right)\right] dt. \tag{3.34}$$

where:

- $A_1, A_2, A_3, A_4, A_5$ are weighting constants representing the importance of reducing bacterial populations.

- $B_1, B_2, B_3, B_4$ are weighting constants representing the economic and operational costs of applying each intervention.
- $t_f$ represents the final simulation time.

The optimal control problem is therefore expressed as:

$$J(U^*) = \min_{U \in \mathcal{U}} J(U). \tag{3.35}$$

The objective functional represents a balance between reducing the concentration of antibiotic-resistant *E. coli* and minimizing the economic or operational cost associated with intervention implementation.

The first component of the functional penalizes high bacterial concentrations, ensuring that the optimal strategy aims to reduce microbial contamination. The second component represents the cost associated with applying control measures. Therefore, the optimization problem seeks control strategies that achieve maximum bacterial reduction while maintaining realistic intervention efforts.

### 3.4.6 Hamiltonian Formulation

According to Pontryagin's Maximum Principle, the optimal control problem can be converted into a Hamiltonian system.

The Hamiltonian function combines the objective functional with the controlled state equations.

The Hamiltonian is defined as:

$$H = L(X, U) + \lambda_1 \frac{dW}{dt} + \lambda_2 \frac{dX}{dt} + \lambda_3 \frac{dY}{dt} + \lambda_4 \frac{dZ}{dt} + \lambda_5 \frac{dT}{dt} + \lambda_6 \frac{dV}{dt} + \lambda_7 \frac{dP}{dt}, \tag{3.36}$$

where:

$$\lambda_i(t), \quad i = 1, 2, \ldots, 7$$

are the adjoint variables associated with the state variables.

The term:

$$L(X, U)$$

represents the integrand of the objective functional. Before constructing the Hamiltonian, the state variables are represented by

$$X(t) = (W(t), X(t), Y(t), Z(t), T(t), V(t), P(t)),$$

while the corresponding adjoint variables are represented by

$$\lambda(t) = (\lambda_1, \lambda_2, \lambda_3, \lambda_4, \lambda_5, \lambda_6, \lambda_7).$$

The control vector is defined as

$$u(t) = (u_1(t), u_2(t), u_3(t), u_4(t)).$$

The Hamiltonian combines the objective functional and the model dynamics to derive the necessary optimality conditions. According to Pontryagin's Maximum Principle, the adjoint variables satisfy the costate equations obtained by differentiating the Hamiltonian with respect to the state variables:

$$\frac{d\lambda_i}{dt} = -\frac{\partial H}{\partial x_i}, \tag{3.37}$$

where $x_i$ represents each state variable of the system.

These equations describe the sensitivity of the objective functional to changes in the state variables and are solved together with the state equations to determine the optimal control strategy.

**Optimality Conditions**

The admissible control set is defined by the bounded measurable controls satisfying

$$U = \{u(t) = (u_1(t), u_2(t), u_3(t), u_4(t)) : 0 \leq u_i(t) \leq 1, \quad i = 1, 2, 3, 4\}.$$

The lower bound $u_i(t) = 0$ represents the absence of the corresponding intervention, whereas $u_i(t) = 1$ represents the maximum feasible application of that intervention. These bounds ensure that the control variables remain within biologically and operationally meaningful limits throughout the treatment period.

### 3.4.7 Adjoint Equations

The adjoint equations were obtained by differentiating the Hamiltonian with respect to the state variables according to Pontryagin's Maximum Principle.

The adjoint system is defined as:

$$\frac{d\lambda_i}{dt} = -\frac{\partial H}{\partial x_i}, \qquad i = 1, 2, \ldots, 7. \tag{3.38}$$

Therefore:

$$\frac{d\lambda_1}{dt} = -\frac{\partial H}{\partial W},$$

$$\frac{d\lambda_2}{dt} = -\frac{\partial H}{\partial X},$$

$$\frac{d\lambda_3}{dt} = -\frac{\partial H}{\partial Y},$$

$$\frac{d\lambda_4}{dt} = -\frac{\partial H}{\partial Z},$$

$$\frac{d\lambda_5}{dt} = -\frac{\partial H}{\partial T},$$

$$\frac{d\lambda_6}{dt} = -\frac{\partial H}{\partial V},$$

$$\frac{d\lambda_7}{dt} = -\frac{\partial H}{\partial P}.$$

The terminal conditions are given by:

$$\lambda_i(t_f) = 0, \qquad i = 1, 2, \ldots, 7. \tag{3.2}$$

subsectionPontryagin Maximum Principle Conditions

The necessary conditions for optimality were obtained using Pontryagin's Maximum Principle. The principle converts the optimal control problem into a system consisting of state equations, adjoint equations, and optimality conditions.

For the optimal control:

$$U^*(t) = (u_1^*(t), u_2^*(t), u_3^*(t), u_4^*(t)),$$

the following conditions must be satisfied:

$$\frac{dX}{dt} = \frac{\partial H}{\partial \lambda}, \tag{3.39}$$

$$\frac{d\lambda}{dt} = -\frac{\partial H}{\partial X}, \tag{3.3}$$

and

$$H(X^*, U^*, \lambda^*) = \min_{U \in \mathcal{U}} H(X, U, \lambda). \tag{3.4}$$

The optimal control variables are obtained by solving:

$$\frac{\partial H}{\partial u_i} = 0, \qquad i = 1, 2, 3, 4. \tag{3.5}$$

Therefore, the characterization of the optimal controls is given by:

$$u_i^* = \min\left(1, \max\left(0, \hat{u_i}\right)\right), \qquad i = 1, 2, 3, 4, \tag{3.39}$$

where $\hat{u_i}$ represents the unconstrained optimal control obtained from the Hamiltonian minimization condition.

The projection ensures that all control variables remain within the admissible control set:

$$0 \leq u_i^*(t) \leq 1. \tag{3.40}$$

### 3.4.8 Existence of Optimal Controls

The existence of optimal controls is guaranteed when the admissible control set is closed and bounded, the state equations satisfy the Lipschitz continuity condition, and the objective functional is convex with respect to the control variables ( Seidu *et al.*(2014)).

The admissible control space is defined as:

$$\mathcal{U} = \{U(t) : 0 \leq u_i(t) \leq 1,\ i = 1, 2, 3, 4\}. \tag{3.41}$$

Since the control functions are bounded and the objective functional contains quadratic control costs, the optimal control problem satisfies the required conditions for the existence of an optimal solution( Seidu *et al.*(2014)).

### 3.4.9 Numerical Solution of the Optimal Control System

The optimal control system consists of the state equations, adjoint equations, and optimality conditions. Due to the nonlinear nature of the system, analytical solutions are difficult to obtain. Therefore, numerical optimization techniques were applied.

The forward-backward sweep method was used to solve the optimal control problem. ur Rahman *et al* ((2021))This approach combines numerical integration of the state and adjoint equations with iterative updating of the control variables( Seidu *et al.*(2014)).

The computational procedure involved the following steps:

1. Initial control functions $u_1, u_2, u_3, u_4$ were selected within the admissible control region.

2. The state equations were solved forward in time using the selected initial control functions.

3. The adjoint equations were solved backward in time using the terminal conditions:

$$\lambda_i(t_f) = 0, \qquad i = 1, 2, \ldots, 7. \tag{3.42}$$

4. The Hamiltonian minimization condition was applied to update the control functions.

5. The updated controls were substituted into the state equations and the process was repeated until convergence was achieved.( Seidu *et al.*(2014))

The forward-backward sweep algorithm provides the optimal intervention strategy that minimises antibiotic-resistant *E. coli* concentration while balancing the associated intervention cost ur Rahman *et al* ((2021)).

### 3.4.10 Numerical Simulation of Model C

Numerical simulations of the optimal control model were performed using MATLAB.

The simulations were conducted to evaluate the effectiveness of different control strategies in reducing antibiotic-resistant *E. coli* concentrations.

The results were presented using graphical comparisons between:

- uncontrolled bacterial dynamics,
- controlled bacterial dynamics,
- individual control strategies,
- combined optimal intervention strategies.

The numerical results provide insight into the most effective intervention combinations for managing antibiotic-resistant *E. coli* persistence in wastewater treatment systems. The optimal control simulations were implemented in MATLAB using the parameter values and initial conditions specified for the proposed model. The controlled state system and corresponding adjoint system were solved iteratively using a forward–backward sweep procedure. The state equations were solved forward in time, while the adjoint equations were solved backward from the terminal conditions. The control variables were subsequently updated subject to the bounds $0 \leq u_i(t) \leq 1$, and the process was repeated until convergence of the state, adjoint, and control variables was achieved.

## 3.5 Chapter Summary

This chapter developed three interconnected mathematical frameworks for analysing antibiotic-resistant *E. coli* dynamics in wastewater treatment systems. Model A established the deterministic foundation by describing bacterial growth, transfer, bacteriophage interaction, resistance persistence, and treatment removal processes. Model B extended the deterministic framework by incorporating Caputo–Fabrizio fractional dynamics to represent biological memory effects associated with previous environmental conditions. Model C further extended the framework through optimal control theory to determine intervention strategies that reduce antibiotic-resistant *E. coli* while considering intervention costs.

Together, the three models provide a comprehensive methodology for understanding, predicting, and controlling antibiotic-resistant bacterial dynamics in wastewater systems. Model A explains the fundamental population behaviour, Model B captures memory-dependent biological processes, and Model C identifies effective control strategies. These frameworks provide the foundation for the numerical results and discussions presented in the following chapter.

# Chapter 4

# RESULTS AND DISCUSSIONS

## 4.1 Introduction

This chapter presents the analytical and numerical results obtained from the three mathematical models developed in Chapter Three. The results are organized according to the specific objectives of the study. First, the deterministic Model A is analysed through positivity, boundedness, equilibrium points, local and global stability, sensitivity analysis, and numerical simulations. Secondly, the Caputo–Fabrizio fractional Model B is investigated to determine the influence of memory effects on the dynamics of Escherichia coli and bacteriophage populations. Finally, the optimal control Model C is analysed using Pontryagin's Maximum Principle and numerical simulations to evaluate the effectiveness of the proposed control strategies.

The chapter is divided into three main sections:

1. Analysis of deterministic Model A.
2. Analysis of Caputo–Fabrizio fractional derivative Model B.
3. Analysis of optimal control Model C.

## 4.2 Analysis of Deterministic Model A

This section presents the results obtained from Deterministic Model A. The analysis is organized into three main components: model formulation, mathematical analysis, and numerical simulation. The mathematical analysis establishes the fundamental properties of the model, including positivity, boundedness, equilibrium behaviour, and stability. Numerical simulations are subsequently used to demonstrate the temporal dynamics of bacterial and bacteriophage populations within the wastewater treatment system.

### 4.2.1 Model A formulation

Before numerical simulation, all microbial concentration parameters were standardized to consistent units. Since wastewater microbiological measurements are reported using different volume standards in the literature, bacterial and bacteriophage concentrations were converted into comparable concentration units to ensure consistency during computational implementation. The parameter values used in the numerical simulations were obtained from previous experimental and mathematical modelling studies where available. Parameters without direct experimental estimates were assigned values based on biologically reasonable assumptions and calibrated to maintain consistency with reported wastewater microbial dynamics.

Table 4.1: Parameters

| **Parameter** | **Description** | **Value** | **Reference** |
|---|---|---|---|
| $\pi_1$ | Represent the recruitment rate of *E. coli* into the treatment plant by storm waters. | 0.32 and 0.35 CFU 100 $mL^{-1}$ | (McCarthy, 2009) |
| $\pi_2$ | Represent the recruitment rate of *E. coli* into the treatment plant. | 5.60–7.11 $\times 10^6$ CFU 100 $mL^{-1}$ | (Raboni, Gavasci, & Torretta, 2016) |
| $\pi_3$ | Represent the bacteriophage recruitment rate into the treatment plant. | Four generations in 6 hours; 1–10 log CFU $L^{-1}$ | (Perulli et al., 2026) |
| $\pi_m$ | Represent the Monod growth rate. | $\mu_{\max} = 1.35$ and $K_s = 0.22 \times 10$ | stimated |
| $\pi_4$ | Represent the recruitment rate of treatment in the plant. | 0.8 CFU 100 $mL^{-1}$ | Estimated |
| $\mu_1$ | Represent the natural death rate of *E. coli* and bacteriophages. | $[3.876 \times 10^{-3},\ 5.382 \times 10^{-4}]$ CFU 100 $mL^{-1}$ | (Demko, Chrást, Dvořák, Damborskỳ, & Šafránek, 2019) |
| $\mu_2$ | Representative induced death rate due to algae. | 0.404 CFU 100 $mL^{-1}$ | Estimated |
| $\beta_1$ | Represent the bacteriophage-induced death rate during the pre-primary stage. | 0.087273 $min^{-1}$; 5.23638 $hour^{-1}$ | (H. Yang et al., 2004) |

| Parameter | Description | Value | Reference |
|---|---|---|---|
| $\beta_2$ | Represent the bacteriophage-induced growth rate in the pre-primary stage. | 0.044930 $min^{-1}$; 2.958 $hour^{-1}$ | (H. Yang et al., 2004) |
| $\omega_1$ | Represent the bacteriophage-induced death rate in the pre-primary stage. | 0.03 CFU 100 $mL^{-1}$ | Estimated |
| $\omega_2$ | Represent bacteriophage predation, induced growth rate in the primary stage. | 0.18 CFU 100 $mL^{-1}$ | Estimated |
| $\gamma_1$ | Represent the *E. coli* recruitment rate in the pre-primary stage. | 6.2 to 9 log 10 CFU 100 $mL^{-1}$ | (Le et al., 2023) |
| $\gamma_2$ | Represent the *E. coli* recruitment rate in the primary stage. | 13 CFU/100 mL | Estimated |
| $\gamma_3$ | Represent the *E. coli* recruitment rate in the secondary stage. | 14 CFU/100 mL | Estimated |
| $\gamma_4$ | Represent the *E. coli* treatment rate in the tertiary stage. | $1.74 \times 10^6$ to 685 MPN 100 $mL^{-1}$, 3.41 log units | (Hernández-Crespo, Fernández-Gonzalvo, Miglio, & Martín, 2022) |
| $\Phi$ | Represent *E. coli* effluent rate. | 0.91–2.60 $\times 10^3$ CFU 100 $mL^{-1}$ | (Raboni et al., 2016) |
| $\Lambda$ | Represent the bacteriophage recruitment rate in the primary stage. | Four generations in 6 hours; 0.04 | (Kigigha, Izah, & Kpea, 2015) |
| $\Omega$ | The representative induced death rate due to treatment. | $[3.876 \times 10^{-3},\ 5.382 \times 10^{-4}]$ CFU 100 $mL^{-1}$ | Estimated |

### 4.2.2 Model analysis methods

The model A was described by a system of seven ordinary differential equations denoted as (3.1). The above model A equations were qualitatively analyzed by determining feasible region of the model,Equilibrium points and stability.Resulting to subsections denoted as ;feasible region of the model,Equilibrium points and stability The total bacterial population within the wastewater treatment system is defined as

$$N(t) = W(t) + X(t) + Y(t) + Z(t) + T(t),$$

where $N(t)$ represents the total *E. coli* population consisting of both susceptible and antibiotic-resistant populations. The parameter $A$ represents the carrying capacity of the bacterial population within the wastewater treatment environment.

## 4.2.2.1 Feasible region of the model

The feasibility of the proposed deterministic Model A is established by demonstrating the positivity and boundedness of its solutions. Positivity ensures that the bacterial and bacteriophage populations remain biologically meaningful since microbial concentrations cannot assume negative values. Boundedness confirms that the model solutions remain restricted within biologically realistic limits and do not exhibit unlimited growth. These properties guarantee that the feasible region of the system is positively invariant and that the mathematical model remains biologically consistent for all $t \geq 0$.

1. **Positivity nature of the solution**

   This study model concerns the *E. coli* and bacteriophage populations; hence, it is essential to demonstrate that all its state variables are non-negative at all times (Prakasha & Veeresha, 2020) .

   **Theorem 1 (Positivity of solutions)**

   Let

$$R = \{W(t), X(t), Y(t), Z(t), T(t), V(t), P(t)\} \in \mathbb{R}^7_+, \tag{4.1}$$

   with initial conditions

$$W(0), X(0), Y(0), Z(0), T(0), V(0), P(0) \geq 0. \tag{4.2}$$

   Then the solutions of the deterministic Model A remain non-negative for all $t \geq 0$. (Gurmu et al., 2020).

   **Proof.**

   The positivity of each state variable is demonstrated using the differential inequality method. It is sufficient to show that each variable remains non-negative whenever its initial value is non-negative.
   Using the differential inequality

$$\frac{dW}{dt} \geq -(\mu_1 + \mu_2 + \beta_1 V + \gamma_1)W, \tag{4.3}$$

and applying separation of variables gives

$$\frac{dW}{W} \geq -(\mu_1 + \mu_2 + \beta_1 V + \gamma_1)dt. \tag{4.4}$$

Integrating both sides from 0 to $t$,

$$W(t) \geq W(0) \exp\left(-\int_0^t (\mu_1 + \mu_2 + \beta_1 V(a) + \gamma_1)\, da\right). \tag{4.5}$$

Since $W(0) \geq 0$ and the exponential term is always positive,

$$W(t) \geq 0. \tag{4. 6}$$

Therefore, the pre-primary *E. coli* population remains non-negative for all $t \geq 0$..

Similarly, from others equations of system (3.1) and applying initial conditions at $t = 0$, and yielded the following.

$$X(t) \geq X(0) \exp\left(-\int_0^t (\mu_1 + \mu_2 + \omega_1 P(a) + \gamma_2)\, da\right) \geq 0 \tag{4.7}$$

Hence,

$$X(t) \geq 0 \tag{4.8}$$

$$Y(t) \geq Y(0) \exp\left(-\int_0^t (\mu_1 + \gamma_3)\, dt\right) \geq 0 \tag{4. 9}$$

Hence,

$$Y(t) \geq 0 \tag{4.10}$$

$$Z(t) \geq Z(0) \exp\left(-\int_0^t (\mu_1 + \mu_4)\left(1 - \frac{N}{A}\right)\, dt\right) \geq 0 \tag{4.11}$$

Hence,

$$Z(t) \geq 0 \tag{4.12}$$

$$T(t) \geq T(0) \exp\left(-\int_0^t (\mu_1 + \Phi)\, dt\right) \geq 0 \tag{4.13}$$

Hence,

$$T(t) \geq 0 \tag{4.14}$$

$$V(t) \geq V(0) \exp\left(-\int_0^t (\mu_1 + \Lambda)\left(1 - \frac{N}{A}\right)\, dt\right) \geq 0 \tag{4.15}$$

Hence,

$$V(t) \geq 0 \tag{4.16}$$

$$P(t) \geq P(0) \exp\left(-\int_0^t \mu_1 \, dt\right) \geq 0 \tag{4.17}$$

Hence,

$$P(t) \geq 0$$

Therefore,

$$W(t), X(t), Y(t), Z(t), T(t), V(t), P(t) \geq 0, \tag{4.18}$$

Consequently, the solution of the deterministic Model A with non-negative initial conditions remains non-negative and exists within the feasible region for all $t \geq 0$. Therefore, $\mathbb{R}_+^7$ is an invariant domain of the system, confirming that the proposed model preserves biological realism (Prakasha & Veeresha, 2020).

## Boundedness of the solution

The boundedness of solutions ensures that the bacterial and bacteriophage populations remain within biologically realistic limits for all time. This property is essential because microbial concentrations in wastewater treatment systems cannot increase indefinitely due to environmental limitations, treatment processes, and resource constraints. Therefore, establishing boundedness confirms that the proposed deterministic Model A remains mathematically valid and biologically meaningful.

Let the total bacterial population within the wastewater treatment system be defined as

$$N(t) = W(t) + X(t) + Y(t) + Z(t) + T(t),$$

where $W(t), X(t), Y(t), Z(t)$ represent the susceptible *E. coli* populations at different treatment stages, while $T(t)$ represents the antibiotic-resistant *E. coli* population. The parameter $A$ represents the carrying capacity of the bacterial population within the wastewater environment(Gurmu et al., 2020).

**Theorem 2 (Boundedness of solutions)**

Let the bacterial population and bacteriophage population be defined as

N(t)=W(t)+X(t)+Y(t)+Z(t)+T(t)

and

$$B(t) = V(t) + P(t).$$

If the initial conditions are non-negative, then the solutions of Model A remain bounded within the feasible region

$$0 \leq N(t) \leq A,$$

and

$$0 \leq B(t) \leq A,$$

for all $t \geq 0$.

**Proof**

N(t)=W(t)+X(t)+Y(t)+Z(t)+T(t) Differentiating $N(t)$ with respect to time gives

$$\frac{dN}{dt} = \frac{dW}{dt} + \frac{dX}{dt} + \frac{dY}{dt} + \frac{dZ}{dt} + \frac{dT}{dt}.$$

Substituting the corresponding equations from Model A and simplifying gives which is differentiated and simplified to,

$$\frac{dN}{dt} \leq \frac{\pi_m NS}{K_2 + S} + (\pi_2 + \pi_1 + \pi_4) - \mu_1 N \left(1 - \frac{N}{A}\right) \tag{4.19}$$

Further integration by the use of Mathematica resulted in,

$$A\left(\log[-A+N] - \log[-S(N+\pi_1+\pi_2+\pi_4)] - \pi_m + NS\mu_1 - K_2(\pi_1+\pi_2+\pi_4 - N\mu_1)\right)((S+K_2 \tag{4.20}$$

$$-\frac{\pi_m + K_2(\pi_1+\pi_2+\pi_4 - A\mu_1)}{S + (\pi_1+\pi_2+\pi_4 - A\mu_1)} = t + C$$

Applying the initial condition and simplifying gives

$$\frac{-A + N(t)}{-N(t)S - S\pi_1 - S\pi_2 - S\pi_4 - K_2\pi_1 - K_2\pi_2 - K_2\pi_4 - \pi_m + N(t)S\mu_1 + N(t)K_2\mu_1} \leq 0 \tag{4.21}$$

Therefore,

$$0 \leq N(t) \leq A,$$

which confirms that the total *E. coli* population remains bounded within the carrying capacity of the wastewater environment.

Similarly, letting $B(t) = V(t) + P(t)$, further differentiated and simplified, resulting in:

$$\frac{dB}{dt} = \left(\beta_2 WV + \omega_2 XP + \pi_3 - \mu_1 B + \frac{\pi_m BS}{K_2 + S}\right)\left(1 - \frac{B}{A}\right) \tag{4.22}$$

Further letting $\beta_2 WV + \omega_2 XP = \alpha B$, and applying initial conditions, it simplifies to:

Which at $\lim_{t\to\infty}$ becomes

$$\frac{-A + B(t)}{K_2\left(B(t)\alpha + \pi_3\right) + S\left(B(t)\alpha + \pi_3 + B(t)\pi_m\right)} \leq 0 \tag{4.23}$$

Then,

$$B(t) \leq A, \text{ hence proved.}$$

Similarly, the bacteriophage population remains bounded as

$$0 \leq B(t) \leq A,$$

indicating that phage dynamics remain constrained within biologically realistic limits.

### 4.2.2.2 Equilibrium points

The equilibrium points are defined as states where all model variables remain constant over time. They are obtained by simultaneously setting all differential equations equal to zero. The deterministic model produces five biologically relevant equilibrium points, representing different possible long-term configurations of the wastewater treatment system.

The five equilibrium points are defined as follows:

$$E^0 = \{0, 0, 0, 0, 0, 0, 0\},$$

representing complete extinction of both *E. coli* and bacteriophage populations.

$$E^1 = \{0, 0, 0, 0, 0, V^1, P^1\},$$

representing bacteriophage persistence in the absence of bacterial populations.

$$E^2 = \{W^2, X^2, Y^2, Z^2, T^2, 0, 0\},$$

representing bacterial persistence without bacteriophage interaction.

$$E^3 = \{W^3, X^3, Y^3, Z^3, 0, V^3, P^3\},$$

representing coexistence of susceptible *E. coli* and bacteriophage populations in the absence of antibiotic-resistant *E. coli*.

$$E^4 = \{W^4, X^4, Y^4, Z^4, T^4, V^4, P^4\},$$

representing the full coexistence equilibrium where susceptible *E. coli*, antibiotic-resistant *E. coli*, and bacteriophage populations persist simultaneously.

## Case 1: Extinction equilibrium

This equilibrium represents complete extinction of susceptible *E. coli*, antibiotic-resistant *E. coli*, and bacteriophage populations within the wastewater treatment system.

$$E^0 = \{W^0, X^0, Y^0, Z^0, T^0, V^0, P^0\} = \{0, 0, 0, 0, 0, 0, 0\} \tag{4.25}$$

## Case 2: Bacteriophage-only equilibrium

The equilibrium point where bacterial populations are absent and only bacteriophage populations persist is denoted as $E^1$.

$$V^1 = \frac{\pi_3}{\left(\mu_1 - \frac{\pi_m S}{K_2+S+\Lambda}\right)} \quad \text{and} \quad P^1 = \frac{\pi_3}{\left(\mu_1 - \frac{\pi_m S}{K_2+S+\Lambda}\right)}. \tag{4.26}$$

Obtaining a solution in the form

$$E^1 = \{0, 0, 0, 0, 0, V^1, P^1\} = \left\{0, 0, 0, 0, 0, \frac{\pi_3}{\left(\mu_1 - \frac{\pi_m S}{K_2+S+\Lambda}\right)}, \frac{\pi_3}{\left(\mu_1 - \frac{\pi_m S}{K_2+S+\Lambda}\right)}\right\}. \tag{4.27}$$

## Case 3: Bacterial persistence without bacteriophages

In this equilibrium scenario, bacteriophage populations are absent while susceptible and antibiotic-resistant *E. coli* populations persist within the wastewater treatment system. This equilibrium represents a condition where bacterial growth, nutrient availability, treatment processes, and antibiotic resistance dynamics continue without the influence of bacteriophage predation. Mathematically, this equilibrium is obtained by setting the bacteriophage compartments $V$ and $P$ equal to zero while maintaining positive values

for the bacterial compartments $W$, $X$, $Y$, $Z$, and $T$. The equilibrium point is therefore denoted by $E^2$, representing bacterial persistence in the absence of bacteriophage control.

The equilibrium conditions are obtained by setting

$$V = P = 0$$

and solving the remaining equations of Model A. The resulting equilibrium components are given by

$$\begin{aligned}
W^2 &= \frac{\pi_1 + \pi_2}{\left(\mu_1 + \mu_2 + \beta_1 \frac{\pi_m S}{K_2 + S + \gamma_1}\right)} \\
X^2 &= \frac{(\gamma_1 W^2 + \pi_1)}{\left(\mu_1 + \mu_2 - \frac{\pi_m S}{K_2 + S + \gamma_2}\right)} \\
Y^2 &= \frac{(\gamma_2 X^2 + \pi_1)}{\left(\mu_1 - \frac{\pi_m S}{K_2 + S + \gamma_3}\right)} \\
Z^2 &= \frac{(\gamma_3 Y^2 + \pi_1)}{\left(\mu_1 - \frac{\pi_m S}{K_2 + S + \gamma_4}\right)} \\
T^2 &= \frac{(\gamma_4 Z^2 (1 - \Omega))}{\left(\mu_1 + \frac{\pi_m S}{K_2 + S + \gamma_5}\right)}
\end{aligned} \tag{4.28}$$

Solution becomes

$$E^2 = \left\{W^2, X^2, Y^2, Z^2, T^2, 0, 0\right\} \tag{4.29}$$

# Case 4: Susceptible bacteria–bacteriophage coexistence equilibrium

When antibiotic resistance is absent, the equilibrium point is denoted as $E^3$. In this case, susceptible *E. coli* populations and bacteriophage populations coexist, while the antibiotic-resistant *E. coli* population is absent.

$$\begin{aligned}
W^3 &= \frac{\pi_1 + \pi_2}{\left(\mu_1 + \mu_2 + \beta_1 - \frac{\pi_m S}{K_2 + S + \gamma_1}\right)}, \quad X^3 = \frac{(\gamma_1 W^3 + \pi_1)}{\left(\mu_1 + \mu_2 - \frac{\pi_m S}{K_2 + S + \gamma_2}\right)}, \\
Y^3 &= \frac{(\gamma_2 X^3 + \pi_1)}{\left(\mu_1 - \frac{\pi_m S}{K_2 + S + \gamma_3}\right)}, \quad Z^3 = \frac{(\gamma_3 Y^3 + \pi_1)}{\left(\mu_1 - \frac{\pi_m S}{K_2 + S + \gamma_4}\right)}, \\
V^3 &= \frac{\pi_3}{\left(\beta_2 W^3 - \mu_1 + \frac{\pi_m S}{K_2 + S + \gamma_5}\right)}, \quad P^3 = \frac{\pi_3}{\left(\beta_2 W^3 - \mu_1 + \frac{\pi_m S}{K_2 + S + \gamma_6}\right)}.
\end{aligned} \tag{4.30}$$

Solution becomes

$$E^3 = \left\{ \begin{array}{l} \frac{\pi_1+\pi_2}{\mu_1+\mu_2+\beta_1-\frac{\pi_m S}{K_2+S+\gamma_1}}, \frac{\gamma_1 W^3+\pi_1}{\mu_1+\mu_2-\frac{\pi_m S}{K_2+S+\gamma_2}}, \frac{\gamma_2 X^3+\pi_1}{\mu_1-\frac{\pi_m S}{K_2+S+\gamma_3}}, \\ \frac{\gamma_3 Y^3+\pi_1}{\mu_1-\frac{\pi_m S}{K_2+S+\gamma_4}}, 0, \frac{\pi_3}{\beta_2 W^3-\mu_1+\frac{\pi_m S}{K_2+S+\gamma_5}}, \frac{\pi_3}{\beta_2 W^3-\mu_1+\frac{\pi_m S}{K_2+S+\gamma_6}} \end{array} \right\}. \tag{4.31}$$

# Case 5: Full microbial coexistence equilibrium

For the coexistence of susceptible *E. coli*, antibiotic-resistant *E. coli*, and bacteriophage populations, the equilibrium point is denoted as $E^4$. In this case, all state variables remain positive, representing the complete coexistence state of the wastewater treatment system.

$$W^4 = \frac{\pi_1+\pi_2}{\left(\mu_1+\mu_2+\beta_1-\frac{\pi_m S}{K_2+S+\gamma_1}\right)}, \quad X^4 = \frac{(\gamma_1 W^4+\pi_1)}{\left(\mu_1+\omega_1\frac{\pi_m S}{K_2+S+\gamma_2}\right)},$$

$$Y^4 = \frac{(\gamma_2 X^4+\pi_1)}{\left(\mu_1-\frac{\pi_m S}{K_2+S+\gamma_3}\right)}, \quad Z^4 = \frac{(\gamma_3 Y^4+\pi_1)}{\left(\mu_1-\frac{\pi_m S}{K_2+S+\gamma_4}\right)},$$

$$T^4 = \frac{(\gamma_4 Z^4(1-\Omega))}{\left(\mu_1+\frac{\pi_m S}{K_2+S+\gamma_5}\right)}, \quad V^4 = \frac{\pi_3}{\left(\beta_2 W^4-\mu_1+\frac{\pi_m S}{K_2+S+\gamma_6}\right)},$$

$$P^4 = \frac{(\Lambda+\omega_2)\, W^4 V^4}{\left(\mu_1+\frac{\pi_m S}{K_2+S}\right)}.$$

$E^4 = \{W^4, X^4, Y^4, Z^4, T^4, V^4, P^4\}$

(4.32)

The equilibrium analysis demonstrates that the wastewater treatment system may exhibit different long-term behaviours depending on the interaction between bacterial growth, the emergence and persistence of antibiotic-resistant *E. coli*, treatment efficiency, and bacteriophage predation. The stability analysis in the following section determines whether these equilibrium states are locally stable or unstable under small perturbations within the wastewater treatment system.

## 4.2.2.3 Stability of the equilibrium points

This study investigated the stability properties of the equilibrium points of Deterministic Model A using local and global stability approaches. Local stability was analysed using the Jacobian matrix and the Routh–Hurwitz criterion, while global stability was examined using the Lyapunov stability theorem. These analyses determine whether small perturbations around an equilibrium state decay with time and whether the system converges towards the equilibrium state.

1. **Local stability**

   The local stability of the equilibrium points of deterministic Model A was investigated using the Jacobian matrix and the Routh–Hurwitz stability criterion. Let the deterministic system be written in the form

   $$\frac{d\mathbf{X}}{dt} = F(\mathbf{X}),$$

   where

   $$\mathbf{X} = (W, X, Y, Z, T, V, P)^T. \tag{4.33}$$

   The local behaviour of the system around an equilibrium point $E^*$ is determined from the Jacobian matrix evaluated at that equilibrium. An equilibrium point is locally asymptotically stable when all eigenvalues of the corresponding Jacobian matrix have negative real parts. The eigenvalues of the Jacobian provide information about the response of each state variable following small deviations from the equilibrium

   **Jacobian Elements**

   The Jacobian matrix of Model A is obtained by differentiating the right-hand side of the system with respect to the state variables $(W, X, Y, Z, T, V, P)$. Therefore,

$$J(\mathbf{X}) = \frac{\partial F}{\partial \mathbf{X}} = \begin{bmatrix} A_1 & A_2 & A_3 & A_4 & A_5 & A_6 & A_7 \\ B_1 & B_2 & B_3 & B_4 & B_5 & B_6 & B_7 \\ C_1 & C_2 & C_3 & C_4 & C_5 & C_6 & C_7 \\ D_1 & D_2 & D_3 & D_4 & D_5 & D_6 & D_7 \\ E_1 & E_2 & E_3 & E_4 & E_5 & E_6 & E_7 \\ F_1 & F_2 & F_3 & F_4 & F_5 & F_6 & F_7 \\ G_1 & G_2 & G_3 & G_4 & G_5 & G_6 & G_7 \end{bmatrix}. \tag{4.34}$$

The entries of the first row are obtained by differentiating the $W(t)$ equation with respect to $W, X, Y, Z, T, V$, and $P$, respectively.

In particular, the bacteriophage interaction term in the $W(t)$ equation is

$$-\beta_1 WV. \tag{4.35}$$

Hence,

$$\frac{\partial}{\partial V}\left(-\beta_1 WV\right) = -\beta_1 W. \tag{4.35}$$

Since the complete right-hand side of the $W(t)$ equation is multiplied by the density-dependent factor

$$\left(1 - \frac{N}{A}\right), \tag{4.36}$$

and $N = W + X + Y + Z + T$ does not contain $V$, the corresponding complete Jacobian element is

$$\boxed{A_6 = -\beta_1 W\left(1 - \frac{N}{A}\right)}. \tag{4.37a}$$

The first governing equation contains no direct dependence on the bacteriophage variable $P(t)$. Therefore,

$$\boxed{A_7 = 0.} \tag{4.37b}$$

Biologically, $A_6 < 0$ shows that an increase in the pre-primary bacteriophage population $V(t)$ contributes to a reduction in the pre-primary *E. coli* population $W(t)$ through bacteriophage predation.

The remaining Jacobian elements are obtained analogously by taking the partial derivatives of each governing equation with respect to the seven state variables.

The resulting Jacobian is then evaluated at the corresponding equilibrium point before determining its eigenvalues.

### Stability Conditions

The characteristic equation associated with the Jacobian matrix evaluated at an equilibrium point $E^*$ is written as

$$\det\left(\lambda I - J(E^*)\right) = 0,$$

which gives a seventh-degree characteristic polynomial of the form

$$a_7\lambda^7 + a_6\lambda^6 + a_5\lambda^5 + a_4\lambda^4 + a_3\lambda^3 + a_2\lambda^2 + a_1\lambda + a_0 = 0. \tag{4.38}$$

The Routh–Hurwitz criterion was used to determine whether all roots of the characteristic polynomial have negative real parts. For a seventh-degree characteristic polynomial, positivity of the coefficients $a_i$ alone is necessary but is not sufficient to establish local asymptotic stability. The corresponding Routh–Hurwitz conditions must also be satisfied.

Equivalently, the relevant Hurwitz determinants must satisfy

Therefore, local asymptotic stability requires satisfaction of the complete Routh–Hurwitz conditions, including positivity of all Hurwitz determinants.

Therefore, an equilibrium point of Model A is locally asymptotically stable when all the required Routh–Hurwitz conditions are satisfied, which ensures that all eigenvalues of $J(E^*)$ have negative real parts. If any required Hurwitz condition fails, local asymptotic stability cannot be concluded.

The Jacobian matrix elements were obtained analytically by differentiating each governing equation with respect to the seven state variables. Mathematica was used only for symbolic verification of the derived expressions.

$$A_1 = \left(1 - \frac{N}{A}\right)\left(\frac{S\pi_m}{S+K_2} - \beta_1 - \gamma_1 - \mu_1 - \mu_2\right)$$
$$- \frac{\pi_1 + \pi_2 + \frac{SW\pi_m}{S+K_2} - W\beta_1 - W\gamma_1 - W\mu_1 - W\mu_2}{A}$$

$$A_2 = \frac{\pi_1 + \pi_2 + \frac{SW\pi_m}{S+K_2} - W\beta_1 - W\gamma_1 - W\mu_1 - W\mu_2}{A}$$

,

$$A_3 = -\frac{\pi_1 + \pi_2 + \frac{SW\pi_m}{S+K_2} - W\beta_1 - W\gamma_1 - W\mu_1 - W\mu_2}{A}$$

$$A_4 = -\frac{\pi_1 + \pi_2 + \frac{SW\pi_m}{S+K_2} - W\beta_1 - W\gamma_1 - W\mu_1 - W\mu_2}{A}$$

,

$$A_5 = -\frac{\pi_1 + \pi_2 + \frac{SW\pi_m}{S+K_2} - W\beta_1 - W\gamma_1 - W\mu_1 - W\mu_2}{A}$$

,

$$B_1 = \left(1 - \frac{N}{A}\right)\gamma_1 - \frac{-PX\omega_1 + \pi_1 + \frac{SX\pi_m}{S+K_2} + W\gamma_1 - X\gamma_2 - X\mu_1 - X\mu_2}{A},$$

$$B_2 = \left(1 - \frac{N}{A}\right)\gamma_1 - \frac{-PX\omega_1 + \pi_1 + \frac{SX\pi_m}{S+K_2} + W\gamma_1 - X\gamma_2 - X\mu_1 - X\mu_2}{A},$$

$$B_3 = -\frac{-PX\omega_1 + \pi_1 + \frac{SX\pi_m}{S+K_2} + W\gamma_1 - X\gamma_2 - X\mu_1 - X\mu_2}{A}.$$

$$B_4 = \frac{-PX\omega 1 + \pi_1 + \frac{SX\pi_m}{S+K_2} + WY_1 - XY_2 - X\mu_1 - X\mu_2}{A}$$

$$B_5 = \frac{-PX\omega 1 + \pi_1 + \frac{SX\pi_m}{S+K_2} + WY_1 - XY_2 - X\mu_1 - X\mu_2}{A}$$

,

$$B_6 = 0, and \quad B_7 = -X\left(1 - \frac{N}{A}\right)\omega 1$$

$$C_1 = \left(1 - \frac{N}{A}\right)Y_2 - \frac{\pi_1 + \frac{S\pi_m}{S+K_2} + WY_2 - Y_3 - Y\mu_1}{A}$$

$$C_2 = -\frac{\pi_1 + \frac{S\pi_m}{S+K_2} + WY_2 - Y_3 - Y\mu_1}{A}$$

$$C_3 = \left(1 - \frac{N}{A}\right)\left(\frac{S\pi_m}{S+K_2} - Y_3 - \mu_1\right)$$

$$C_4 = \frac{\pi_1 + \frac{S\pi_m}{S+K_2} + WY_2 - Y_3 - Y\mu_1}{A}, \quad C_5 = \frac{\pi_1 + \frac{S\pi_m}{S+K_2} + WY_2 - Y_3 - Y\mu_1}{A}$$

$$C_6 = 0, \quad C_7 = 0$$

$$D_1 = \left(1 - \frac{N}{A}\right) Y_3 - \frac{\pi_1 + \frac{SZ\pi_m}{S+K_2} + WY_3 - ZY_4 - Z\mu_1}{A}$$

$$D_2 = \frac{\pi_1 + \frac{SZ\pi_m}{S+K_2} + WY_3 - ZY_4 - Z\mu_1}{A}$$

$$D_3 = -\frac{\pi_1 + \frac{SZ\pi_m}{S+K_2} + WY_3 - ZY_4 - Z\mu_1}{A}$$

$$D_4 = 1 - \frac{S\pi_m}{S + K_2} - Y_4 - \mu_1$$

$$D_5 = \frac{\pi_1 + \frac{SZ\pi_m}{S+K_2} + WY_3 - ZY_4 - Z\mu_1}{A}, \quad D_6 = 0, \quad D_7 = 0$$

$$E_1 = -T\Phi + \frac{ST\pi_m}{S + K_2} + (1 - \Omega) ZY_4 - T\mu_1$$

$$E_2 = -T\Phi + \frac{ST\pi_m}{S + K_2} + (1 - \Omega) ZY_4 - T\mu_1$$

$$E_3 = -T\Phi + \frac{ST\pi_m}{S + K_2} + (1 - \Omega) ZY_4 - T\mu_1$$

$$E_4 = \frac{(1 - \Omega)\left(1 - \frac{N}{A}\right) Y_4 - T\Phi + \frac{ST\pi_m}{S+K_2} + (1 - \Omega) ZY_4 - T\mu_1}{A}$$

$$E_5 = \left(1 - \frac{T+W+X+Y+Z}{A}\right)\left(-\Phi + \frac{S\pi_m}{S+K_2} - \mu_1\right) - \frac{-T\Phi + \frac{ST\pi_m}{S+K_2} + (1-\Omega)Z\gamma_4 - T\mu}{A}$$

$$E_6 = 0, \qquad E_7 = 0,$$

$$F_1 = V\left(1 - \frac{P+V}{A}\right)\beta_2, \qquad F_2 = 0, \qquad F_3 = 0, \qquad F_4 = 0,$$

$$F_5 = \left(1 - \frac{P+V}{A}\right)(-\Lambda + W\beta_2 - \mu_1),$$

$$F_6 = -\frac{-V\Lambda + \pi_3 + \frac{VS\pi_m}{S+K_2} + VW\beta_2 - V\mu_1}{A},$$

$$F_7 = -\frac{-V\Lambda + \pi_3 + \frac{VS\pi_m}{S+K_2} + VW\beta_2 - V\mu_1}{A},$$

$$G_1 = V\left(1 - \frac{P+V}{A}\right)\omega_2, \qquad G_2 = 0, \qquad G_3 = 0, \qquad G_4 = 0, \qquad G_5 = 0,$$

$$G_6 = \left(1 - \frac{P+V}{A}\right)(\Lambda + W\omega_2) - \frac{V\Lambda + \pi_3 + \frac{PS\pi_m}{S+K_2} - P\mu_1 + VW\omega_2}{A},$$

$$G_7 = \left(1 - \frac{P+V}{A}\right)\left(\frac{S\pi_m}{S+K_2} - \mu_1\right) - \frac{V\Lambda + \pi_3 + \frac{PS\pi_m}{S+K_2} - P\mu_1 + VW\omega_2}{A}. \tag{4.39}$$

The local stability of the system (3.1) was determined by the nature of the eigenvalues of this Jacobian matrix; the Routh-Hurwitz criterion was used to determine the stability. In which characteristic polynomial was obtained as follows

$a_7\lambda^7 + a_6\lambda^6 + a_5\lambda^5 + a_4\lambda^4 + a_3\lambda^3 + a_2\lambda^2 + a_1\lambda^1 + a_0 = 0$ Where the expression $a_i i = 1$ for the system (3.1) was obtained and placed in the supplementary material.
The characteristic polynomial values of $a_7, a_6, a_5, a_4, a_3, a_2, a_1$ are determined using Mathematica Software and exhibited using Routh's Criteria for stability in terms of $R_0$ as shown.

**Ruoth Criterion Table**

| | | | | |
|---|---|---|---|---|
| $\lambda^7$ | $a_0$ | $a_2$ | $a_4$ | $a_6$ |
| $\lambda^6$ | $a_1$ | $a_3$ | $a_5$ | $a_7$ |
| $\lambda^5$ | $b_1$ | $b_2$ | $b_3$ | |
| $\lambda^4$ | $c_1$ | $c_2$ | $c_3$ | |
| $\lambda^3$ | $d_1$ | $d_2$ | | |
| $\lambda^2$ | $e_1$ | $e_2$ | | |
| $\lambda^1$ | $f_1$ | | | |
| $\lambda^0$ | $g_1$ | | | |

$$b_1 = \frac{a_1a_2 - a_0a_3}{a_1}, \quad b_2 = \frac{a_1a_4 - a_0a_5}{a_1}, \quad b_3 = \frac{a_1a_6 - a_0a_7}{a_1}, \quad b_4 = 0$$

$$c_1 = \frac{b_1a_3 - a_1b_2}{b_1}, \quad c_2 = \frac{b_1a_5 - a_1b_3}{b_1}, \quad c_3 = \frac{b_1a_7}{b_1}$$

$$d_1 = \frac{c_1b_2 - b_1c_2}{c_1}, \quad d_2 = \frac{c_1b_2 - b_1c_2}{c_1}$$

$$e_1 = \frac{d_1c_2 - c_1d_2}{d_1}, \quad e_2 = \frac{d_1c_3}{d_1}$$

$$f_1 = \frac{e_1d_2 - d_1e_2}{e_1}$$

$$g_1 = \frac{f_1e_2 - d_1e_2}{e_1} \tag{4.40}$$

$a_7, a_6, a_5, a_4, a_3, a_2, a_1, a_0$ were also obtained and provided in the appendix supplementary materials.

For the seventh-order characteristic polynomial, positivity of all coefficients is a necessary condition but does not independently guarantee local asymptotic stability. Therefore, the Routh–Hurwitz stability criterion was applied by evaluating the corresponding Hurwitz determinants. The equilibrium point is locally asymptotically stable when all Hurwitz determinants are positive, ensuring that all eigenvalues of the Jacobian matrix have negative real parts.

If any Hurwitz determinant changes sign, the equilibrium point cannot be considered locally asymptotically stable. Therefore, an equilibrium point of Model A is locally asymptotically stable when all the required Routh–Hurwitz conditions are satisfied, which ensures that all eigenvalues of $J(E^*)$ have negative real parts. If any required Hurwitz condition fails, local asymptotic stability cannot be concluded.

2. **Global stability**

Global stability was established by examining the convergence of the equilibrium point $E^*$ using a Lyapunov function approach.The approach used in studying the global asymptotically stable state of this study was the using the Lyapunov function (Odhiambo, 2023).

**Theorem 3**

Let

$$\begin{aligned} V =& \frac{1}{2}(W - W^*)^2 + \frac{\delta_1}{2}(X - X^*)^2 + \frac{\delta_2}{2}(Y - Y^*)^2 \\ &+ \frac{\delta_3}{2}(Z - Z^*)^2 + \frac{\delta_4}{2}(T - T^*)^2 \\ &+ \frac{\delta_5}{2}(V - V^*)^2 + \frac{\delta_6}{2}(P - P^*)^2. \end{aligned} \tag{4.41}$$

be the Lyapunov function, where

$$\delta_1, \delta_2, \delta_3, \delta_4, \delta_5, \delta_6 > 0 \tag{4.42}$$

were correctly taken such that the above function satisfied the Lyapunov conditions below.

$$V'(E^*) \text{ where } E^* = W^*, X^*, Y^*, Z^*, T^*, V^*, P^* \text{ and } V(W, X, Y, Z, T, V, P).$$

**Proof**

$$\begin{aligned} V = & \frac{(W - W^*)^2}{2} + \delta_1 \frac{(X - X^*)^2}{2} + \delta_2 \frac{(Y - Y^*)^2}{2} + \delta_3 \frac{(Z - Z^*)^2}{2} \\ & + \delta_4 \frac{(T - T^*)^2}{2} + \delta_5 \frac{(V - V^*)^2}{2} + \delta_6 \frac{(P - P^*)^2}{2} \end{aligned} \tag{4.43}$$

Deriving the above equation and substituting (3.1), then factorising $W, X, Y, Z, T, V,$ and $P$, we obtain the following result. In the special case

$$W = W^*, \quad X = X^*, \quad Y = Y^*, \quad Z = Z^*, \quad T = T^*, \quad V = V^*, \quad P = P^*, \tag{4.44}$$

this implies that

$$\begin{aligned} & W - W^* = 0, \quad X - X^* = 0, \quad Y - Y^* = 0, \quad Z - Z^* = 0, \\ & T - T^* = 0, \quad V - V^* = 0, \quad P - P^* = 0. \end{aligned} \tag{4.45}$$

These are also equilibrium points, and substituting them gives

$$\frac{dV}{dt} = 0,$$

since

$$(W - W^*)^2 = 0, \quad \ldots, \quad (P - P^*)^2 = 0,$$

because

$$W = W^*, \quad X = X^*, \quad Y = Y^*, \quad Z = Z^*, \quad T = T^*, \quad V = V^*, \quad P = P^*. \tag{4.46}$$

Also, since

$$\delta_1 > 0, \quad \delta_2 > 0, \quad \delta_3 > 0, \quad \delta_4 > 0, \quad \delta_5 > 0, \quad \delta_6 > 0,$$

they are chosen such that

$$\frac{dV}{dt} \leq 0, \tag{4.47}$$

By LaSalle's invariance principle, the equilibrium point $E^*$ is globally asymptotically stable if the largest invariant set contained in $\frac{dV}{dt} = 0$ consists only of the equilibrium point $E^*$.

### 4.2.3 Model simulation

The numerical simulations of Model A were performed using MATLAB to investigate the temporal behaviour of susceptible *E. coli*, antibiotic-resistant *E. coli*, bacteriophage populations, and treatment-related compartments. The simulations were conducted to complement the analytical results obtained from positivity, boundedness, equilibrium, and stability analyses.

Before numerical implementation, all microbial concentration parameters were standardized into consistent units to ensure compatibility during computational analysis. Parameter values were obtained from previous experimental and mathematical modelling studies where available, while parameters without direct experimental estimates were assigned biologically reasonable values and calibrated according to reported wastewater microbial dynamics.

The resulting system of ordinary differential equations was solved numerically using the Runge–Kutta method implemented in MATLAB. The numerical simulations were conducted over the selected time interval using the defined initial conditions and parameter

values to examine the long-term behaviour of the wastewater microbial system

$$N(t_f) = W(t_f) + X(t_f) + Y(t_f) + Z(t_f) + T(t_f), \tag{4.48}$$

where $t_f$ represents the final simulation time. This study used Partial Rank Correlation Coefficient (PRCC) and Latin hypercube sampling (LHS)in sensitivity analysis; The PRCC an efficient tool was used in uncertainty analysis in exploring parameter space of the model entirel. The strength of inputs and output of the model was measured using PRCC through LHS method. The main aim of LHS/PRCC analysis was to identify the parameters which were more important in uncertainty contributions to rank them by their significance and prediction to this imprecision . The PRCC always ranges from -1 to +1 and its absolute value describe how the relationship between x and y variables strength. If the value is close to -1 or +1 then the linear relationship is stronger between x and y and if the value is far much from -1 or +1 then the weaker relationship between x and y. From Figure x, the two values on the top [x, y] in each plot, represents the PRCC and p-value respectively(Ngari, Muthuri, Kitavi, et al., 2022) .
The figures of sensitivity analysis analysis were as shown

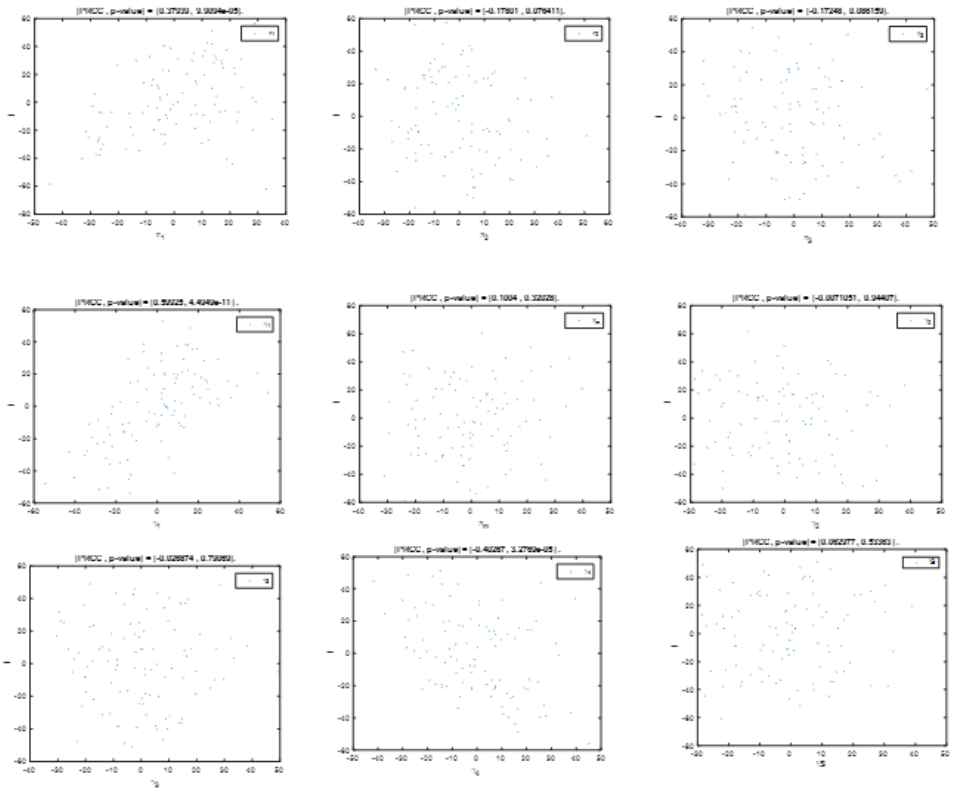

Figure 4.1: PRCC

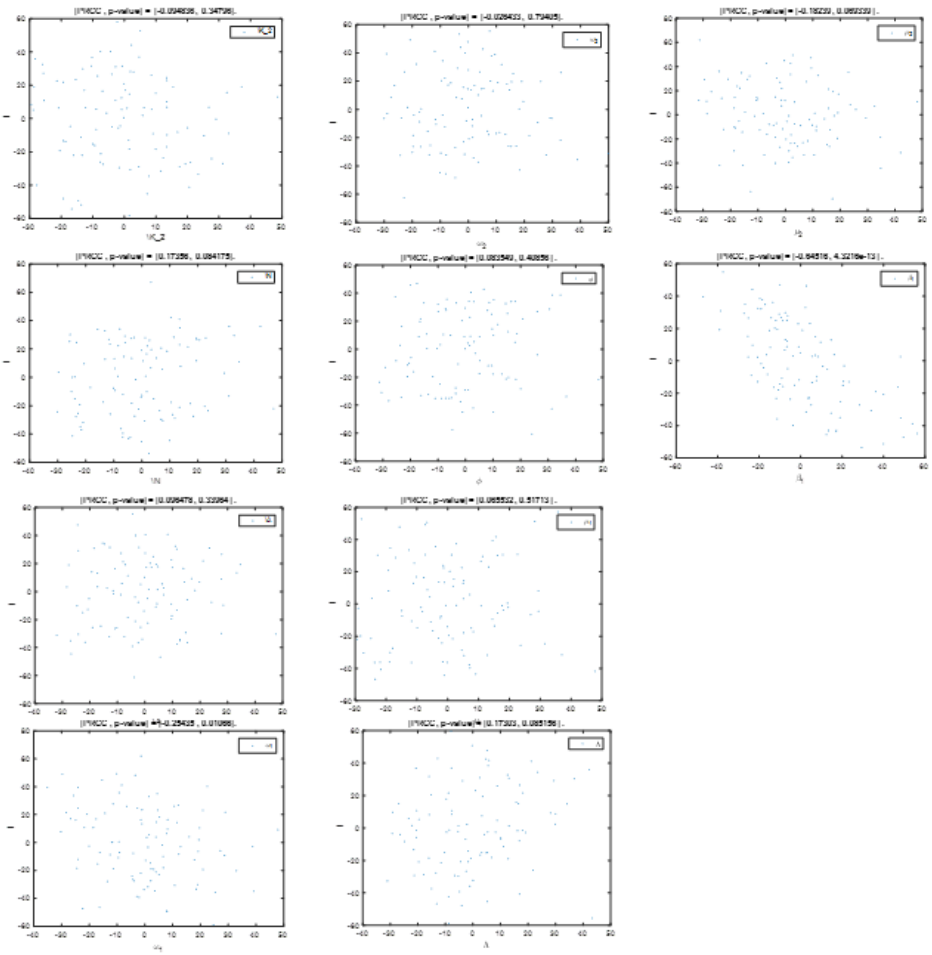

Figure 4.2: PRCC continues

The PRCC ranges from -1 to +1 and its absolute value described the relationship between x and y variables strength.When value was close to -1 or +1 then the linear relationship was stronger between x and y and when the value was far much from -1 or +1 then represented weaker relationship between x and yFrom Figure 4.4, the two values on the top [x, y] in each plot, represents the PRCC and p-value respectively

The PRCC always ranges from -1 to +1 and its absolute value describe how the relationship between x and y variables strength. If the value is close to -1 or +1 then the linear relationship is stronger between x and y and if the value is far much from -1 or +1 then the weaker relationship between x and y.

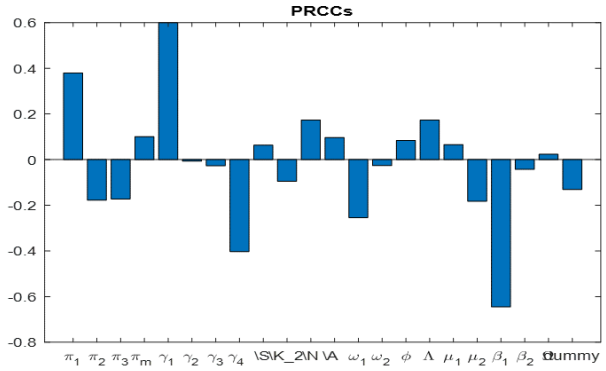


Figure 4.3: PRCC and p-values

From Figure 4.4, The two values on the top [x, y] in each plot, represents the PRCC and p-value respectively
This information is further summarised in a table as shown

Table 4.2: PRCC values and corresponding p-values

| Parameter Symbol | PRCC | $p$-values |
|---|---|---|
| $\pi_1$ | 0.4466 | $3.2021 \times 10^{-6}$ |
| $\pi_2$ | -0.036901 | 0.71549 |
| $\pi_3$ | 0.14363 | 0.15398 |
| $\pi_m$ | 0.047649 | 0.63781 |
| $\gamma_1$ | 0.40187 | $3.4085 \times 10^{-5}$ |
| $\gamma_2$ | 0.16649 | 0.09782 |
| $\gamma_3$ | -0.23424 | 0.018992 |
| $\gamma_4$ | -0.065812 | 0.51533 |
| $S$ | 0.047082 | 0.64182 |
| $K_2$ | 0.040344 | 0.69024 |
| $N$ | 0.12048 | 0.23249 |
| $A$ | -0.03593 | 0.72267 |
| $\omega_1$ | -0.088145 | 0.38317 |
| $\omega_2$ | -0.012077 | 0.90508 |
| $\phi$ | 0.154 | 0.12607 |
| $\Lambda$ | -0.041982 | 0.67834 |
| $\mu_1$ | -0.19124 | 0.056648 |
| $\mu_2$ | -0.047424 | 0.63939 |
| $\beta_1$ | -0.05831 | $9.8345 \times 10^{-14}$ |
| $\beta_2$ | 0.076511 | 0.44929 |
| $\Omega$ | 0.14255 | 0.15712 |

The figures and tables present a Partial Rank Correlation Coefficient (PRCC) sensitivity analysis. PRCC measures the monotonic influence of each parameter on the model output while controlling for the effects of the remaining parameters.

The following was exhibited as mathematical interpretation of the Sensitivity Analysis Using PRCC results of this study.

**Sensitivity Analysis Using PRCC**

A Partial Rank Correlation Coefficient (PRCC) analysis was performed to determine the influence of model parameters on the response variable. The PRCC method measured the monotonic relationship between each parameter and the model output while accounting for the effects of the remaining parameters.

For a parameter $x_i$, the PRCC satisfies

$$-1 \leq \text{PRCC}(x_i) \leq 1.$$

A positive PRCC value indicated increasing the parameter increased response variable, whereas a negative PRCC value implies that increasing the parameter decreases the response variable. Parameters with large absolute PRCC values had stronger effects on the model dynamics. Statistical significance was determined using the associated $p$-values,

with

$$p < 0.05$$

considered statistically significant.

The PRCC results revealed the parameters

$$\pi_1, \quad \gamma_1, \quad \gamma_3, \quad \beta_1$$

statistically significant effects on the model output.

The parameter $\pi_1$ has a PRCC value of

$$\text{PRCC}(\pi_1) = 0.4466,$$

with

$$p = 3.2021 \times 10^{-6},$$

indicating a strong positive relationship with the response variable. This suggests that increasing $\pi_1$ significantly increases the model output.

Similarly, the parameter $\gamma_1$ has

$$\text{PRCC}(\gamma_1) = 0.40187,$$

with

$$p = 3.4085 \times 10^{-5},$$

showing that $\gamma_1$ also strongly enhances the system response.

The parameter $\gamma_3$ has a negative PRCC value,

$$\text{PRCC}(\gamma_3) = -0.23424,$$

with

$$p = 0.018992,$$

which indicates that increasing $\gamma_3$ reduces the response variable.

Among all parameters, $\beta_1$ exhibits the largest magnitude of sensitivity,

$$\text{PRCC}(\beta_1) = -0.65831,$$

with a highly significant $p$-value,

$$p = 9.8345 \times 10^{-14}.$$

This result indicates that $\beta_1$ has a very strong negative influence on the model output

and acts as the dominant controlling parameter in the system.

Several parameters, including

$$\pi_2,\ \pi_m,\ \gamma_4,\ S,\ K_2,\ A,\ \omega_2,\ \mu_2,$$

have relatively small PRCC values and large $p$-values, indicating weak or statistically insignificant influence on the model response within the investigated parameter ranges.

Furthermore, the parameters

$$\mu_1,\ \gamma_2,\ \phi$$

show moderate PRCC values but are not statistically significant at the 5% level. These parameters may become influential under different parameter regimes or larger sample sizes.

Ranking the parameters according to the magnitude of their PRCC values gives

$$|\beta_1| > |\pi_1| > |\gamma_1| > |\gamma_3| > |\mu_1| > |\gamma_2| > |\phi|.$$

Hence, the model dynamics are primarily governed by the parameters

$$\beta_1, \quad \pi_1, \quad \gamma_1.$$

Overall, the PRCC analysis demonstrates that increasing $\pi_1$ and $\gamma_1$ enhances the system response, whereas increasing $\beta_1$ and $\gamma_3$ suppresses it. Therefore, $\beta_1$ represents the most effective parameter for reducing the model output and may serve as an important control parameter in the system.

### 4.2.4 Model A Simulations

The numerical simulations of Model A were performed to investigate the temporal dynamics of susceptible *E. coli*, antibiotic-resistant *E. coli*, bacteriophage populations, and wastewater treatment compartments. The numerical analysis was conducted to complement the analytical results obtained from the positivity, boundedness, equilibrium, and stability analyses. The simulations provide insight into how bacterial growth, antibiotic resistance development, bacteriophage predation, and treatment processes interact within the wastewater system.

Before numerical implementation, all microbial concentration parameters were standardized into consistent units. Since wastewater microbial measurements may be reported using different volume scales, all bacterial and bacteriophage concentrations were converted into a common concentration basis to ensure mathematical consistency during computation.

The parameter values used in the simulations were obtained from previously reported experimental studies and mathematical modelling literature where available. Parameters without direct experimental estimates were assigned biologically reasonable values and calibrated to ensure that the resulting system behaviour remained consistent with reported wastewater microbial dynamics. The numerical solutions were obtained using the adaptive Runge–Kutta–Fehlberg method (RK45) implemented in MATLAB.

The baseline initial conditions for Model A were defined as

$$(W(0), X(0), Y(0), Z(0), T(0), V(0), P(0)) = (W_0, X_0, Y_0, Z_0, T_0, V_0, P_0).$$

These initial conditions represent the initial microbial state of the wastewater treatment system before significant changes occur due to bacterial growth, resistance evolution, treatment processes, and bacteriophage interactions.

The total microbial population within the treatment system was considered as

$$N(t) = W(t) + X(t) + Y(t) + Z(t) + T(t),$$

where $N(t)$ represents the combined bacterial population across the different treatment compartments.

The simulations were conducted over the selected time interval using the defined parameter values and initial conditions. The resulting trajectories were analysed to determine whether bacterial populations increased, decreased, or approached a stable equilibrium state under different biological scenarios.

### 4.2.5 Sensitivity Analysis Using PRCC

A Partial Rank Correlation Coefficient (PRCC) analysis was performed to identify the parameters that have the greatest influence on the model output. The analysis was conducted using Latin Hypercube Sampling (LHS), which provides an efficient method for exploring the multidimensional parameter space.

For each parameter $x_i$, the PRCC value satisfies

$$-1 \leq \text{PRCC}(x_i) \leq 1.$$

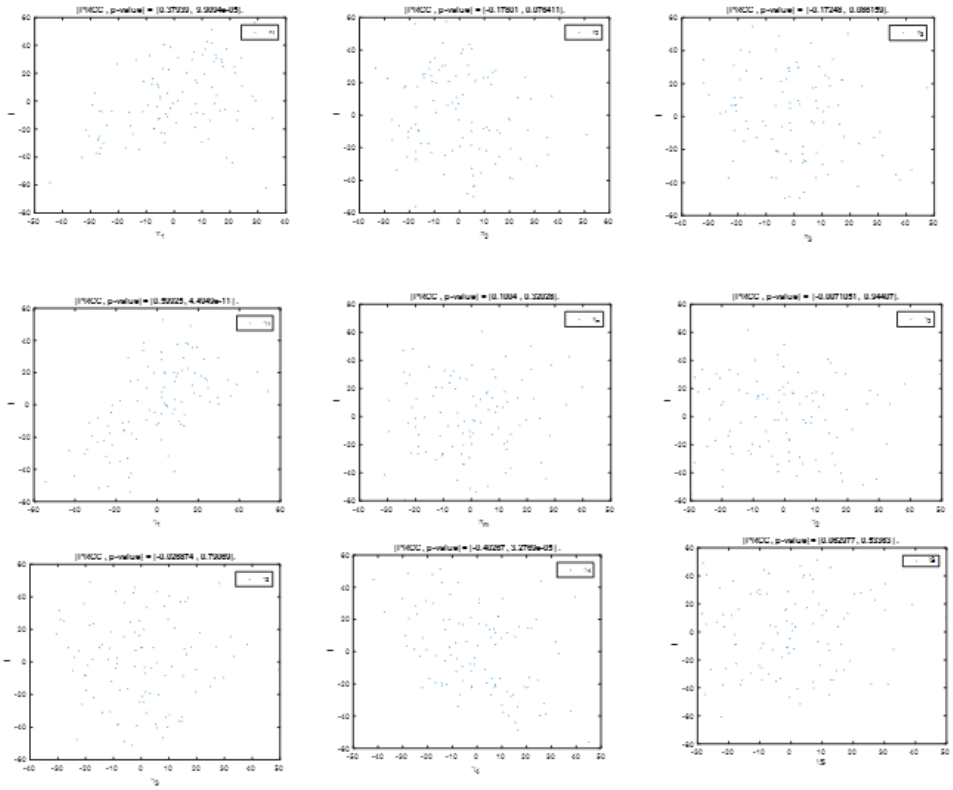

Figure 4.4: PRCC

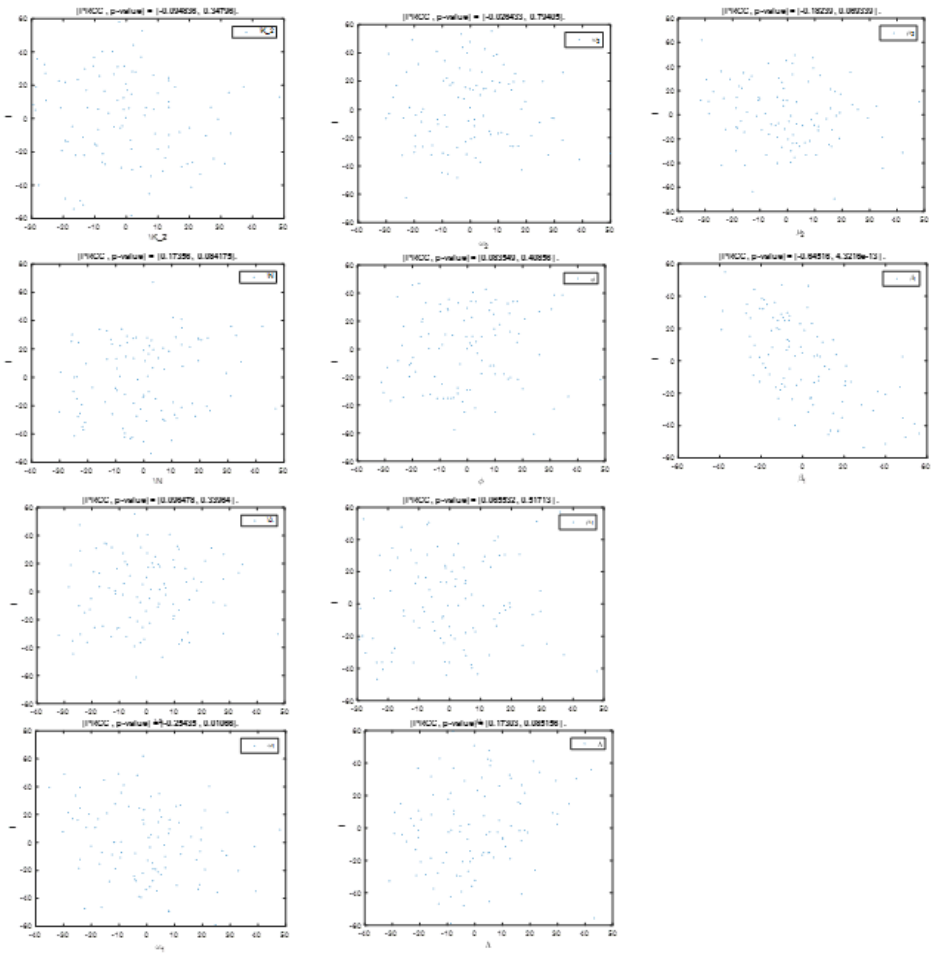

Figure 4.5: PRCC

| **Parameter Symbol** | **PRCC** | **p-value** |
|---|---|---|
| $\pi_1$ | 0.4466 | $3.2021 \times 10^{-6}$ |
| $\pi_2$ | $-0.036901$ | 0.71549 |
| $\pi_3$ | 0.14363 | 0.15398 |
| $\pi_m$ | 0.047649 | 0.63781 |
| $\gamma_1$ | 0.40187 | $3.4085 \times 10^{-5}$ |
| $\gamma_2$ | 0.16649 | 0.09782 |
| $\gamma_3$ | $-0.23424$ | 0.018992 |
| $\gamma_4$ | $-0.065812$ | 0.51533 |
| $S$ | 0.047082 | 0.64182 |
| $K_2$ | 0.040344 | 0.69024 |
| $N$ | 0.12048 | 0.23249 |
| $A$ | $-0.03593$ | 0.72267 |

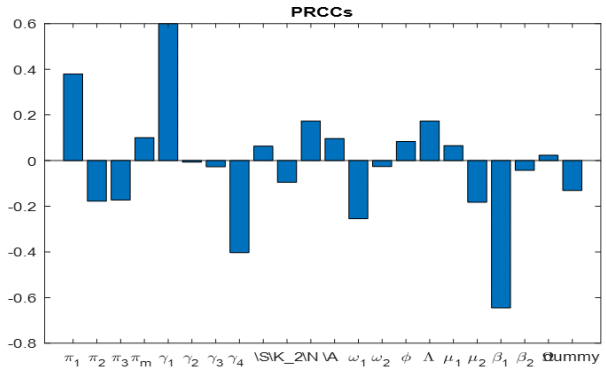


Figure 4.6: PRCC and p-values

The parameter $\pi_1$ exhibited a positive influence on the model output with

$$\text{PRCC}(\pi_1) = 0.4466,$$

and

$$p = 3.2021 \times 10^{-6}.$$

This indicates that increasing $\pi_1$ increases the response variable, suggesting that this parameter promotes bacterial persistence within the wastewater system.

Similarly, the parameter $\gamma_1$ demonstrated a significant positive relationship:

$$\text{PRCC}(\gamma_1) = 0.40187,$$

with

$$p = 3.4085 \times 10^{-5}.$$

Therefore, increases in $\gamma_1$ contribute to an increase in the model response under the investigated parameter range.

The parameter $\gamma_3$ showed a significant negative relationship:

$$\text{PRCC}(\gamma_3) = -0.23424,$$

with

$$p = 0.018992.$$

This indicates that increasing $\gamma_3$ reduces the bacterial population, demonstrating its potential contribution to bacterial removal within the treatment process.

Among all investigated parameters, $\beta_1$ showed the strongest influence:

$$\text{PRCC}(\beta_1) = -0.65831,$$

with

$$p = 9.8345 \times 10^{-14}.$$

The negative sign indicates that increasing bacteriophage predation intensity reduces the model output. Therefore, $\beta_1$ represents a dominant parameter controlling bacterial suppression within the wastewater system.

The parameters were ranked according to the magnitude of their PRCC values as

$$|\beta_1| > |\pi_1| > |\gamma_1| > |\gamma_3| > |\mu_1| > |\gamma_2| > |\phi|.$$

The sensitivity analysis demonstrates that the wastewater microbial dynamics are mainly influenced by parameters associated with bacterial input, treatment interactions, and bacteriophage predation. Among the investigated parameters, $\beta_1$ exhibited the largest absolute PRCC value, indicating that changes in the bacteriophage predation rate have a strong influence on the predicted *E. coli* concentration. The positive influence of $\pi_1$ and $\gamma_1$ suggests that bacterial introduction and compartmental transfer processes contribute to persistence, whereas the negative influence of $\gamma_3$ and $\beta_1$ indicates their potential role in reducing bacterial levels. These results identify the parameters that require particular attention during model calibration and future wastewater management interventions.

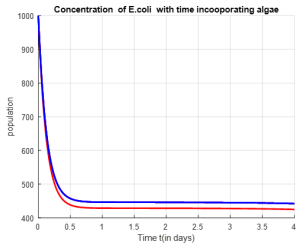


Figure 4.7: Concentration of E.coli with time incooporating algae

Figure 4.7 illustrates both curves drop very rapidly in the first 0.5 days, then level off. Blue stabilizes near 443–445. Red stabilizes near 427–430. Red remains lower than blue by about 15–18 units throughout the steady phase.
The figure indicates that the E. coli concentration decreases sharply from about 1000 to a stable positive equilibrium within less than 1 day. The equilibrium is approximately 443–445 for the blue case and 427–430 for the red case. Hence, the algae-incorporated case achieves an additional reduction of about 15–18 units, corresponding to roughly 3.5–4.5 percent lower long-term bacterial concentration. Therefore, the model predicts that algae has a measurable suppressive effect, but the effect is moderate and leads to persistence at a reduced endemic equilibrium rather than eradication.

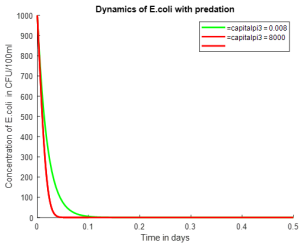


Figure 4.8: Dynamics of E.coli with predation

Figure 4.8 The absence of oscillations indicates that the simulated trajectories approach a stable equilibrium behaviour under the assumed predation conditions. The results demonstrate that increased predation intensity accelerates bacterial decline and reduces the long-term concentration of *E. coli.*,

$$\frac{dE(t)}{dt} < 0,$$

where $E(t)$ represents the concentration of *E. coli* at time $t$.The decay may be approximated by an exponential model,

$$E(t) = E_0 e^{-kt},$$

where $E_0$ is the initial concentration and $k$ is the decay rate. Since thered curve decreases faster than the green curve, its decay rate is larger, so

$$k_{\text{red}} > k_{\text{green}}.$$

The absence of oscillations indicates that the system is stable under predation.Both curves converge smoothly to the bacteria-free equilibrium,

$$\lim_{t\to\infty} E(t) = 0.$$

.

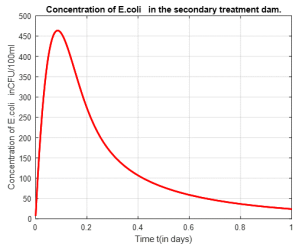


Figure 4.9: Concentration of E.coli in the secondary treatment dam

The figure 4.9 the secondary treatment dam contributes to the reduction of *E. coli* concentration. Since the concentration continues to decline without oscillations, the trajectory approaches stable equilibrium behaviour consistent with the analytical stability analysis.

$$E_{\max} \approx 460 \text{ CFU}/100 \text{ ml}$$

at about

$$t \approx 0.09 \text{ days}.$$

After this peak, the concentration decreases continuously with time. By $t = 1$ day,

the concentration has reduced to approximately

$$E(1) \approx 25 \text{ CFU}/100 \text{ ml}.$$

Mathematically, the behaviour is non-monotonic. During the early stage,

$$\frac{dE(t)}{dt} > 0,$$

which indicates rapid growth or accumulation of *E. coli*. At the peak point,

$$\frac{dE(t)}{dt} = 0,$$

and after the maximum concentration is reached,

$$\frac{dE(t)}{dt} < 0.$$

This shows that the system first experiences a transient increase in *E. coli* concentration before treatment effects dominate and reduce the bacterial load. The decreasing phase indicates that the secondary treatment dam has a strong removal effect on *E. coli*. Since the concentration continues to decline toward a low value without oscillations, the system is stable and tends toward a bacteria-free or low-concentration equilibrium.

Therefore, the figure demonstrates that although *E. coli* concentration initially increases in the secondary treatment dam, the treatment process eventually suppresses the bacterial population and drives the system toward stability.

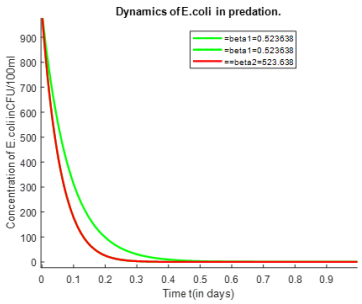


Figure 4.10: Dynamics of E.coli in predation

Figure 4.10 s the solution trajectory approaches a low-concentration equilibrium behaviour consistent with the stability properties of the mathematical model.

$$E_{\max} \approx 460 \text{ CFU/100 ml},$$

which occurs at about

$$t \approx 0.08 \text{ days}.$$

After reaching this maximum value, the *E. coli* concentration decreases continuously. By the end of the simulation period, at $t = 1$ day, the concentration has reduced to approximately

$$E(1) \approx 25 \text{ CFU/100 ml}.$$

Mathematically, the behaviour of the system is non-monotonic. During the early stage,

$$\frac{dE(t)}{dt} > 0,$$

showing that the bacterial concentration is increasing. At the peak point,

$$\frac{dE(t)}{dt} = 0,$$

and after the peak,

$$\frac{dE(t)}{dt} < 0.$$

This means that the concentration begins to decline after the maximum point is reached. The decreasing phase suggests that the secondary treatment dam has a strong removal effect on *E. coli*. Since the curve decreases smoothly without oscillations, the system is stable and tends toward a low-concentration equilibrium.

Therefore, the figure demonstrates that although *E. coli* initially increases in the secondary treatment dam, the treatment process eventually reduces the bacterial population and drives the system toward stability

The figure 4.8 shows the dynamics of *E. coli* concentration in thepre-primary dam under different predation levels. All curves begin from the same initial concentration,

$$E(0) \approx 1000 \text{ CFU/100 ml}.$$

When there is no predation, represented by the yellow curve with $V(t) = 0$, the*E. coli* concentration increases continuously throughout the simulationperiod. By $t = 5$ days, the concentration reaches approximately

$$E(5) \approx 4700 \text{ CFU/100 ml}.$$

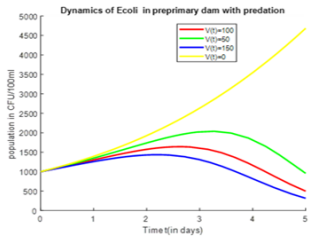


Figure 4.11: Dynamics of E.coli in preprimary dam with predation

This indicates that in the absence of predators, the bacterial population growsrapidly and remains uncontrolled.For the cases with predation, the concentration initially increases but laterdecreases after reaching a maximum value. The green curve, corresponding to$V(t) = 50$, reaches a peak of about

$$E_{\max} \approx 2000 \text{ CFU/100 ml}$$

before decreasing to approximately 1000 CFU/100 ml at $t = 5$ days. The redcurve, corresponding to $V(t) = 100$, reaches a lower peak of about

$$E_{\max} \approx 1650 \text{ CFU/100 ml},$$

and then decreases to approximately 500 CFU/100 ml. The blue curve,corresponding to $V(t) = 150$, shows the strongest reduction effect. It reaches apeak of about

$$E_{\max} \approx 1450 \text{ CFU/100 ml},$$

and then decreases to nearly 300 CFU/100 ml by the end of the simulation.Therefore, increasing the predator population reduces both the maximum*E. coli* concentration and the final bacterial concentration. This shows that predation has a strong suppressive effect on *E. coli*growth in the pre-primary dam.

$$V(t) = 150 > V(t) = 100 > V(t) = 50 > V(t) = 0$$

in terms of bacterial suppression efficiency.

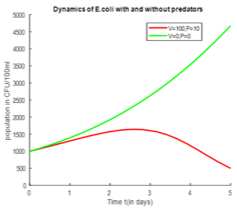


Figure 4.12: Dynamics of E.coli with and without predation

The figure 4.12 compares the dynamics of *E. coli* concentration with and without predators. The green curve represents the case without predators,where $V = 0$ and $P = 0$. In this case, the *E. coli* population increasescontinuously from

$$E(0) \approx 1000 \text{ CFU/100 ml}$$

to approximately

$$E(5) \approx 4700 \text{ CFU/100 ml.}$$

This shows that without predation, the bacterial population grows freely andv does not approach a stable lower level within the simulation period.The red curve represents the case with predators, where $V = 100$ and $P = 10$.Here, the *E. coli* concentration initially increases and reaches amaximum value of approximately

$$E_{\max} \approx 1650 \text{ CFU/100 ml}$$

at about

$$t \approx 2.5 \text{ days.}$$

After this peak, the concentration decreases steadily and reaches approximately

$$E(5) \approx 500 \text{ CFU/100 ml.}$$

Mathematically, the red curve is non-monotonic. During the early stage,

$$\frac{dE(t)}{dt} > 0,$$

showing bacterial growth. At the maximum point,

$$\frac{dE(t)}{dt} = 0,$$

and after the peak,

$$\frac{dE(t)}{dt} < 0,$$

showing that predation dominates and reduces the bacterial concentration.Therefore, the right figure confirms that predators significantly reduce*E. coli* concentration. In the absence of predators, the bacterialpopulation continues to increase, while in the presence of predators,the population growth is suppressed and the concentration decreases towards a lower equilibrium level.

Figur 4.7 shows the dynamics of *E. coli* concentration under predation for different values of the predation-related parameters.

At the initial time, the *E. coli* concentration is approximately

$$970 \text{ CFU}/100\,\text{ml}.$$

For all parameter cases, the concentration decreases rapidly within the first few fractions of a day, indicating a strong predation effect on the bacterial population.

The green curve, corresponding to the lower predation parameter case, shows a comparatively slower decline. The *E. coli* concentration remains above

$$100 \text{ CFU}/100\,\text{ml}$$

until approximately

$$t \approx 0.18 \text{ days}.$$

This suggests that weaker predation allows the bacterial population to persist for a longer period before approaching extinction.

In contrast, the blue and red curves show a much faster decay. The concentration falls below

$$100 \text{ CFU}/100\,\text{ml}$$

at approximately

$$t \approx 0.12 \text{ days},$$

and approaches zero shortly afterwards. This indicates that higher predation intensity accelerates the removal of *E. coli* from the system.

Overall, Figure 4.7 demonstrates that predation has a strong suppressive effect on *E. coli* concentration. Increasing the predation-related parameter increases the decay rate of the bacterial population, causing the concentration to approach zero more rapidly. There-

fore, predation plays an important role in reducing and controlling *E. coli* contamination levels.

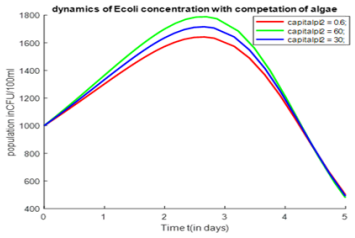


Figure 4.13: Dynamics of E.coli concentration with competation of algae

Figure 4. 13 presents the dynamics of *E. coli* concentration under the effect of algae competition for different values of the parameter $P_2$.

At the beginning of the simulation, the *E. coli* concentration is approximately

$$1000 \text{ CFU}/100\,\text{ml}.$$

For all considered values of $P_2$, the bacterial concentration initially increases with time, indicating that the growth effect dominates during the early stage of the system.

The concentration reaches its maximum between

$$t \approx 2.5 \text{ days} \quad \text{and} \quad t \approx 3 \text{ days}.$$

Among the three cases, the curve corresponding to $P_2 = 60$ attains the highest peak, reaching approximately

$$1780 \text{ CFU}/100\,\text{ml}.$$

The case $P_2 = 30$ gives an intermediate peak of about

$$1720 \text{ CFU}/100\,\text{ml},$$

while the case $P_2 = 0.6$ produces the lowest peak, approximately

$$1640 \text{ CFU}/100\,\text{ml}.$$

After the peak point, the *E. coli* concentration decreases rapidly for all parameter values. The three curves become very close after

$$t \approx 4 \text{ days},$$

showing that the long-term behaviour of the system is nearly the same regardless of the value of $P_2$. By the end of the simulation at

$$t = 5 \text{ days},$$

the concentration decreases to approximately

$$500 \text{ CFU}/100\,\text{ml}.$$

Overall 4.8 shows that algae competition influences the transient growth of *E. coli*, especially the peak concentration. Larger values of $P_2$ produce higher maximum bacterial concentrations during the early and middle stages. However, as time progresses, the suppressive effect becomes dominant, and all solutions decline toward a lower concentration level.

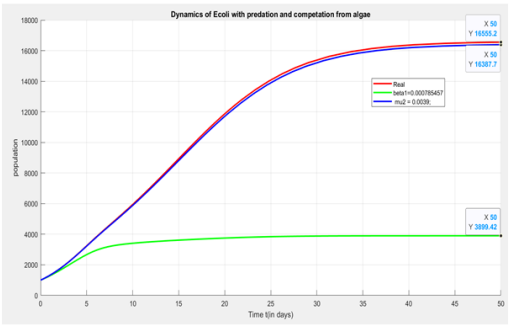


Figure 4.14: Dynamics of E.coli with predation and competation from algae

Figure 4.14 shows the dynamics of *E. coli* concentration under the combined effects of predation and competition from algae.At the initial time, the *E. coli* population is approximately

$$1000.$$

For the reference case, represented by the red curve, the bacterial population increases rapidly during the early stage of the simulation. The population continues to grow until it approaches a steady state value of approximately

$$16555.2$$

at

$$t = 50 \text{ days.}$$

This indicates that, under the reference parameter values, the system tends toward a high equilibrium population level.The blue curve, corresponding to the parameter case

$$\mu_2 = 0.0039,$$

follows almost the same pattern as the reference solution. It increases rapidly at first and then gradually approaches a steady state value of about

$$16387.7$$

at

$$t = 50 \text{ days.}$$

The closeness of the blue and red curves shows that this value of $\mu_2$ produces only a small reduction in the *E. coli* population compared with the reference case.In contrast, the green curve, corresponding to

$$\beta_1 = 0.000785457,$$

shows a much stronger suppressive effect on the bacterial population. Although the *E. coli* concentration initially increases, its growth rate is significantly reduced. The population approaches a much lower equilibrium value of approximately

$$3899.42$$

at

$$t = 50 \text{ days.}$$

Therefore, Figure 4.12 demonstrates that the parameter $\beta_1$ has a stronger controlling effect on *E. coli* growth than $\mu_2$. While the reference and $\mu_2$ cases lead to high equilibrium concentrations above

$$1.6 \times 10^4,$$

the $\beta_1$ case limits the population to below

$$4.0 \times 10^3.$$

This suggests that competition from algae, represented through $\beta_1$, plays an important role in suppressing *E. coli* concentration and reducing the final population level in the system.

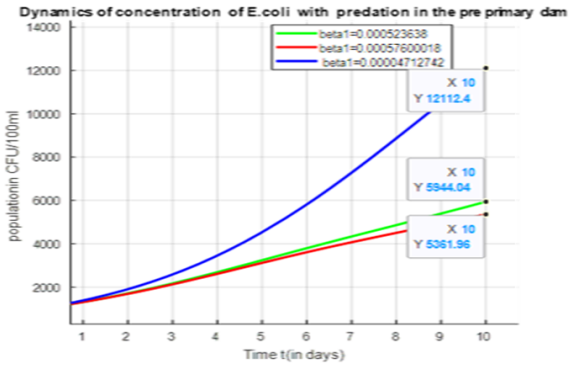


Figure 4.15: Dynamics of concentration of E.coli with predation in the preprimary dam

Figure 4.15 illustrates the dynamics of *E. coli* concentration under the effect of predation in the pre-primary dam for different values of the parameter $\beta_1$.

At the initial stage, the *E. coli* concentration is approximately

$$1200 \text{ CFU}/100\,\text{ml}.$$

For all considered values of $\beta_1$, the concentration increases with time, indicating that bacterial growth remains active throughout the simulation period. However, the rate of increase differs significantly depending on the value of $\beta_1$.

The blue curve, corresponding to the smaller value

$$\beta_1 = 0.000471274,$$

shows the fastest growth. The *E. coli* concentration increases rapidly and reaches approximately

$$12112.4 \text{ CFU}/100\,\text{ml}$$

at

$$t = 10 \text{ days}.$$

This indicates that a lower predation-related parameter allows the bacterial population to grow more strongly.

The green curve, corresponding to

$$\beta_1 = 0.000523638,$$

shows a moderate increase in concentration. At

$$t = 10 \text{ days},$$

the population reaches approximately

$$5844.04 \text{ CFU}/100\,\text{ml}.$$

The red curve, corresponding to the larger value

$$\beta_1 = 0.00057600018,$$

produces the lowest bacterial concentration among the three cases. At the final time, the concentration reaches approximately

$$5361.96 \text{ CFU}/100\,\text{ml}.$$

Overall, Figure 4.10 shows that the parameter $\beta_1$ has a strong influence on *E. coli* growth in the pre-primary dam. A smaller value of $\beta_1$ results in rapid bacterial growth and a much higher final concentration, while increasing $\beta_1$ suppresses the growth rate and reduces the final *E. coli* population. Therefore, stronger predattion effects help control the accumulation of *E. coli* in the system.

The simulation results demonstrate the combined influence of bacterial growth, antibiotic resistance development, treatment effects, and bacteriophage predation on wastewater microbial dynamics. The numerical outcomes support the analytical findings by illustrating the long-term behaviour of the system under different parameter scenarios. However, since several parameters are obtained from literature-based estimates, further validation using wastewater treatment plant data is recommended before direct operational application.the solution trajectory approaches stable equilibrium behaviour consistent with the analytical stability analysis

Overall, the numerical results demonstrate the interaction between microbial growth, antibiotic resistance development, treatment effects, and bacteriophage predation within

the wastewater system. The simulations support the analytical findings by illustrating how different biological mechanisms influence the persistence or reduction of *E. coli* populations. These results provide a basis for evaluating possible intervention strategies for controlling antibiotic-resistant bacteria in wastewater environments.

**NOTE**;Part of this section is published in the article named;
**Modeling Escherichia Coli Dynamics in Multi-Stage Wastewater Treatment Systems**.
DOI: 10.51584/IJRIAS.2026.11010083

## 4.3 Analysis of Caputo–Fabrizio fractional derivatives form model B

In order to comprehend the movement, permanence, and management of microbiological pollutants in wastewater systems, mathematical modeling has emerged as a crucial tool. Models of classical integer-order differential equations have been used extensively to explain the dynamics of contaminants and their treatment procedures(Ahmed et al., 2023). The memory, latency, and genetic consequences that result from biological and environmental processes—such as bacterial adaptability, resistance development, and treatment history which may not be sufficiently captured by such models ,Ali *et al.* ((2020)),

The ability to handle derivatives of non-integer order in fractional calculus makes it a logical extension of classical modeling frameworks. Complex dynamical systems with memory effects can be more accurately and flexibly represented using fractional-order models.Because it uses a non-singular exponential kernel, the Caputo–Fabrizio fractional derivative, in particular, avoids the singularity that occurs in the traditional Caputo derivative and has been effectively used in several biological and environmental applications(Ahmed et al., 2023).

For *E. coli* dynamics, this study developed a multi-stage wastewater treatment model incorporating antibiotic resistance mechanisms, bacteriophage predation, and Monod-type bacterial growth. Both the classical integer-order formulation and the Caputo–Fabrizio fractional-order extension were considered to investigate how memory effects influence microbial behaviour within the wastewater treatment system ,Ali *et al.* ((2020)), Biologically, the fractional memory effect represents the influence of previous environmental conditions, treatment exposure, and microbial adaptation history on the current population dynamics. In wastewater systems, bacterial populations do not respond instantaneously to environmental changes because growth, resistance development, and treatment responses may depend on previous states of the system. Therefore, the Caputo–Fabrizio fractional formulation provides a more flexible framework for representing delayed microbial responses that may not be completely captured by conventional integer-order differ-

ential models. The Caputo–Fabrizio fractional derivative extends classical differentiation by introducing a non-integer order operator capable of describing systems with memory effects(2020)). Unlike the traditional Caputo derivative, the Caputo–Fabrizio operator uses a non-singular exponential kernel, making it suitable for modelling biological systems where previous states influence current dynamics ,Ali *et al.* ((2020)),.

In this study, the integer-order Model A was transformed into the Caputo–Fabrizio fractional-order Model B by replacing the classical derivatives with fractional operators(ur Rahman *et al* (2021)). The resulting system preserves the biological mechanisms of the original model while incorporating memory effects associated with microbial adaptation, resistance development, and wastewater treatment history(ur Rahman *et al* (2021)).

### 4.3.1 Caputo–Fabrizio fractional derivatives form model B

**Existence and uniqueness**

This study used fixed point theorems to demonstrate the existence and uniqueness of model solutions, hence expressed as (Ahmed et al., 2023),(Edessa, 2022).

$$
\begin{aligned}
{}^{CF}D^{\alpha}W &= K_1(\kappa, W),\\
{}^{CF}D^{\alpha}X &= K_2(\kappa, X),\\
{}^{CF}D^{\alpha}Y &= K_3(\kappa, Y),\\
{}^{CF}D^{\alpha}Z &= K_4(\kappa, Z),\\
{}^{CF}D^{\alpha}T &= K_5(\kappa, T),\\
{}^{CF}D^{\alpha}V &= K_6(\kappa, V),\\
{}^{CF}D^{\alpha}P &= K_7(\kappa, P).
\end{aligned} \tag{4.1}
$$

Where

$$
\begin{aligned}
K_1(\kappa, W) &= \left(\pi_1 + \pi_2 - \mu_1 W - \mu_2 W - \beta_1 WV + \frac{\pi_m WS}{K_2 + S} - \gamma_1 W\right)\left(1 - \frac{N}{A}\right), \\
K_2(\kappa, X) &= \left(\gamma_1 W + \pi_1 - \mu_1 X - \mu_2 X - \omega_1 XP + \frac{\pi_m XS}{K_2 + S} - \gamma_2 X\right)\left(1 - \frac{N}{A}\right), \\
K_3(\kappa, Y) &= \left(\gamma_2 X + \pi_1 - \mu_1 Y + \frac{\pi_m YS}{K_2 + S} - \gamma_3 Y\right)\left(1 - \frac{N}{A}\right), \\
K_4(\kappa, Z) &= \left(\gamma_3 Y + \pi_1 + \pi_4 - \mu_2 Z + \frac{\pi_m ZS}{K_2 + S} - \gamma_4 Z\right)\left(1 - \frac{N}{A}\right), \\
K_5(\kappa, T) &= \left(\gamma_4 Z(1 - \Omega) - \mu_1 T + \frac{\pi_m TS}{K_2 + S} - \Phi T\right)\left(1 - \frac{N}{A}\right), \\
K_6(\kappa, V) &= \left(\beta_2 WV + \pi_3 - \mu_1 V + \frac{\pi_m VS}{K_2 + S} + \Lambda V\right)\left(1 - \frac{B}{A}\right), \\
K_7(\kappa, P) &= \left(\Lambda V + \beta_2 \omega_2 XP - \mu_1 P + \frac{\pi_m PS}{K_2 + S}\right)\left(1 - \frac{B}{A}\right). \qquad (4.49)
\end{aligned}
$$

Applying the fractional integral operator, system (4.49) reduces to a Volterra integral type of order $0 < \alpha < 1$, which is represented as follows(Ali *et al.* (2020)(Edessa, 2022)).

.

$$
\begin{aligned}
W(k) &= W(0) + \frac{2(1-\alpha)}{(2-\alpha)\mathcal{M}(\alpha)} K_1(\kappa, W) + \frac{2\alpha}{(2-\alpha)\mathcal{M}(\alpha)} \int_0^k K_1(y, W)\, dy, \\
X(k) &= X(0) + \frac{2(1-\alpha)}{(2-\alpha)\mathcal{M}(\alpha)} K_2(\kappa, X) + \frac{2\alpha}{(2-\alpha)\mathcal{M}(\alpha)} \int_0^k K_2(y, X)\, dy, \\
Y(k) &= Y(0) + \frac{2(1-\alpha)}{(2-\alpha)\mathcal{M}(\alpha)} K_3(\kappa, Y) + \frac{2\alpha}{(2-\alpha)\mathcal{M}(\alpha)} \int_0^k K_3(y, Y)\, dy, \\
Z(k) &= Z(0) + \frac{2(1-\alpha)}{(2-\alpha)\mathcal{M}(\alpha)} K_4(\kappa, Z) + \frac{2\alpha}{(2-\alpha)\mathcal{M}(\alpha)} \int_0^k K_4(y, Z)\, dy, \\
T(k) &= T(0) + \frac{2(1-\alpha)}{(2-\alpha)\mathcal{M}(\alpha)} K_5(\kappa, T) + \frac{2\alpha}{(2-\alpha)\mathcal{M}(\alpha)} \int_0^k K_5(y, T)\, dy, \\
V(k) &= V(0) + \frac{2(1-\alpha)}{(2-\alpha)\mathcal{M}(\alpha)} K_6(\kappa, V) + \frac{2\alpha}{(2-\alpha)\mathcal{M}(\alpha)} \int_0^k K_6(y, V)\, dy, \\
P(k) &= P(0) + \frac{2(1-\alpha)}{(2-\alpha)\mathcal{M}(\alpha)} K_7(\kappa, P) + \frac{2\alpha}{(2-\alpha)\mathcal{M}(\alpha)} \int_0^k K_7(y, P)\, dy. \qquad (4.50)
\end{aligned}
$$

Next,under some assumptions, we display the kernels $K_1, K_2, K_3, K_4, K_5, K_6$ and $K_7$ obey the Lipschitz and contraction conditions by proving the following lemma.

**Lemma 1:** The autonomous system (4.50) is Lipschitz continuous (Ahmed et al., 2023)(Edessa, 2022).

**Proof for $W$ and $W^*$:** Equation (4.50) this study obtained

$$\|K_1(\kappa,W)-K_1(\kappa,W^*)\| = \left(\mu_1+\mu_2+\beta_1 V+\gamma_1+\frac{\pi_m S}{K_2+S}\right)\left(1-\frac{N}{A}\right)\|W(k)-W^*(k)\|$$

$$\leq \beta_1 V(k)\left(\mu_1+\mu_2+\gamma_1+\frac{\pi_m S}{K_2+S}\right)\left(1-\frac{N}{A}\right)\|W(k)-W^*(k)\|$$

$$\leq \beta_1\epsilon_1+\left(\mu_1+\mu_2+\gamma_1+\frac{\pi_m S}{K_2+S}\right)\left(1-\frac{N}{A}\right)\|W(k)-W^*(k)\|$$

$$\leq l_1\|W(k)-W^*(k)\| \tag{4.51}$$

Where $0 < l_1 = \beta_1\epsilon_1 + \left(\mu_1+\mu_2+\gamma_1+\frac{\pi_m S}{K_2+S}\right)\left(1-\frac{N}{A}\right)$ and $\|V(k)\| \leq \epsilon_1$ is bounded.

**From $X$ and $X^*$ this study obtains**

$$\|K_2(\kappa,X)-K_2(X^*)\| = \left(\mu_1+\mu_2+\omega_1 P+\frac{\pi_m S}{K_2+S}+\gamma_2\right)\left(1-\frac{N}{A}\right)\|X(k)-X^*(k)\|$$

$$\leq \|\omega_1 P\|+\left(\mu_1+\mu_2+\frac{\pi_m S}{K_2+S}+\gamma_2\right)\left(1-\frac{N}{A}\right)\|X(k)-X^*(k)\|$$

$$\leq \|\omega_1\epsilon_2\|-\left(\mu_1+\mu_2+\frac{\pi_m S}{K_2+S}+\gamma_2\right)\left(1-\frac{N}{A}\right)\|X(k)-X^*(k)\|$$

$$\leq l_2\|X(k)-X^*(k)\| \tag{4.52}$$

Where

$$0 < l_2 = \omega_1\epsilon_2+\left(-\mu_1-\mu_2+\frac{\pi_m S}{K_2+S}+\gamma_2\right)\left(1-\frac{N}{A}\right) \quad \text{and} \quad \|P(k)\| \leq \epsilon_2 \text{ is bounded.} \tag{4.53}$$

**From $Y$ and $Y^*$ from (4.50),this study obtains**

$$\|K_3(\kappa,Y)-K_3(\kappa,Y^*)\| = \left(\mu_1+\frac{\pi_m S}{K_2+S}+\gamma_3\right)\left(1-\frac{N}{A}\right)\|Y(k)-Y^*(k)\|$$

$$\leq l_3\|Y(k)-Y^*(k)\|$$

$$0 < l_3 = \left(\mu_1+\frac{\pi_m S}{K_2+S}+\gamma_3\right)\left(1-\frac{N}{A}\right) \tag{4.54}$$

**From $Z$ and $Z^*$ from (4.50),this study obtains**

$$\|K_4(\kappa, Z) - K_4(\kappa, Z^*)\| = \mu_1 + \frac{\pi_m S}{K_2 + S} + \gamma_4 \left(1 - \frac{N}{A}\right) \|Z(k) - Z^*(k)\|$$

$$\leq l_4 \|Y(k) - Y^*(k)\|$$

$$0 < l_4 = \mu_1 + \frac{\pi_m S}{K_2 + S} + \gamma_4 \left(1 - \frac{N}{A}\right) \tag{4.55}$$

**From $T$ and $T^*$from (4.50),this study obtains**

$$\|K_5(\kappa, T) - K_3(\kappa, T^*)\| = \left(\mu_1 + \frac{\pi m S}{K_2 + S} - \Phi\right) \left(1 - \frac{N}{A}\right) \|T(k) - T^*(k)\|$$

$$\leq l_5 \|T(k) - T^*(k)\|$$

$$0 < l_5 = \left(\mu_1 + \frac{\pi m S}{K_2 + S} - \Phi\right) \left(1 - \frac{N}{A}\right) \tag{4.56}$$

**From $V$ and $V^*$from (4.50),this study obtains**

$$\|K_6(\kappa, V) - K_6(\kappa, V^*)\| = \left(\|\beta_2 W + \mu_1 + \frac{\pi m S}{K_2 + S} + \Lambda\right) \left(1 - \frac{B}{A}\right) \|V(k) - V^*(k)\|$$

$$\leq \beta_2 \|W\| + \left(\mu_1 + \frac{\pi m S}{K_2 + S} + \Lambda\right) \left(1 - \frac{B}{A}\right) \|V(k) - V^*(k)\|$$

$$\leq \beta_2 \epsilon_3 + \left(\mu_1 + \frac{\pi m S}{K_2 + S} + \Lambda\right) \left(1 - \frac{B}{A}\right) \|V(k) - V^*(k)\|$$

$$\leq l_6 \|V(k) - V^*(k)\| \tag{4.57}$$

Where

$$0 < l_6 = \beta_2 \epsilon_3 + \left(\mu_1 + \frac{\pi m S}{K_2 + S} + \Lambda\right) \left(1 - \frac{B}{A}\right) \quad \text{and} \quad \|W(k)\| \leq \epsilon_3 \text{ is bounded.}$$

**From $P$ and $P^*$ we have from (4.50),give**
$\Delta V + \omega_2 X P - \mu_1 P + \frac{\pi m P S}{K_2 + S}$

$$\|K_6(\kappa, P) - K_6(\kappa, P^*)\| = \left(\omega_2 X + \mu_1 + \frac{\pi m S}{K_2 + S}\right) \left(1 - \frac{B}{A}\right) \|P(k) - P^*(k)\|$$

$$\|K_6(\kappa, P) - K_6(\kappa, P^*)\| = \left(\omega_2 X + \mu_1 + \frac{\pi m S}{K_2 + S}\right)\left(1 - \frac{B}{A}\right)\|P(k) - P^*(k)\|$$

$$\leq \omega_2\|X\| + \left(\mu_1 + \frac{\pi m S}{K_2 + S}\right)\left(1 - \frac{B}{A}\right)\|P(k) - P^*(k)\|$$

$$\leq \omega_2\|X\| + \left(\mu_1 + \frac{\pi m S}{K_2 + S}\right)\left(1 - \frac{B}{A}\right)\|P(k) - P^*(k)\|$$

$$\leq l_7\|P(k) - P^*(k)\| \tag{4.58}$$

Where

$$0 < l_7 = \omega_2\epsilon_4 + \left(\mu_1 + \frac{\pi m S}{K_2 + S}\right)\left(1 - \frac{B}{A}\right) \quad \text{and} \quad \|X(k)\| \leq \epsilon_4 \text{ is bounded.}$$

Hence, it's Lipschitz continuous, and the proof of the lemma is complete. The system (4.51) can be written in recursive form by the difference between the successive terms as shown in system (4.52), shown below (Edessa, 2022) ,(Ahmed et al., 2023) (Ahmad et

al., 2025).

$$
\begin{aligned}
X_{1n} = W_n(K) - W_{n-1}(k) &= \frac{2(1-\alpha)}{(2-\alpha)\mathcal{M}(\alpha)} K_1(\kappa, W_{n-1}) - K_1(\kappa, W_{n-2}) \\
&\quad + \frac{2\alpha}{(2-\alpha)\mathcal{M}(\alpha)} \int_0^k \left(K_1(\kappa, W_{n-1}) - K_1(\kappa, W_{n-2})\right) dy, \\
X_{2n} = X_n(K) - X_{n-1}(k) &= \frac{2(1-\alpha)}{(2-\alpha)\mathcal{M}(\alpha)} K_2(\kappa, X_{n-1}) - K_2(\kappa, X_{n-2}) \\
&\quad + \frac{2\alpha}{(2-\alpha)\mathcal{M}(\alpha)} \int_0^k \left(K_2(\kappa, X_{n-1}) - K_2(\kappa, X_{n-2})\right) dy, \\
X_{3n} = Y(K) - Y_{n-1}(k) &= \frac{2(1-\alpha)}{(2-\alpha)\mathcal{M}(\alpha)} K_3(\kappa, Y_{n-1}) - K_3(\kappa, Y_{n-2}) \\
&\quad + \frac{2\alpha}{(2-\alpha)\mathcal{M}(\alpha)} \int_0^k \left(K_3(\kappa, Y_{n-1}) - K_3(\kappa, Y_{n-2})\right) dy, \\
X_{4n} = Z_n(K) - Z_{n-1}(k) &= \frac{2(1-\alpha)}{(2-\alpha)\mathcal{M}(\alpha)} K_4(\kappa, Z_{n-1}) - K_4(\kappa, Z_{n-2}) \\
&\quad + \frac{2\alpha}{(2-\alpha)\mathcal{M}(\alpha)} \int_0^k \left(K_4(\kappa, Z_{n-1}) - K_4(\kappa, Z_{n-2})\right) dy, \\
X_{5n} = T_n(K) - T_{n-1}(k) &= \frac{2(1-\alpha)}{(2-\alpha)\mathcal{M}(\alpha)} K_5(\kappa, T_{n-1}) - K_5(\kappa, T_{n-2}) \\
&\quad + \frac{2\alpha}{(2-\alpha)\mathcal{M}(\alpha)} \int_0^k \left(K_5(\kappa, T_{n-1}) - K_5(\kappa, T_{n-2})\right) dy, \\
X_{6n} = V_n(K) - V_{n-1}(k) &= \frac{2(1-\alpha)}{(2-\alpha)\mathcal{M}(\alpha)} K_6(\kappa, V_{n-1}) - K_6(\kappa, V_{n-2}) \\
&\quad + \frac{2\alpha}{(2-\alpha)\mathcal{M}(\alpha)} \int_0^k \left(K_6(\kappa, V_{n-1}) - K_6(\kappa, V_{n-2})\right) dy, \\
X_{7n} = P_n(K) - P_{n-1}(k) &= \frac{2(1-\alpha)}{(2-\alpha)\mathcal{M}(\alpha)} K_7(\kappa, P_{n-1}) - K_7(\kappa, P_{n-2}) \\
&\quad + \frac{2\alpha}{(2-\alpha)\mathcal{M}(\alpha)} \int_0^k \left(K_7(\kappa, P_{n-1}) - K_7(\kappa, P_{n-2})\right) dy. \quad (4.59)
\end{aligned}
$$

Subject to initial conditions

$$W_0(k) = W(0),\ X_0(k) = X(0),\ Y_0(k) = Y(0),\ Z_0(k) = Z(0),\ T_0(k) = T(0),\ V_0(k) = V(0),$$

and

$$P_0(k) = P(0).$$

From the equations of system (4.51) , taking the norm and applying the triangular

inequality, we obtain

$$\begin{aligned}
\|W_n(K) - W_{n-1}(k)\| &= \frac{2(1-\alpha)}{(2-\alpha)\mathcal{M}(\alpha)}\|K_1(\kappa, W_{n-1}) - K_1(\kappa, W_{n-2})\| \\
&\quad + \frac{2\alpha}{(2-\alpha)\mathcal{M}(\alpha)}\int_0^k \|K_1(\kappa, W_{n-1}) - K_1(\kappa, W_{n-2})\|\, dy, \\
\|X_n(K) - X_{n-1}(k)\| &= \frac{2(1-\alpha)}{(2-\alpha)\mathcal{M}(\alpha)}\|K_2(\kappa, X_{n-1}) - K_2(\kappa, X_{n-2})\| \\
&\quad + \frac{2\alpha}{(2-\alpha)\mathcal{M}(\alpha)}\int_0^k \|K_2(\kappa, X_{n-1}) - K_2(\kappa, X_{n-2})\|\, dy, \\
\|Y_n(K) - Y_{n-1}(k)\| &= \frac{2(1-\alpha)}{(2-\alpha)\mathcal{M}(\alpha)}\|K_3(\kappa, Y_{n-1}) - K_3(\kappa, Y_{n-2})\| \\
&\quad + \frac{2\alpha}{(2-\alpha)\mathcal{M}(\alpha)}\int_0^k \|K_3(\kappa, Y_{n-1}) - K_3(\kappa, Y_{n-2})\|\, dy, \\
\|Z_n(K) - Z_{n-1}(k)\| &= \frac{2(1-\alpha)}{(2-\alpha)\mathcal{M}(\alpha)}\|K_4(\kappa, Z_{n-1}) - K_4(\kappa, Z_{n-2})\| \\
&\quad + \frac{2\alpha}{(2-\alpha)\mathcal{M}(\alpha)}\int_0^k \|K_4(\kappa, Z_{n-1}) - K_4(\kappa, Z_{n-2})\|\, dy, \\
\|T_n(K) - T_{n-1}(k)\| &= \frac{2(1-\alpha)}{(2-\alpha)\mathcal{M}(\alpha)}\|K_5(\kappa, T_{n-1}) - K_5(\kappa, T_{n-2})\| \\
&\quad + \frac{2\alpha}{(2-\alpha)\mathcal{M}(\alpha)}\int_0^k \|K_5(\kappa, T_{n-1}) - K_5(\kappa, T_{n-2})\|\, dy, \\
\|V_n(K) - V_{n-1}(k)\| &= \frac{2(1-\alpha)}{(2-\alpha)\mathcal{M}(\alpha)}\|K_6(\kappa, V_{n-1}) - K_6(\kappa, V_{n-2})\| \\
&\quad + \frac{2\alpha}{(2-\alpha)\mathcal{M}(\alpha)}\int_0^k \|K_6(\kappa, V_{n-1}) - K_6(\kappa, V_{n-2})\|\, dy, \\
\|P_n(K) - P_{n-1}(k)\| &= \frac{2(1-\alpha)}{(2-\alpha)\mathcal{M}(\alpha)}\|K_7(\kappa, P_{n-1}) - K_7(\kappa, P_{n-2})\| \\
&\quad + \frac{2\alpha}{(2-\alpha)\mathcal{M}(\alpha)}\int_0^k \|K_7(\kappa, P_{n-1}) - K_7(\kappa, P_{n-2})\|\, dy. \qquad (4.60)
\end{aligned}$$

Given Lemma 1, the study obtained according to (Edessa, 2022).

$$
\begin{aligned}
\|W_n(K) - W_{n-1}(k)\| &= \frac{2(1-\alpha)}{(2-\alpha)\mathcal{M}(\alpha)} l_1 \|W_{n-1} - W_{n-2}\| \\
&\quad + \frac{2\alpha}{(2-\alpha)\mathcal{M}(\alpha)} \int_0^k \|W_{n-1} - W_{n-2}\| \, dy, \\
\|X_n(K) - X_{n-1}(k)\| &= \frac{2(1-\alpha)}{(2-\alpha)\mathcal{M}(\alpha)} l_2 \|X_{n-1} - X_{n-2}\| \\
&\quad + \frac{2\alpha}{(2-\alpha)\mathcal{M}(\alpha)} \int_0^k \|X_{n-1} - X_{n-2}\| \, dy, \\
\|Y_n(K) - Y_{n-1}(k)\| &= \frac{2(1-\alpha)}{(2-\alpha)\mathcal{M}(\alpha)} l_3 \|Y_{n-1} - Y_{n-2}\| \\
&\quad + \frac{2\alpha}{(2-\alpha)\mathcal{M}(\alpha)} \int_0^k \|Y_{n-1} - Y_{n-2}\| \, dy, \\
\|Z_n(K) - Z_{n-1}(k)\| &= \frac{2(1-\alpha)}{(2-\alpha)\mathcal{M}(\alpha)} l_4 \|Z_{n-1} - Z_{n-2}\| \\
&\quad + \frac{2\alpha}{(2-\alpha)\mathcal{M}(\alpha)} \int_0^k \|Z_{n-1} - Z_{n-2}\| \, dy, \\
\|T_n(K) - T_{n-1}(k)\| &= \frac{2(1-\alpha)}{(2-\alpha)\mathcal{M}(\alpha)} l_5 \|T_{n-1} - T_{n-2}\| \\
&\quad + \frac{2\alpha}{(2-\alpha)\mathcal{M}(\alpha)} \int_0^k \|T_{n-1} - T_{n-2}\| \, dy, \\
\|V_n(K) - V_{n-1}(k)\| &= \frac{2(1-\alpha)}{(2-\alpha)\mathcal{M}(\alpha)} l_6 \|V_{n-1} - V_{n-2}\| \\
&\quad + \frac{2\alpha}{(2-\alpha)\mathcal{M}(\alpha)} \int_0^k \|V_{n-1} - V_{n-2}\| \, dy, \\
\|P_n(K) - P_{n-1}(k)\| &= \frac{2(1-\alpha)}{(2-\alpha)\mathcal{M}(\alpha)} l_7 \|P_{n-1} - P_{n-2}\| \\
&\quad + \frac{2\alpha}{(2-\alpha)\mathcal{M}(\alpha)} \int_0^k \|P_{n-1} - P_{n-2}\| \, dy. \qquad (4.61)
\end{aligned}
$$

Therefore,the study obtained

$$\|\chi_{1n}(k)\| = \frac{2(1-\alpha)}{(2-\alpha)\mathcal{M}(\alpha)} l_1 \|\chi_{1(n-1)}(k)\| + \frac{2\alpha}{(2-\alpha)\mathcal{M}(\alpha)} l_1 \int_0^k \|\chi_{1(n-1)}(y)\| \, dy,$$
$$\|\chi_{2n}(k)\| = \frac{2(1-\alpha)}{(2-\alpha)\mathcal{M}(\alpha)} l_2 \|\chi_{2(n-1)}(k)\| + \frac{2\alpha}{(2-\alpha)\mathcal{M}(\alpha)} l_2 \int_0^k \|\chi_{2(n-1)}(y)\| \, dy,$$
$$\|\chi_{3n}(k)\| = \frac{2(1-\alpha)}{(2-\alpha)\mathcal{M}(\alpha)} l_3 \|\chi_{3(n-1)}(k)\| + \frac{2\alpha}{(2-\alpha)\mathcal{M}(\alpha)} l_3 \int_0^k \|\chi_{3(n-1)}(y)\| \, dy,$$
$$\|\chi_{4n}(k)\| = \frac{2(1-\alpha)}{(2-\alpha)\mathcal{M}(\alpha)} l_4 \|\chi_{4(n-1)}(k)\| + \frac{2\alpha}{(2-\alpha)\mathcal{M}(\alpha)} l_4 \int_0^k \|\chi_{4(n-1)}(y)\| \, dy,$$
$$\|\chi_{5n}(k)\| = \frac{2(1-\alpha)}{(2-\alpha)\mathcal{M}(\alpha)} l_5 \|\chi_{5(n-1)}(k)\| + \frac{2\alpha}{(2-\alpha)\mathcal{M}(\alpha)} l_5 \int_0^k \|\chi_{5(n-1)}(y)\| \, dy,$$
$$\|\chi_{6n}(k)\| = \frac{2(1-\alpha)}{(2-\alpha)\mathcal{M}(\alpha)} l_6 \|\chi_{6(n-1)}(k)\| + \frac{2\alpha}{(2-\alpha)\mathcal{M}(\alpha)} l_6 \int_0^k \|\chi_{6(n-1)}(y)\| \, dy,$$
$$\|\chi_{7n}(k)\| = \frac{2(1-\alpha)}{(2-\alpha)\mathcal{M}(\alpha)} l_7 \|\chi_{7(n-1)}(k)\| + \frac{2\alpha}{(2-\alpha)\mathcal{M}(\alpha)} l_7 \int_0^k \|\chi_{7(n-1)}(y)\| \, dy. \quad (4.61)$$

Hence

$$\begin{cases} W_n(k) = \sum_{k=1}^{n} \chi_1(k) \\ X_n(k) = \sum_{k=1}^{n} \chi_2(k) \\ Y_n(k) = \sum_{k=1}^{n} \chi_3(k) \\ Z_n(k) = \sum_{k=1}^{n} \chi_4(k) \\ T_n(k) = \sum_{k=1}^{n} \chi_5(k) \\ V_n(k) = \sum_{k=1}^{n} \chi_6(k) \\ P_n(k) = \sum_{k=1}^{n} \chi_7(k) \end{cases} \quad (4.62)$$

The following theorem guarantees the existence of a solution

**Theorem 5**

Consider the model given by (4.49); then there exists a solution if one can find $k_1$ for which

$$\frac{2(1-\alpha)}{(2-\alpha)\mathcal{M}(\alpha)} l_k + \frac{2\alpha k_1}{(2-\alpha)\mathcal{M}(\alpha)} l_k < 1, \quad k = 1, 2, \ldots, 4. \quad (4.63)$$

**Proof:** From Lemma 1 and Equation (4.55), applying the recursive technique we obtained

below

$$\|\chi_{1n}(k)\| \leq \|W_n(0)\| \left[\frac{2(1-\alpha)}{(2-\alpha)\mathcal{M}(\alpha)}l_1 + \frac{2\alpha k_1}{(2-\alpha)\mathcal{M}(\alpha)}l_1\right]^n,$$
$$\|\chi_{2n}(k)\| \leq \|X_n(0)\| \left[\frac{2(1-\alpha)}{(2-\alpha)\mathcal{M}(\alpha)}l_2 + \frac{2\alpha k_1}{(2-\alpha)\mathcal{M}(\alpha)}l_2\right]^n,$$
$$\|\chi_{3n}(k)\| \leq \|Y_n(0)\| \left[\frac{2(1-\alpha)}{(2-\alpha)\mathcal{M}(\alpha)}l_3 + \frac{2\alpha k_1}{(2-\alpha)\mathcal{M}(\alpha)}l_3\right]^n,$$
$$\|\chi_{4n}(k)\| \leq \|Z_n(0)\| \left[\frac{2(1-\alpha)}{(2-\alpha)\mathcal{M}(\alpha)}l_4 + \frac{2\alpha k_1}{(2-\alpha)\mathcal{M}(\alpha)}l_4\right]^n,$$
$$\|\chi_{5n}(k)\| \leq \|T_n(0)\| \left[\frac{2(1-\alpha)}{(2-\alpha)\mathcal{M}(\alpha)}l_5 + \frac{2\alpha k_1}{(2-\alpha)\mathcal{M}(\alpha)}l_5\right]^n,$$
$$\|\chi_{6n}(k)\| \leq \|V_n(0)\| \left[\frac{2(1-\alpha)}{(2-\alpha)\mathcal{M}(\alpha)}l_6 + \frac{2\alpha k_1}{(2-\alpha)\mathcal{M}(\alpha)}l_6\right]^n,$$
$$\|\chi_{7n}(k)\| \leq \|P_n(0)\| \left[\frac{2(1-\alpha)}{(2-\alpha)\mathcal{M}(\alpha)}l_7 + \frac{2\alpha k_1}{(2-\alpha)\mathcal{M}(\alpha)}l_7\right]^n. \tag{4.64}$$

Showing that the system solution exists and is continuous. Next, we show that (4.56) constructs the solution for the model (4.49). We proceed as follows;

$$\begin{aligned}
W(t) - W(0) &= W_n(k) - \beta_1 n(k),\\
X(t) - X(0) &= X_n(k) - \beta_2 n(k),\\
Y(t) - Y(0) &= Y_n(k) - \beta_3 n(k),\\
Z(t) - Z(0) &= Z_n(k) - \beta_4 n(k),\\
T(t) - T(0) &= T_n(k) - \beta_5 n(k),\\
V(t) - V(0) &= V_n(k) - \beta_6 n(k),\\
P(t) - P(0) &= P_n(k) - \beta_7 n(k).
\end{aligned} \tag{4.65}$$

Thus we obtain

$$\|\beta_1 n(k)\| = \left\| \frac{2(1-\alpha)}{(2-\alpha)\mathcal{M}(\alpha)} \left(K_1(\kappa, W) - K_1(\kappa, W_{n-1})\right) K_1(\kappa, W_{n-1}) \right\| dy$$

$$\leq \frac{2(1-\alpha)}{(2-\alpha)\mathcal{M}(\alpha)} \|(K_1(\kappa, W) - K_1(\kappa, W_{n-1}))\| + \frac{2\alpha}{(2-\alpha)\mathcal{M}(\alpha)} \int_0^k \|(K_1(\kappa, W) - K_1(\kappa, W_{n-1}))\|$$

$$\leq \frac{2(1-\alpha)}{(2-\alpha)\mathcal{M}(\alpha)} l_1 \|W - W_{n-1}\| + \frac{2\alpha k}{(2-\alpha)\mathcal{M}(\alpha)} l_1 \|W - W_{n-1}\|$$

$$\|\beta_2 n(k)\| = \left\| \frac{2(1-\alpha)}{(2-\alpha)\mathcal{M}(\alpha)} \left(K_2(\kappa, X) - K_2(\kappa, X_{n-1})\right) K_2(\kappa, X_{n-1}) \right\| dy$$

$$\leq \frac{2(1-\alpha)}{(2-\alpha)\mathcal{M}(\alpha)} \|(K_2(\kappa, X) - K_2(\kappa, X_{n-1}))\| + \frac{2\alpha}{(2-\alpha)\mathcal{M}(\alpha)} \int_0^k \|(K_2(\kappa, X) - K_2(\kappa, X_{n-1}))\|$$

$$\leq \frac{2(1-\alpha)}{(2-\alpha)\mathcal{M}(\alpha)} l_2 \|X - X_{n-1}\| + \frac{2\alpha k}{(2-\alpha)\mathcal{M}(\alpha)} l_2 \|X - X_{n-1}\|$$

$$\|\beta_3 n(k)\| = \left\| \frac{2(1-\alpha)}{(2-\alpha)\mathcal{M}(\alpha)} \left(K_3(\kappa, Y) - K_3(\kappa, Y_{n-1})\right) K_3(\kappa, Y_{n-1}) \right\| dy$$

$$\leq \frac{2(1-\alpha)}{(2-\alpha)\mathcal{M}(\alpha)} \|K_3(\kappa, Y) - K_3(\kappa, Y_{n-1})\| + \frac{2\alpha}{(2-\alpha)\mathcal{M}(\alpha)} \int_0^k \|K_3(\kappa, Y) - K_3(\kappa, Y_{n-1})\|$$

$$\leq \frac{2(1-\alpha)}{(2-\alpha)\mathcal{M}(\alpha)} l_1 \|Y - Y_{n-1}\| + \frac{2\alpha k}{(2-\alpha)\mathcal{M}(\alpha)} l_1 \|Y - Y_{n-1}\|$$

$$\|\beta_4 n(k)\| = \left\| \frac{2(1-\alpha)}{(2-\alpha)\mathcal{M}(\alpha)} \left(K_4(\kappa, Z) - K_4(\kappa, Z_{n-1})\right) K_4(\kappa, Z_{n-1}) \right\| dy$$

$$\leq \frac{2(1-\alpha)}{(2-\alpha)\mathcal{M}(\alpha)} \|K_4(\kappa, Z) - K_4(\kappa, Z_{n-1})\| + \frac{2\alpha}{(2-\alpha)\mathcal{M}(\alpha)} \int_0^k \|K_4(\kappa, Z) - K_4(\kappa, Z_{n-1})\|$$

$$\leq \frac{2(1-\alpha)}{(2-\alpha)\mathcal{M}(\alpha)} l_4 \|Z - Z_{n-1}\| + \frac{2\alpha k}{(2-\alpha)\mathcal{M}(\alpha)} l_4 \|Z - Z_{n-1}\|$$

$$\|\beta_5 n(k)\| = \left\| \frac{2(1-\alpha)}{(2-\alpha)\mathcal{M}(\alpha)} \left(K_5(\kappa, P) - K_5(\kappa, T_{n-1})\right) K_5(\kappa, T_{n-1}) \right\| dy$$

$$\leq \frac{2(1-\alpha)}{(2-\alpha)\mathcal{M}(\alpha)} \|(K_5(\kappa, P) - K_5(\kappa, T_{n-1}))\| + \frac{2\alpha}{(2-\alpha)\mathcal{M}(\alpha)} \int_0^k \|(K_5(\kappa, T) - K_5(\kappa, T_{n-1}))\|$$

$$\leq \frac{2(1-\alpha)}{(2-\alpha)\mathcal{M}(\alpha)} l_7 \|P - P_{n-1}\| + \frac{2\alpha k}{(2-\alpha)\mathcal{M}(\alpha)} l_7 \|P - P_{n-1}\|$$

$$\|\beta_6 n(k)\| = \left\| \frac{2(1-\alpha)}{(2-\alpha)\mathcal{M}(\alpha)} \left(K_6(\kappa, V) - K_6(\kappa, V_{n-1})\right) K_6(\kappa, V_{n-1}) \right\| dy$$

$$\leq \frac{2(1-\alpha)}{(2-\alpha)\mathcal{M}(\alpha)} \|(K_6(\kappa, V) - K_6(\kappa, V_{n-1}))\| + \frac{2\alpha}{(2-\alpha)\mathcal{M}(\alpha)} \int_0^k \|(K_6(\kappa, V) - K_6(\kappa, V_{n-1}))\|$$

$$\leq \frac{2(1-\alpha)}{(2-\alpha)\mathcal{M}(\alpha)} l_6 \|V - V_{n-1}\| + \frac{2\alpha k}{(2-\alpha)\mathcal{M}(\alpha)} l_6 \|V - V_{n-1}\|$$

$$\|\beta_7 n(k)\| = \left\| \frac{2(1-\alpha)}{(2-\alpha)\mathcal{M}(\alpha)} \left(K_7(\kappa, P) - K_7(\kappa, P_{n-1})\right) K_7(\kappa, P_{n-1}) \right\| dy$$

$$\leq \frac{2(1-\alpha)}{(2-\alpha)\mathcal{M}(\alpha)} \|(K_7(\kappa, P) - K_7(\kappa, P_{n-1}))\| + \frac{2\alpha}{(2-\alpha)\mathcal{M}(\alpha)} \int_0^k \|(K_7(\kappa, P) - K_7(\kappa, P_{n-1}))\|$$

$$\leq \frac{2(1-\alpha)}{(2-\alpha)\mathcal{M}(\alpha)} l_7 \|P - P_{n-1}\| + \frac{2\alpha k}{(2-\alpha)\mathcal{M}(\alpha)} l_7 \|P - P_{n-1}\|$$

()4.58)

Using the process above,the study obtained the following solution(Ahmed et al., 2023)
;

$$\begin{aligned}
\|\beta_{1n}(k)\| &\leq \left( \frac{2(1-\alpha)}{(2-\alpha)\mathcal{M}(\alpha)} + \frac{2\alpha k}{(2-\alpha)\mathcal{M}(\alpha)} \right)^{n+1} l_1^{n+1} b, \\
\|\beta_{2n}(k)\| &\leq \left( \frac{2(1-\alpha)}{(2-\alpha)\mathcal{M}(\alpha)} + \frac{2\alpha k}{(2-\alpha)\mathcal{M}(\alpha)} \right)^{n+1} l_2^{n+1} b, \\
\|\beta_{3n}(k)\| &\leq \left( \frac{2(1-\alpha)}{(2-\alpha)\mathcal{M}(\alpha)} + \frac{2\alpha k}{(2-\alpha)\mathcal{M}(\alpha)} \right)^{n+1} l_3^{n+1} b, \\
\|\beta_{4n}(k)\| &\leq \left( \frac{2(1-\alpha)}{(2-\alpha)\mathcal{M}(\alpha)} + \frac{2\alpha k}{(2-\alpha)\mathcal{M}(\alpha)} \right)^{n+1} l_4^{n+1} b, \\
\|\beta_{5n}(k)\| &\leq \left( \frac{2(1-\alpha)}{(2-\alpha)\mathcal{M}(\alpha)} + \frac{2\alpha k}{(2-\alpha)\mathcal{M}(\alpha)} \right)^{n+1} l_5^{n+1} b, \\
\|\beta_{6n}(k)\| &\leq \left( \frac{2(1-\alpha)}{(2-\alpha)\mathcal{M}(\alpha)} + \frac{2\alpha k}{(2-\alpha)\mathcal{M}(\alpha)} \right)^{n+1} l_6^{n+1} b, \\
\|\beta_{7n}(k)\| &\leq \left( \frac{2(1-\alpha)}{(2-\alpha)\mathcal{M}(\alpha)} + \frac{2\alpha k}{(2-\alpha)\mathcal{M}(\alpha)} \right)^{n+1} l_7^{n+1} b.
\end{aligned} \tag{4.59}$$

We therefore obtained the following for the rest.

$$\begin{aligned}
\|\beta_{2n}(k)\| &\leq \left(\frac{2(1-\alpha)}{(2-\alpha)\mathcal{M}(\alpha)} + \frac{2\alpha k_2}{(2-\alpha)\mathcal{M}(\alpha)}\right)^{n+1} l_2^{n+1} b, \\
\|\beta_{3n}(k)\| &\leq \left(\frac{2(1-\alpha)}{(2-\alpha)\mathcal{M}(\alpha)} + \frac{2\alpha k_3}{(2-\alpha)\mathcal{M}(\alpha)}\right)^{n+1} l_3^{n+1} b, \\
\|\beta_{4n}(k)\| &\leq \left(\frac{2(1-\alpha)}{(2-\alpha)\mathcal{M}(\alpha)} + \frac{2\alpha k_4}{(2-\alpha)\mathcal{M}(\alpha)}\right)^{n+1} l_4^{n+1} b, \\
\|\beta_{5n}(k)\| &\leq \left(\frac{2(1-\alpha)}{(2-\alpha)\mathcal{M}(\alpha)} + \frac{2\alpha k_5}{(2-\alpha)\mathcal{M}(\alpha)}\right)^{n+1} l_5^{n+1} b, \\
\|\beta_{6n}(k)\| &\leq \left(\frac{2(1-\alpha)}{(2-\alpha)\mathcal{M}(\alpha)} + \frac{2\alpha k_6}{(2-\alpha)\mathcal{M}(\alpha)}\right)^{n+1} l_6^{n+1} b, \\
\|\beta_{7n}(k)\| &\leq \left(\frac{2(1-\alpha)}{(2-\alpha)\mathcal{M}(\alpha)} + \frac{2\alpha k_2}{(2-\alpha)\mathcal{M}(\alpha)}\right)^{n+1} l_7^{n+1} b.
\end{aligned} \tag{4.60}$$

As $n \to \infty$, (4.60) yields $\|\beta_{1n}(k)\| \to 0$
$\|\beta_{2n}(k)\| \to 0$, $\|\beta_{3n}(k)\| \to 0$, $\|\beta_{4n}(k)\| \to 0$, $\|\beta_{5n}(k)\| \to 0$, $\|\beta_{6n}(k)\| \to 0$ and $\|\beta_{7n}(k)\| \to 0$.

$$
\begin{aligned}
\|W(k)-W_1(k)\| &= \frac{2(1-\alpha)}{(2-\alpha)\mathcal{M}(\alpha)}\|K_1(k,W)-K_1(k,W_1)\| \\
&\quad + \frac{2\alpha}{(2-\alpha)\mathcal{M}(\alpha)}\int_0^k \|K_1(y,W)-K_1(y,W_1)\|\,dy, \\
\|X(k)-X_1(k)\| &= \frac{2(1-\alpha)}{(2-\alpha)\mathcal{M}(\alpha)}\|K_2(k,X)-K_2(k,X_1)\| \\
&\quad + \frac{2\alpha}{(2-\alpha)\mathcal{M}(\alpha)}\int_0^k \|K_2(y,X)-K_2(y,X_1)\|\,dy, \\
\|Y(k)-Y_1(k)\| &= \frac{2(1-\alpha)}{(2-\alpha)\mathcal{M}(\alpha)}\|K_3(k,Y)-K_3(k,Y_1)\| \\
&\quad + \frac{2\alpha}{(2-\alpha)\mathcal{M}(\alpha)}\int_0^k \|K_3(y,Y)-K_3(y,Y_1)\|\,dy, \\
\|Z(k)-Z_1(k)\| &= \frac{2(1-\alpha)}{(2-\alpha)\mathcal{M}(\alpha)}\|K_4(k,Z)-K_4(k,Z_1)\| \\
&\quad + \frac{2\alpha}{(2-\alpha)\mathcal{M}(\alpha)}\int_0^k \|K_4(y,Z)-K_4(y,Z_1)\|\,dy, \\
\|T(k)-T_1(k)\| &= \frac{2(1-\alpha)}{(2-\alpha)\mathcal{M}(\alpha)}\|K_5(k,T)-K_5(k,T_1)\| \\
&\quad + \frac{2\alpha}{(2-\alpha)\mathcal{M}(\alpha)}\int_0^k \|K_5(y,T)-K_5(y,T_1)\|\,dy, \\
\|V(k)-V_1(k)\| &= \frac{2(1-\alpha)}{(2-\alpha)\mathcal{M}(\alpha)}\|K_6(k,V)-K_6(k,V_1)\| \\
&\quad + \frac{2\alpha}{(2-\alpha)\mathcal{M}(\alpha)}\int_0^k \|K_6(y,V)-K_6(y,V_1)\|\,dy, \\
\|P(k)-P_1(k)\| &= \frac{2(1-\alpha)}{(2-\alpha)\mathcal{M}(\alpha)}\|K_7(k,P)-K_7(k,P_1)\| \\
&\quad + \frac{2\alpha}{(2-\alpha)\mathcal{M}(\alpha)}\int_0^k \|K_7(y,P)-K_7(y,P_1)\|\,dy. \qquad (4.61)
\end{aligned}
$$

Taking the norm of (4.61) and from Lemma 1, the study gets

$$\begin{aligned}
\|W(k)-W_1(k)\| &\leq \frac{2(1-\alpha)}{(2-\alpha)\mathcal{M}(\alpha)}\|K_1(k,W)-K_1(k,W_1)\| \\
&\quad+\frac{2\alpha}{(2-\alpha)\mathcal{M}(\alpha)}\int_0^k \|K_1(y,W)-K_1(y,W_1)\|\,dy \\
&\leq \frac{2(1-\alpha)l_1}{(2-\alpha)\mathcal{M}(\alpha)}\|W(k)-W_1(k)\| \\
&\quad+\frac{2\alpha l_1}{(2-\alpha)\mathcal{M}(\alpha)}\int_0^k \|W(y)-W_1(y)\|\,dy \\
&\leq \frac{2((1-\alpha)+\alpha k)l_1}{(2-\alpha)\mathcal{M}(\alpha)}D, \\
\|X(k)-X_1(k)\| &\leq \frac{2(1-\alpha)}{(2-\alpha)\mathcal{M}(\alpha)}\|K_2(k,X)-K_2(k,X_1)\| \\
&\quad+\frac{2\alpha}{(2-\alpha)\mathcal{M}(\alpha)}\int_0^k \|K_2(y,X)-K_2(y,X_1)\|\,dy \\
&\leq \frac{2(1-\alpha)l_2}{(2-\alpha)\mathcal{M}(\alpha)}\|X(k)-X_1(k)\| \\
&\quad+\frac{2\alpha l_2}{(2-\alpha)\mathcal{M}(\alpha)}\int_0^k \|X(y)-X_1(y)\|\,dy \\
&\leq \frac{2((1-\alpha)+\alpha k)l_2}{(2-\alpha)\mathcal{M}(\alpha)}D, \\
\|Y(k)-Y_1(k)\| &\leq \frac{2(1-\alpha)}{(2-\alpha)\mathcal{M}(\alpha)}\|K_3(k,Y)-K_3(k,Y_1)\| \\
&\quad+\frac{2\alpha}{(2-\alpha)\mathcal{M}(\alpha)}\int_0^k \|K_3(y,Y)-K_3(y,Y_1)\|\,dy \\
&\leq \frac{2(1-\alpha)l_3}{(2-\alpha)\mathcal{M}(\alpha)}\|Y(k)-Y_1(k)\| \\
&\quad+\frac{2\alpha l_3}{(2-\alpha)\mathcal{M}(\alpha)}\int_0^k \|Y(y)-Y_1(y)\|\,dy \\
&\leq \frac{2((1-\alpha)+\alpha k)l_3}{(2-\alpha)\mathcal{M}(\alpha)}D, \\
\|Z(k)-Z_1(k)\| &\leq \frac{2(1-\alpha)}{(2-\alpha)\mathcal{M}(\alpha)}\|K_4(k,Z)-K_4(k,Z_1)\| \\
&\quad+\frac{2\alpha}{(2-\alpha)\mathcal{M}(\alpha)}\int_0^k \|K_4(y,Z)-K_4(y,Z_1)\|\,dy \\
&\leq \frac{2(1-\alpha)l_4}{(2-\alpha)\mathcal{M}(\alpha)}\|Z(k)-Z_1(k)\| \\
&\quad+\frac{2\alpha l_4}{(2-\alpha)\mathcal{M}(\alpha)}\int_0^k \|Z(y)-Z_1(y)\|\,dy \\
&\leq \frac{2((1-\alpha)+\alpha k)l_4}{(2-\alpha)\mathcal{M}(\alpha)}D. \qquad (4.62a)
\end{aligned}$$

$$
\begin{aligned}
\|T(k)-T_1(k)\| &\le \frac{2(1-\alpha)}{(2-\alpha)\mathcal{M}(\alpha)}\|K_5(k,T)-K_5(k,T_1)\| \\
&\quad+\frac{2\alpha}{(2-\alpha)\mathcal{M}(\alpha)}\int_0^k \|K_5(y,T)-K_5(y,T_1)\|\,dy \\
&\le \frac{2(1-\alpha)l_5}{(2-\alpha)\mathcal{M}(\alpha)}\|T(k)-T_1(k)\| \\
&\quad+\frac{2\alpha l_5}{(2-\alpha)\mathcal{M}(\alpha)}\int_0^k \|T(y)-T_1(y)\|\,dy \\
&\le \frac{2((1-\alpha)+\alpha k)l_5}{(2-\alpha)\mathcal{M}(\alpha)}D, \\
\|V(k)-V_1(k)\| &\le \frac{2(1-\alpha)}{(2-\alpha)\mathcal{M}(\alpha)}\|K_6(k,V)-K_6(k,V_1)\| \\
&\quad+\frac{2\alpha}{(2-\alpha)\mathcal{M}(\alpha)}\int_0^k \|K_6(y,V)-K_6(y,V_1)\|\,dy \\
&\le \frac{2(1-\alpha)l_6}{(2-\alpha)\mathcal{M}(\alpha)}\|V(k)-V_1(k)\| \\
&\quad+\frac{2\alpha l_6}{(2-\alpha)\mathcal{M}(\alpha)}\int_0^k \|V(y)-V_1(y)\|\,dy \\
&\le \frac{2((1-\alpha)+\alpha k)l_6}{(2-\alpha)\mathcal{M}(\alpha)}D, \\
\|P(k)-P_1(k)\| &\le \frac{2(1-\alpha)}{(2-\alpha)\mathcal{M}(\alpha)}\|K_7(k,P)-K_7(k,P_1)\| \\
&\quad+\frac{2\alpha}{(2-\alpha)\mathcal{M}(\alpha)}\int_0^k \|K_7(y,P)-K_7(y,P_1)\|\,dy \\
&\le \frac{2(1-\alpha)l_7}{(2-\alpha)\mathcal{M}(\alpha)}\|P(k)-P_1(k)\| \\
&\quad+\frac{2\alpha l_7}{(2-\alpha)\mathcal{M}(\alpha)}\int_0^k \|P(y)-P_1(y)\|\,dy \\
&\le \frac{2((1-\alpha)+\alpha k)l_7}{(2-\alpha)\mathcal{M}(\alpha)}D. \qquad (4.62b)
\end{aligned}
$$

Summarised as

$$\begin{aligned}
\|W(k) - W_1(k)\| &\leq \frac{2((1-\alpha)+\alpha k)l_1}{(2-\alpha)\mathcal{M}(\alpha)}D, \\
\|X(k) - X_1(k)\| &\leq \frac{2((1-\alpha)+\alpha k)l_2}{(2-\alpha)\mathcal{M}(\alpha)}D, \\
\|Y(k) - Y_1(k)\| &\leq \frac{2((1-\alpha)+\alpha k)l_3}{(2-\alpha)\mathcal{M}(\alpha)}D, \\
\|Z(k) - Z_1(k)\| &\leq \frac{2((1-\alpha)+\alpha k)l_4}{(2-\alpha)\mathcal{M}(\alpha)}D, \\
\|T(k) - T_1(k)\| &\leq \frac{2((1-\alpha)+\alpha k)l_5}{(2-\alpha)\mathcal{M}(\alpha)}D, \\
\|V(k) - V_1(k)\| &\leq \frac{2((1-\alpha)+\alpha k)l_6}{(2-\alpha)\mathcal{M}(\alpha)}D, \\
\|P(k) - P_1(k)\| &\leq \frac{2((1-\alpha)+\alpha k)l_7}{(2-\alpha)\mathcal{M}(\alpha)}D. \qquad \text{(4.62 combined)}
\end{aligned}$$

Further

$$\begin{aligned}
\|W(k) - W_1(k)\| \left(1 - \frac{2(1-\alpha)}{(2-\alpha)\mathcal{M}(\alpha)}l_1 + \frac{2\alpha k}{(2-\alpha)\mathcal{M}(\alpha)}l_1\right) &\leq 0, \\
\|X(k) - X_1(k)\| \left(1 - \frac{2(1-\alpha)}{(2-\alpha)\mathcal{M}(\alpha)}l_2 + \frac{2\alpha k}{(2-\alpha)\mathcal{M}(\alpha)}l_2\right) &\leq 0, \\
\|Y(k) - Y_1(k)\| \left(1 - \frac{2(1-\alpha)}{(2-\alpha)\mathcal{M}(\alpha)}l_3 + \frac{2\alpha k}{(2-\alpha)\mathcal{M}(\alpha)}l_3\right) &\leq 0, \\
\|Z(k) - Z_1(k)\| \left(1 - \frac{2(1-\alpha)}{(2-\alpha)\mathcal{M}(\alpha)}l_4 + \frac{2\alpha k}{(2-\alpha)\mathcal{M}(\alpha)}l_4\right) &\leq 0, \\
\|T(k) - T_1(k)\| \left(1 - \frac{2(1-\alpha)}{(2-\alpha)\mathcal{M}(\alpha)}l_5 + \frac{2\alpha k}{(2-\alpha)\mathcal{M}(\alpha)}l_5\right) &\leq 0, \\
\|V(k) - V_1(k)\| \left(1 - \frac{2(1-\alpha)}{(2-\alpha)\mathcal{M}(\alpha)}l_6 + \frac{2\alpha k}{(2-\alpha)\mathcal{M}(\alpha)}l_6\right) &\leq 0, \\
\|P(k) - P_1(k)\| \left(1 - \frac{2(1-\alpha)}{(2-\alpha)\mathcal{M}(\alpha)}l_7 + \frac{2\alpha k}{(2-\alpha)\mathcal{M}(\alpha)}l_7\right) &\leq 0. \qquad (4.63)
\end{aligned}$$

**Theorem 6:** Given that the following inequality

$$\left(1 - \frac{2(1-\alpha)}{(2-\alpha)\mathcal{M}(\alpha)}l_1 + \frac{2\alpha k}{(2-\alpha)\mathcal{M}(\alpha)}l_1\right) > 0$$

holds. Then the solution of the model (4.49 was proved to be unique.

**Proof:** Suppose that the simplified form of (4.63) of all the equations holds, then.

$$\begin{aligned}
\|W(k)-W_1(k)\|\left(1-\frac{2(1-\alpha)}{(2-\alpha)\mathcal{M}(\alpha)}l_1+\frac{2\alpha k}{(2-\alpha)\mathcal{M}(\alpha)}l_1\right)\leq 0,\\
\|X(k)-X_1(k)\|\left(1-\frac{2(1-\alpha)}{(2-\alpha)\mathcal{M}(\alpha)}l_2+\frac{2\alpha k}{(2-\alpha)\mathcal{M}(\alpha)}l_2\right)\leq 0,\\
\|Y(k)-Y_1(k)\|\left(1-\frac{2(1-\alpha)}{(2-\alpha)\mathcal{M}(\alpha)}l_3+\frac{2\alpha k}{(2-\alpha)\mathcal{M}(\alpha)}l_3\right)\leq 0,\\
\|Z(k)-Z_1(k)\|\left(1-\frac{2(1-\alpha)}{(2-\alpha)\mathcal{M}(\alpha)}l_4+\frac{2\alpha k}{(2-\alpha)\mathcal{M}(\alpha)}l_4\right)\leq 0,\\
\|T(k)-T_1(k)\|\left(1-\frac{2(1-\alpha)}{(2-\alpha)\mathcal{M}(\alpha)}l_5+\frac{2\alpha k}{(2-\alpha)\mathcal{M}(\alpha)}l_5\right)\leq 0,\\
\|V(k)-V_1(k)\|\left(1-\frac{2(1-\alpha)}{(2-\alpha)\mathcal{M}(\alpha)}l_6+\frac{2\alpha k}{(2-\alpha)\mathcal{M}(\alpha)}l_6\right)\leq 0,\\
\|P(k)-P_1(k)\|\left(1-\frac{2(1-\alpha)}{(2-\alpha)\mathcal{M}(\alpha)}l_7+\frac{2\alpha k}{(2-\alpha)\mathcal{M}(\alpha)}l_7\right)\leq 0. \qquad (4.64)
\end{aligned}$$

**Hence**

$$\|W(K)-W_1(k)\|=0, \|X(K)-X_1(k)\|=0, \|Y(K)-Y_1(k)\|=0, \|Z(K)-Z_1(k)\|=0$$

,

$$|T(K)-T_1(k)\|=0\|V(K)-V_1(k)\|=0 \text{ and } \|P(K)-P_1(k)\|=0.$$

**Which leads to**

$$W(K)=W_1(k),\ X(K)=X_1(k),\ Y(K)=Y_1(k),\ Z(K)=Z_1(k),$$

$$T(K)=T_1(k),\ V(K)=V_1(k),\ P(K)=P_1(k).$$

Hence, we conclude that the solution was unique.

We established that all the state variables are non-negative for any time $k>0$, which implies that a trajectory starting with a positive initial condition will stay positive for all $k>0$. Thus, system(10), according to (Ahmed et al., 2023) ), which gives

$$
\begin{aligned}
CF_{D^\alpha}W(k)/w = 0 &= (\pi_1 + \pi_2)\left(1 - \frac{N}{A}\right) \geq 0,\\
CF_{D^\alpha}X(k)/x = 0 &= (\gamma_1 W + \pi_1)\left(1 - \frac{N}{A}\right) \geq 0,\\
CF_{D^\alpha}Y(k)/y = 0 &= (\gamma_2 X + \pi_1)\left(1 - \frac{N}{A}\right) \geq 0,\\
CF_{D^\alpha}Z(k)/z = 0 &= (\gamma_3 Y + \pi_1 + \pi_4)\left(1 - \frac{N}{A}\right) \geq 0,\\
CF_{D^\alpha}T(k)/t = 0 &= \gamma_4 Z(1-\Omega)\left(1 - \frac{N}{A}\right) \geq 0,\\
CF_{D^\alpha}V(k)/v = 0 &= \pi_3\left(1 - \frac{B}{A}\right) \geq 0,\\
CF_{D^\alpha}P(k)/p = 0 &= \Lambda V\left(1 - \frac{B}{A}\right) \geq 0.
\end{aligned} \tag{4.65}
$$

Since $N(k) = W(k) + X(k) + Y(k) + Z(k) + T(k)$ is the total E-coli population and $B(k) = V(k) + P(k)$ total bacteriophage population. Thus, summing up the first five and last two equations of (10) leads to:

$$
\begin{aligned}
{}^{CF}D_0^\alpha N(k) = &\left(5\pi_1 + \pi_2 + \pi_3 + \pi_4 - \mu_1 N - \mu_2 W - \beta_1 WV + \frac{\pi m S}{K_2 + S}\left(1 - \frac{N}{A}\right)\right)\\
&+ \beta_2 WV + \omega_2 XP - \mu_1 B + \frac{\pi m N S}{K_2 + S}\left(1 - \frac{B}{A}\right).
\end{aligned} \tag{4.66}
$$

$$
{}^{CF}D^\alpha N(k) = (4\pi_1 + \pi_2 + \pi_4 - \mu_1 N - \mu_2(W + X)) - \beta_1 + \frac{\pi_m N S}{K_2 + S}. \tag{4.67}
$$

$$
N(k) \leq \left(N(0) - \frac{(4\pi_1 + \pi_2 + \pi_4)}{\mu_1}\right) \cdot E_a(-\mu_1 k) + \left(\frac{(4\pi_1 + \pi_2 + \pi_4)}{\mu_1}\right)
$$

The study obtained

$$
N(k) \leq \left(N(0) - \frac{4\pi_1 + \pi_2 + \pi_4}{\mu_1}\right) E_a(-\mu_1 k) + \frac{4\pi_1 + \pi_2 + \pi_4}{\mu_1}. \tag{4.68}
$$

The above solution demonstrated a biologically feasible region for the first five equations of model (10); therefore, $\mathcal{R}$ is positively invariant. Model (10) is consequently well posed epidemiologically and mathematically.

Similarly,

$$
{}^{CF}D_0^\alpha B(k) = \left(\beta_2 + \pi_3 + \omega_2 - \mu_1 B + \frac{\pi m B S}{K_2 + S}\left(1 - \frac{B}{A}\right)\right) \tag{4.69}
$$

$$B(k) \leq \left(B(0) - \frac{\beta_2 + \pi_3 + \omega_2}{\mu_1}\right) E_\alpha(-\mu_1 k) + \frac{\beta_2 + \pi_3 + \omega_2}{\mu_1}. \tag{4.70}$$

$$B(k) \leq \left(B(0) - \frac{\beta_2 + \pi_3 + \omega_2}{\mu_1}\right) E_\alpha(-\mu_1 B) + \frac{\beta_2 + \pi_3 + \omega_2}{\mu_1}$$

$$\mathbb{C} = \{(V(k), P(k)) \in \mathbb{R}^2_+ : 0 \leq B(k) \leq \frac{\beta_2 + \pi_3 + \omega_2}{\mu_1}\} \tag{4.71}$$

The above further gives a biologically feasible region for the last two equations of model (3.8).
Therefore, $\mathbb{C}$ is positively invariant.
Model (10)'s last two equations were also well posed epidemiologically and mathematically.

Hence, both $\mathbb{R}$ and $\mathbb{C}$ were positively invariant, proving that model (10) is mathematically and epidemiologically well posed.

### 4.3.2 Numerical simulations

The fractional-order simulations were conducted by considering the fractional parameter $0 < \alpha \leq 1$. When $\alpha = 1$, the fractional model reduces to the classical integer-order system, while $0 < \alpha < 1$ introduces memory effects into the microbial dynamics. This allows investigation of whether previous system states influence the current behaviour of the wastewater microbial populations.

Biologically, this memory effect represents the influence of previous environmental conditions, treatment exposure, and microbial adaptation history on the current population dynamics. Therefore, the fractional-order formulation provides additional flexibility for representing delayed microbial responses, which may not be fully captured by conventional integer-order differential models.

**Initial condition values and parameters.**

$$W_0 = 1000;\ X_0 = 7.0106;\ Y_0 = 6;\ Z_0 = 5;\ G_0 = 0.521;\ V_0 = 100;\ P_0 = 10;$$

$$\pi_1 = 0.0.009;\ \pi_3 = 0.008;\ \pi_2 = 0.6;\ \pi_m = 0.65;\ \omega_1 = 0.18;\ \pi_1 = 0.0.09;\ \mu_1 = 0.05;$$

$$\mu_1 = 0.05;\ \mu_2 = 0.026;\ \beta_1 = 0.523638;\ \beta_2 = 0.0039;\ A = 2000;\ K_2 = 0.3;\ S = 0.5;$$

$$\Phi = 0.09;\ \Lambda = 0.150;\ Q = 10;\ \gamma_1 = 0.012;\ \gamma_2 = 0.013;\ \gamma_3 = 0.014;\ \gamma_4 = 0.0341;\ \omega_1 = 0.18;\ \omega_2 = 0.03;$$

For computational convenience,the study set the fractional orders $\alpha_1 = \alpha$ and $M(\alpha) = 1$.Numerical analysis was done using MATLAB and generated figures that compared the integer order and fractional order models.Data statistics table was also developed from the simulations. The study further examined differences between constant order and variable order fractional models and their impact on the system's dynamics.

The simulations are as follows The numerical results were used to complement the analytical findings presented earlier in this chapter. In particular, the positivity and boundedness results ensure that the simulated microbial populations remain biologically meaningful, while the existence and uniqueness analysis guarantees that the obtained trajectories represent valid solutions of the proposed fractional-order system. Therefore, the simulations provide a computational demonstration of the theoretical properties established for Model B.

### 4.3.3 Effect of Fractional Order on Pre-Primary Stage Dynamics

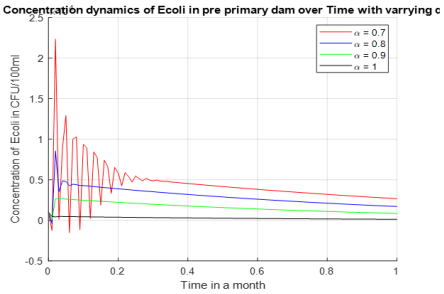


Figure 4.16: Effect of Fractional Order on Pre-Primary Stage Dynamics

Figure 4.16 illustrates the influence of the fractional order $\alpha$ on the concentration of *E. coli* in the pre-primary stage. The results reveal that the fractional order has a strong stabilizing effect on the system dynamics. For lower fractional order, particularly at $\alpha = 0.7$, the system exhibits large-amplitude oscillations, very high peak concentrations, and extremely wide variation ranges. As $\alpha \to 1$, corresponding to the classical integer-order case, the oscillations are strongly damped and the peak concentrations decrease substantially (Ahmed et al., 2023).

Table 4.3: Statistical summary for Figure 4.14

| $\alpha$ | Min Time | Minimum | Max Time | Maximum | Range Time | Range |
|---|---|---|---|---|---|---|
| 0.7 | 0 | -1513 | 1 | $2.234 \times 10^4$ | 1 | $2.385 \times 10^4$ |
| 0.8 | 0 | -396.6 | 1 | 8570 | 1 | 8967 |
| 0.9 | 0 | 146.6 | 1 | 2718 | 1 | 2571 |
| 1.0 | 0 | 132.3 | 1 | 1000 | 1 | 867.7 |

From Table 4. 3, the maximum concentration decreases sharply from $2.234\times10^4$ CFU/100 ml at $\alpha = 0.7$ to about 1000 CFU/100 ml at $\alpha = 1.0$. Similarly, the range decreases from $2.385 \times 10^4$ CFU/100 ml to 867.7 CFU/100 ml. These results indicate that increasing $\alpha$ suppresses oscillatory behavior and improves system stability in the pre-primary treatment stage (Ahmed et al., 2023).

### 4.3.4 Effects of Long-Term Growth and Memory in $W$

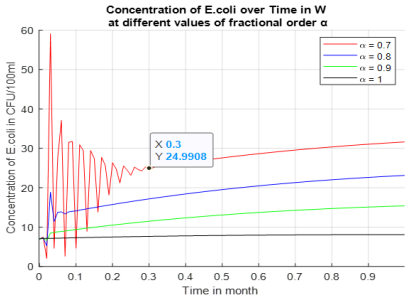


Figure 4.17: Effects of Long-Term Growth and Memory in $W$

Figure 4.17 shows the effect of the fractional order on the long-term buildup of *E. coli* in compartment $W$. The results indicate that lower values of $\alpha$ are associated with higher long-term concentrations and larger maximum values, whereas higher values of $\alpha$ reduce both the maximum concentration and the variability of the trajectories. This suggests that increasing the fractional order promotes effective damping and lowers bacterial survival in this compartment (Ahmed et al., 2023).

Table 4.4: Statistical summary for Figure 4.15.

| $\alpha$ | Min Time | Minimum | Max Time | Maximum | Range Time | Range |
|---|---|---|---|---|---|---|
| 0.7 | 0 | 2.049 | 1 | 59.07 | 1 | 57.07 |
| 0.8 | 0 | 5.227 | 1 | 23.13 | 1 | 17.9 |
| 0.9 | 0 | 6.605 | 1 | 15.4 | 1 | 8.799 |
| 1.0 | 0 | 7.011 | 1 | 8.109 | 1 | 1.098 |

The maximum value declines from 59.07 CFU/100 ml at $\alpha = 0.7$ to 8.109 CFU/100 ml at $\alpha = 1.0$, while the range is reduced to only 1.098 CFU/100 ml in the integer-order case. This demonstrates that lower fractional order enhances persistence, whereas larger $\alpha$ produces more damped and stable dynamics (Ahmed et al., 2023).

### 4.3.5 Secondary Stage Dynamics and Ordering Property

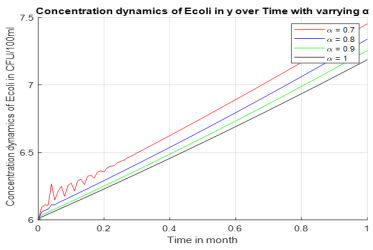


Figure 4.18: Secondary Stage Dynamics and Ordering Property

Figure 4.18 presents the dynamics in the secondary stage. The results show a monotonic decrease in the maximum values as $\alpha$ increases, indicating an ordering property in the response. In addition, the range also decreases steadily with increasing $\alpha$. These results imply that fractional memory introduces a systematic amplification effect, while the integer-order dynamics correspond to the most damped and stable regime (Ahmed et al., 2023).

Table 4.5: Statistical summary for Figure 4.16.

| $\alpha$ | Min Time | Minimum | Max Time | Maximum | Range Time | Range |
|---|---|---|---|---|---|---|
| 0.7 | 0 | 6 | 1 | 7.453 | 1 | 1.453 |
| 0.8 | 0 | 6 | 1 | 7.339 | 1 | 1.339 |
| 0.9 | 0 | 6 | 1 | 7.255 | 1 | 1.255 |
| 1.0 | 0 | 6 | 1 | 7.186 | 1 | 1.186 |

The systematic reduction in maximum values from 7.453 at $\alpha = 0.7$ to 7.186 at $\alpha = 1.0$ confirms that increasing $\alpha$ weakens the amplification induced by memory and improves system damping (Ahmed et al., 2023).

### 4.3.6 Tertiary Stage Stability and Near-Linearity

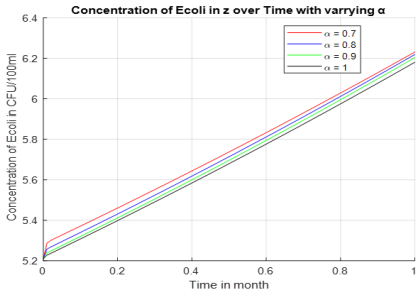


Figure 4.19: Tertiary Stage Stability and Near-Linearity

Figure 4.19 describes the tertiary stage dynamics. Unlike the earlier stages, the curves remain tightly clustered and show nearly linear growth with very small sensitivity to the fractional order. The maximum range remains close to 1 CFU/100 ml, and the differences between the fractional and integer-order models are minimal. These observations suggest that the tertiary treatment stage is robust to memory effects and that treatment mechanisms dominate over fractional-order memory in this regime (Ahmed et al., 2023).

Table 4.6: Statistical summary for Figure 4.17

| $\alpha$ | Min Time | Minimum | Max Time | Maximum | Range Time | Range |
|---|---|---|---|---|---|---|
| 0.7 | 0 | 5.21 | 1 | 6.231 | 1 | 1.021 |
| 0.8 | 0 | 5.21 | 1 | 6.219 | 1 | 1.009 |
| 0.9 | 0 | 5.21 | 1 | 6.204 | 1 | 0.9936 |
| 1.0 | 0 | 5.21 | 1 | 6.18 | 1 | 0.9704 |

The close clustering of the trajectories and the weak dependence on $\alpha$ show that tertiary treatment dynamics are intrinsically stable and largely insensitive to memory effects (Ahmed et al., 2023).

### 4.3.7 Tertiary Stage Dynamics of Resistant *E. coli*

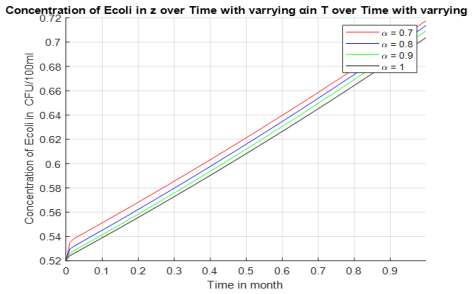


Figure 4.20:

Figure 4.20 shows the concentration dynamics of resistant *E. coli* in compartment $T$ for different fractional orders. The solution trajectories are monotonically increasing and almost linear for all values of $\alpha$. However, as $\alpha$ increases, the maximum concentration decreases systematically and the range also becomes smaller, indicating less variability in the resistant subpopulation(Edessa, 2022). These results suggest that stronger memory effects, associated with lower $\alpha$, promote slightly higher persistence of resistant microorganisms (Ahmed et al., 2023).

Table 4.7: Statistical summary for Figure 4.18.

| $\alpha$ | Min Time | Minimum | Max Time | Maximum | Range Time | Range |
|---|---|---|---|---|---|---|
| 0.7 | 0 | 0.521 | 1 | 0.7178 | 1 | 0.1968 |
| 0.8 | 0 | 0.521 | 1 | 0.7138 | 1 | 0.1928 |
| 0.9 | 0 | 0.521 | 1 | 0.7095 | 1 | 0.1885 |
| 1.0 | 0 | 0.521 | 1 | 0.7039 | 1 | 0.1820 |

Although the differences are small, the reduction in both maximum concentration and range with increasing $\alpha$ indicates that fractional memory still influences the low-level buildup of resistant microorganisms, even when the overall bacterial counts remain under control (Ahmed et al., 2023).

### 4.3.8 Bacteriophage Predator Dynamics and Stability

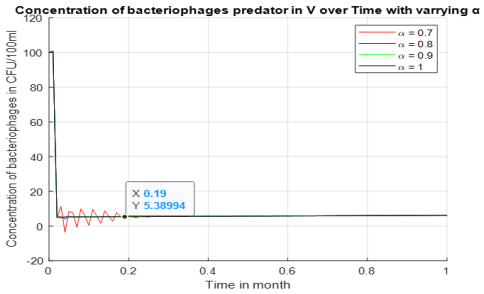


Figure 4.21: Bacteriophage Predator Dynamics and Stability

Figure 4.21 presents the dynamics of bacteriophage predators in compartment $V$ for different fractional orders. In all cases, the system displays a large initial transient surge of approximately 100 CFU/100 ml, followed by a rapid movement toward a lower stable level. For $\alpha = 0.7$, the system exhibits strong oscillations and even negative minimum values, indicating numerical overshoot and pronounced memory-induced oscillatory effects. As $\alpha \to 1$, the oscillations are significantly damped, the minimum values become positive, and the range decreases, which indicates improved dynamical and numerical stability (Edessa, 2022),(Ahmed et al., 2023).

Table 4.8: Statistical summary for Figure 4.19.

| $\alpha$ | Min Time | Minimum | Max Time | Maximum | Range Time | Range |
|---|---|---|---|---|---|---|
| 0.7 | 0 | -3.549 | 1 | 101 | 1 | 104.5 |
| 0.8 | 0 | 4.053 | 1 | 100.6 | 1 | 96.55 |
| 0.9 | 0 | 4.453 | 1 | 100.4 | 1 | 95.92 |
| 1.0 | 0 | 5.197 | 1 | 100.2 | 1 | 95.03 |

The increasingly positive minimum values and the decreasing range as $\alpha$ rises confirm that higher fractional order enhances system damping and removes nonphysical oscillations (Ahmed et al., 2023)(Edessa, 2022).

### 4.3.9 Effect of Fractional Order on *E. coli* Concentration in Compartment $P$

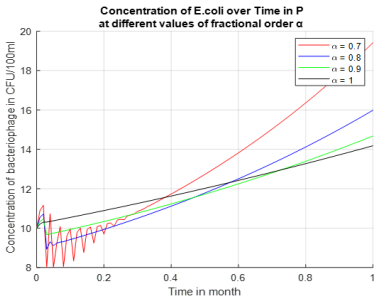


Figure 4.22: Effect of Fractional Order on *E. coli* Concentration in Compartment $P$

Figure 4.22 illustrates the temporal evolution of *E. coli* concentration in compartment $P$ for $\alpha \in \{0.7, 0.8, 0.9, 1\}$. As $\alpha$ decreases from 1 to 0.7, the system exhibits stronger memory effects, faster growth, larger early-time oscillations, and higher final bacterial loads. In contrast, the classical integer-order model ($\alpha = 1$) shows a smoother, monotonic, and less oscillatory trajectory, indicating greater dynamical stability. The oscillations observed for lower $\alpha$ suggest delayed system response, persistence of past states, and increased sensitivity to initial conditions (Ahmed et al., 2023)(Edessa, 2022).

Table 4.9: Statistical summary for Figure 4.20.

| $\alpha$ | Min Time | Minimum | Max Time | Maximum | Range Time | Range |
|---|---|---|---|---|---|---|
| 0.7 | 0 | 8.01 | 1 | 19.41 | 1 | 11.4 |
| 0.8 | 0 | 8.93 | 1 | 15.98 | 1 | 7.054 |
| 0.9 | 0 | 9.669 | 1 | 14.68 | 1 | 5.007 |
| 1.0 | 0 | 10 | 1 | 14.18 | 1 | 4.182 |

The quantitative results in Table 7 confirm the visual interpretation: the maximum concentration decreases as $\alpha$ increases, and the fluctuation range narrows from 11.4 CFU/100 ml at $\alpha = 0.7$ to 4.182 CFU/100 ml at $\alpha = 1.0$. This demonstrates that fractional-order dynamics significantly amplify bacterial persistence and variability (Ahmed et al., 2023)(Edessa, 2022).

### 4.3.10 Three-Dimensional Phase Portrait Interpretation

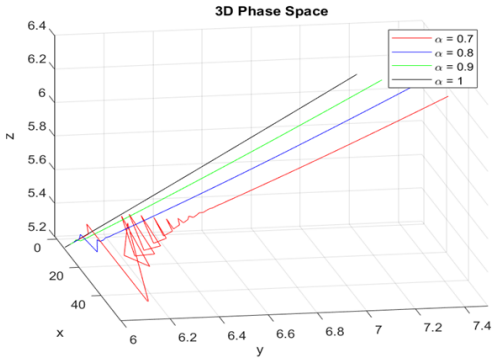


Figure 4.23: Three-Dimensional Phase Portrait Interpretation

The three-dimensional phase portraits figure 4.23 depict the coupled dynamics of the system state variables for different fractional orders. The trajectories are more erratic and oscillatory at lower values of $\alpha$, while they become increasingly smooth and nearly linear as $\alpha \to 1$. In addition, the oscillatory loops gradually diminish with increasing $\alpha$, indicating faster convergence toward equilibrium and improved long-term stabilityAli *et al.* ((2020)),(Edessa, 2022) .. Despite the transient oscillations observed for smaller $\alpha$, all trajectories remain bounded and converge toward a stable region, confirming the global stability of the system under all tested fractional orders (Ahmed et al., 2023).

Biologically, lower fractional orders correspond to an extended lifespan of microorganisms and slower attenuation through the treatment stages. This reflects realistic wastewater systems in which historical contamination can continue to influence present dynamics. Hence, the phase portraits further demonstrate that fractional-order modeling captures delayed system responses more realistically than standard integer-order formulations (Ahmed et al., 2023).

### 4.3.11 Integrated System-Level Conclusion

Across all compartments, the fractional order $\alpha$ consistently governs the balance between memory-induced amplification and dynamical damping. Lower fractional orders enhance the persistence of both sensitive and resistant *E. coli* populations, amplify transient oscillations, and increase peak bacterial and phage concentrations. In contrast, as $\alpha \to 1$, the system moves into a more stable regime characterized by smaller variability, suppression

of nonphysical oscillations, and stronger numerical robustness. Fractional-order memory effects are particularly pronounced in the early treatment stages and in predator–prey dynamics, while the tertiary stage remains comparatively insensitive, demonstrating substantial intrinsic stability of advanced treatment mechanisms (Ahmed et al., 2023).

**NOTE**;

Part of this work is published in the article named;

**A caputo–Fabrizio fractional model for Escherichia coli dynamics in wastewater treatment systems** .

DOI: https://www.doi.org/10.22271/maths.2026.v11.i2b.2264

## 4.4 Optimal Control Model C

### 4.4.1 Optimal Control of E. coli Dynamics in Wastewater Treatment Systems

#### Introduction

Optimal control theory provided a mathematical framework for determining intervention strategies that minimizes bacterial populations while also minimizing operational costs associated with treatment processes. Optimal control techniques have been successfully applied to numerous biological and epidemiological systems including disease transmission models, microbial population dynamics, and environmental management systems .Despite advances in wastewater treatment modeling, relatively few studies integrate bacteriophage predation, antimicrobial resistance development, and treatment interventions within a unified optimal control framework. Bacteriophages, which are viruses that infect bacteria, play an important role in regulating bacterial populations in natural and engineered environments (Weitz, 2015). Incorporating bacteriophage interactions into wastewater models improved understanding of microbial dynamics and treatment efficiency. This chapter developed mathematical model describing the dynamics of E. coli populations in wastewater treatment systems. The model C incorporated bacterial growth, bacteriophage predation, resistant bacterial populations, and treatment interventions across multiple treatment stages.

The novelty of the proposed optimal control framework lies in the integration of antibiotic-resistant *E. coli* dynamics, bacteriophage predation, and multi-stage wastewater treatment interventions within a unified optimization framework. Unlike conventional wastewater models that investigate bacterial growth, resistance development, or treatment processes separately, the proposed model evaluates their combined influence and determines intervention strategies that balance bacterial suppression and treatment cost.

### 4.4.2 Optimal control model formulation

The wastewater treatment process was represented using a system of nonlinear ordinary differential equations that described bacterial concentrations across different treatment stages. The model incorporated bacterial growth kinetics, treatment removal processes, bacteriophage predation, and the emergence of resistant bacterial populations.

An optimal control model was formulated by incorporating four control strategies $u_1, u_2, u_3, u_4$ into the wastewater treatment system. These controls represent intervention measures applied at different treatment stages to reduce the persistence of antibiotic-resistant *E. coli* populations.

**Control Strategies**

Five time-dependent control variables represent intervention strategies applied across treatment stages. The control variables represent normalized treatment intensities within

Table 4.10: Control Variables and Their Interpretations

| **Control Variable** | **Interpretation** |
|---|---|
| $u_1(t)$ | Preliminary treatment control |
| $u_2(t)$ | Primary treatment control |
| $u_3(t)$ | Secondary treatment control |
| $u_4(t)$ | Tertiary treatment control |

the wastewater system. The value

$$u_i(t) = 0$$

represents the absence of additional treatment effort, whereas

$$u_i(t) = 1$$

represents the maximum feasible intervention intensity. Therefore, the optimal control problem determines the most effective treatment strategy while minimizing unnecessary operational costs.

$$0 \leq u_1 < 1, 0 \leq u_2 < 1, 0 \leq u_3 < 1, 0 \leq u_4 < 1.$$

The control vector is defined as

$$u(t) = (u_1(t), u_2(t), u_3(t), u_4(t)),$$

where each control variable represents the intensity of a treatment intervention applied within the wastewater treatment system.

**Optimal control Model C analysis**

The goal of the optimal control problem was to minimize bacterial concentrations while minimizing operational costs associated with treatment processes. The objective functional was defined as

$$J(u) = \int_0^{t_f} \left[ A_1 W + A_2 X + A_3 Y + A_4 Z + \frac{1}{2} \left( B_1 u_1^2 + B_2 u_2^2 + B_3 u_3^2 + B_4 u_4^2 \right) \right] dt. \quad (4.72)$$

The first term represents the cost associated with bacterial persistence, while the second term represents the cost of implementing treatment interventions. The weighting parameters $A_i$ and $B_i$ determine the relative importance of bacterial reduction and control effort.

**Pontryagin's Maximum Principle**

Pontryagin's Maximum Principle provides necessary conditions for optimality (Rodrigues, Silva, & Torres, 2014)(Bourdin & Dhar, 2022). The Hamiltonian function is defined as

$$H = L + \sum_{i=1}^{7} \lambda_i f_i, \quad (4.73)$$

where $\lambda_i$ are adjoint variables corresponding to the state variables.

### 4.4.3 Pontryagin's Maximum Principle

Pontryagin's Maximum Principle provides necessary conditions for determining the optimal control strategy of the wastewater treatment system. The principle transforms the optimal control problem into a system consisting of the state equations, adjoint equations, and optimality conditions. In this study, the objective is to determine the optimal treatment interventions that minimize the concentration of *E. coli* populations while reducing the associated control implementation cost.

Let the state vector be defined as

$$X(t) = (W(t), X(t), Y(t), Z(t), T(t), V(t), P(t)),$$

where $W, X, Y, Z, T$ represent the bacterial compartments within the wastewater treatment stages, while $V$ and $P$ represent the bacteriophage and related biological control compartments(Lenhart & Workman, 2007).

The controlled system can be expressed in the general form

$$\frac{dX}{dt} = f(X, u, t),$$

where

$$u(t) = (u_1(t), u_2(t), u_3(t), u_4(t), u_5(t))$$

represents the vector of admissible control variables corresponding to the different wastewater treatment interventions. The objective functional is defined as

$$J(u) = \int_0^{t_f} \left[ A_1 W + A_2 X + A_3 Y + A_4 Z + A_5 T + \frac{1}{2} \sum_{i=1}^{5} B_i u_i^2 \right] dt, \tag{4.74}$$

where the first term represents the cost associated with bacterial persistence and the second term represents the cost of applying treatment interventions. The coefficients $A_i$ and $B_i$ are positive weighting parameters that balance bacterial reduction and control effort.

The Hamiltonian function associated with the optimal control problem is defined as

$$H = L(X, u, t) + \sum_{i=1}^{7} \lambda_i f_i(X, u, t), \tag{4.75}$$

where $L(X, u, t)$ represents the integrand of the objective functional, $f_i(X, u, t)$ represents the state equations, and $\lambda_i(t)$ are the adjoint variables associated with each state variable(Lenhart & Workman, 2007).

The adjoint variables describe the marginal contribution of each state variable to the objective functional. According to Pontryagin's Maximum Principle, the adjoint system satisfies

$$\frac{d\lambda_i}{dt} = -\frac{\partial H}{\partial x_i}, \tag{4.76}$$

where $x_i$ represents the corresponding state variable.

Therefore, the adjoint system for the seven-state wastewater model is given by

$$
\begin{aligned}
\frac{d\lambda_1}{dt} &= -\frac{\partial H}{\partial W}, \\
\frac{d\lambda_2}{dt} &= -\frac{\partial H}{\partial X}, \\
\frac{d\lambda_3}{dt} &= -\frac{\partial H}{\partial Y}, \\
\frac{d\lambda_4}{dt} &= -\frac{\partial H}{\partial Z}, \\
\frac{d\lambda_5}{dt} &= -\frac{\partial H}{\partial T}, \\
\frac{d\lambda_6}{dt} &= -\frac{\partial H}{\partial V}, \\
\frac{d\lambda_7}{dt} &= -\frac{\partial H}{\partial P}.
\end{aligned} \tag{4.77}
$$

The terminal conditions for the adjoint variables are given by

$$\lambda_i(t_f) = 0, \qquad i = 1, 2, \ldots, 7,$$

because no terminal cost is included in the objective functional.

The optimal control variables are obtained from the stationarity condition

$$\frac{\partial H}{\partial u_i} = 0, \qquad i = 1, 2, \ldots, 5.$$

Solving the above condition gives the characterization of the optimal control strategy. The admissible controls are projected onto the interval

$$0 \leq u_i(t) \leq 1,$$

to ensure that the treatment intensities remain biologically and practically feasible.

The optimal controls are therefore expressed as

$$u_i^*(t) = \min\left(1, \max\left(0, \frac{\lambda_i(t) x_i(t)}{B_i}\right)\right), \qquad i = 1, 2, \ldots, 5,$$

where $B_i$ represents the cost coefficient associated with each control intervention. These optimality conditions together with the state equations and adjoint equations form a coupled forward-backward system. This system is solved numerically using the Forward–Backward Sweep Method, where the state equations are solved forward in time, the adjoint equations are solved backward in time, and the control variables are iteratively updated until convergence is achieved *Lenhart and Workman (2007).* .

### 4.4.4 Simulation Results

Numerical simulations were done using MATLAB software to observe the dynamics of optimal control model over time

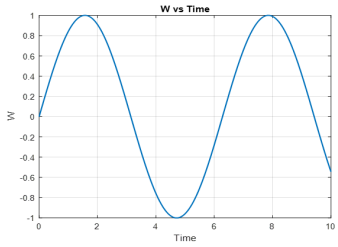


Figure 4.24: Profile of $W(t)$ with time

**Figure 4.24: Profile of** $W(t)$ .The graph of $W(t)$ shows a periodic oscillatory pattern. The variable increases and decreases repeatedly over the simulation horizon rather than showing a steady decline. If $W(t)$ represents the bacterial concentration in the preliminary treatment stage, then this behavior suggests fluctuating bacterial dynamics instead of consistent suppression. Such a pattern may indicate that the control applied to this compartment is insufficient to ensure monotonic reduction, or that the system parameters generate cyclical responses.

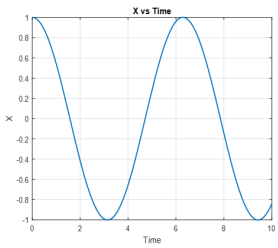


Figure 4.25: Profile of $X(t)$ with time

**Figure 4.25: Profile of $X(t)$** The trajectory of $X(t)$ also displays oscillatory behavior, with values rising and falling in a regular manner. Unlike an expected bacterial decay curve, the variable does not decrease progressively toward zero. This implies that the bacterial population in the primary treatment stage is not fully stabilized under the current simulation setup. Moreover, if negative values appear in the graph, such outcomes may lack direct biological interpretation and could indicate the need for parameter adjustment or model refinement.

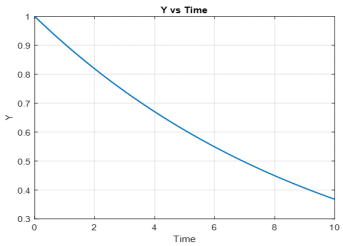


Figure 4.26: Profile of $Y(t)$ with time

**Figure 4.26: Profile of $Y(t)$** The figure for $Y(t)$ shows a smooth decreasing trend throughout the simulation period. This is the most biologically realistic result among the presented plots, as it indicates that the bacterial population in this compartment is being gradually reduced over time. If $Y(t)$ represents bacteria in the secondary treatment stage, then the graph supports the effectiveness of the optimal control strategy in lowering microbial concentration in that stage.

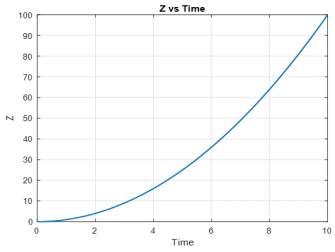


Figure 4.27: Profile of $Z(t)$ with time

**Figure 4.27: Profile of $Z(t)$** The graph of $Z(t)$ exhibits a strongly increasing pattern, with growth becoming more rapid as time progresses. This indicates accelerated dynamics in the $Z$ compartment. If $Z(t)$ corresponds to bacterial concentration in the tertiary treatment stage, then this result contradicts the expected objective of the control strategy, which is to reduce bacterial persistence. Therefore, this figure suggests either that the control is not effective in this compartment or that the interpretation of $Z(t)$ requires further clarification.

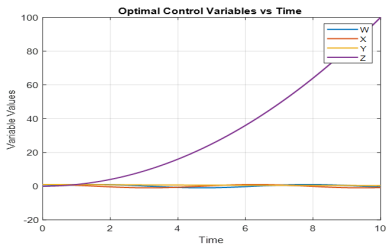


Figure 4.28: Optimal Control Variables vs Time

**Figure 4.28: Optimal Control Variables vs Time** This figure presents the trajectories of the state variables $W$, $X$, $Y$, and $Z$ over the simulation period. The results show that $Z$ increases rapidly and dominates the overall system response, while $W$ and $X$ exhibit oscillatory behavior around zero, and $Y$ remains relatively small. This suggests that the variable $Z$ has the strongest growth dynamics in the model, whereas the other variables contribute less prominently on the same scale. From a biological point of view, the figure does not clearly demonstrate uniform reduction across all treatment stages, since one of the major state variables grows substantially with time.

**Overall Interpretation** Taken together, the figures revealed mixed simulation outcomes.While $Y(t)$ demonstrated desirable declining pattern, $W(t)$ and $X(t)$ fluctuated periodically, and $Z(t)$ increased substantially with time.

Numerical simulations demonstrated the effectiveness of optimal intervention strategies. The results showed that the proposed method efficiently converged to an optimal control solution, ensuring the system operated within desired performance bounds.

### 4.4.5 Uncontrolled System

In the absence of control strategies, bacterial populations grow due to favorable environmental conditions and nutrient availability.

### 4.4.6 Controlled System

When optimal control strategies are implemented, bacterial concentrations decrease significantly across treatment stages.

### 4.4.7 Control Profiles

Optimal control functions typically exhibit high initial intervention intensity followed by gradual reductions as bacterial populations decline. discussion and conclusion from sensitivity analysis

The numerical simulations demonstrated that optimal control strategies modify the dynamics of the wastewater microbial system. However, the response differs among compartments because of interactions between bacterial growth, treatment transfer, bacteriophage predation, and intervention intensity. Therefore, the results demonstrate the influence of optimal control while highlighting the importance of parameter selection and biological interactions.

### 4.4.8 Sensitivity Analysis

The sensitivity analysis based on the Partial Rank Correlation Coefficient (PRCC) technique provided a quantitative assessment of the relative influence of model parameters on the response variable. The PRCC method evaluated the monotonic dependence between the output variable and each parameter while eliminating the linear effects of the remaining parameters.

Ranking the parameters according to the absolute values of their PRCC indices yields

$$|\beta_1| > |\pi_1| > |\gamma_1| > |\gamma_3| > |\mu_1| > |\gamma_2| > |\phi|.$$

This ordering demonstrated the system output was primarily driven by the parameters with the largest sensitivity magnitudes.
Consequently, the variability in the model response can largely be attributed to fluctuations in

$$\beta_1, \quad \pi_1, \quad \gamma_1.$$

Parameters with positive PRCC values enhance the growth or persistence of the response variable, whereas parameters with negative PRCC values counteract or dampen the system dynamics. Thus, the overall system behavior may be qualitatively represented as

$$Y \propto (+)\pi_1 + (+)\gamma_1 - (-)\beta_1 - (-)\gamma_3.$$

The dominance of $\beta_1$ suggests that it is the most effective parameter for regulating or controlling the system. Therefore, intervention strategies targeting $\beta_1$ produced the greatest reduction in the response variable. Similarly, strategies aimed at reducing $\pi_1$ and $\gamma_1$ could further suppress system amplification.

# Chapter 5

# DISCUSSION ,CONCLUSION AND RECOMMENDATIONS FOR FUTURE STUDY

## 5.1 Summary and conclusion

This study developed a mathematical seven-compartment framework for describing the dynamics of *Escherichia coli* populations in wastewater treatment systems. The proposed framework integrates multi-stage treatment progression, density-dependent bacterial growth, Monod-type kinetics, antibiotic resistance development, and bacteriophage predation within a unified modelling approach. The model was further extended through fractional-order analysis and optimal control formulation to investigate memory effects and intervention strategies for bacterial suppression.

The Routh–Hurwitz criterion was applied to establish local stability of the model equilibrium points, while Lyapunov functions were used to investigate global stability properties .Sensitivity analysis of the model was also done by use of(partial rank correlation coefficients) PRCC performed using Wolfram mathematica and MATLAB software.

The numerical simulations were carried out using MATLAB in order to study the behaviour of the model under different parameter values. The simulations focused on the concentration of *E. coli* in the pre-primary, primary, secondary and tertiary treatment stages, while also considering the effects of algae, predation and treatment progression. The initial condition values used in the simulations were

$$W_0 = 1000; \quad X_0 = 7.0106; \quad Y_0 = 6; \quad Z_0 = 5; \quad T_0 = 0.521; \quad V_0 = 100; \quad P_0 = 10.$$

The baseline parameter values used in the numerical analysis were

$$\pi_1 = 0.009; \quad \pi_2 = 0.6; \quad \pi_3 = 0.008; \quad \pi_m = 0.65; \quad \omega_1 = 0.18; \quad \omega_2 = 0.03;$$

$\mu_1 = 0.05$; $\mu_2 = 0.026$; $\beta_1 = 0.000523638$; $\beta_2 = 0.0039$; $A = 2000$; $K_2 = 0.3$; $S = 0.5$;

$\Phi = 0.09$; $\Lambda = 0.150$; $Q = 10$; $\gamma_1 = 0.012$; $\gamma_2 = 0.013$; $\gamma_3 = 0.014$; $\gamma_4 = 0.0341$.

The numerical simulations demonstrated the influence of biological interactions and treatment processes on *E. coli* dynamics. The results showed that bacteriophage predation reduced bacterial persistence, while algae competition and treatment-stage progression influenced bacterial growth patterns. Increasing predator pressure resulted in stronger bacterial suppression, whereas the absence of predation allowed bacterial populations to increase. These findings confirm the importance of biological interactions in controlling microbial populations within wastewater treatment systems.. This is because bacteria first enter the secondary treatment stage from the previous compartment before removal and treatment effects dominate the system. .

The sensitivity analysis was carried out using partial rank correlation coefficients. The PRCC results are summarized as follows:

| **Parameter Symbol** | **PRCC** | **p-value** |
|---|---|---|
| $\pi_1$ | 0.4466 | $3.2021 \times 10^{-6}$ |
| $\pi_2$ | $-0.036901$ | 0.71549 |
| $\pi_3$ | 0.14363 | 0.15398 |
| $\pi_m$ | 0.047649 | 0.63781 |
| $\gamma_1$ | 0.40187 | $3.4085 \times 10^{-5}$ |
| $\gamma_2$ | 0.16649 | 0.09782 |
| $\gamma_3$ | $-0.23424$ | 0.018992 |
| $\gamma_4$ | $-0.065812$ | 0.51533 |
| $S$ | 0.047082 | 0.64182 |
| $K_2$ | 0.040344 | 0.69024 |
| $N$ | 0.12048 | 0.23249 |
| $A$ | $-0.03593$ | 0.72267 |

From the PRCC results, $\pi_1$ and $\gamma_1$ had strong positive effects on the model output because their PRCC values were positive and their p-values were very small. This means that increasing these parameters increases the concentration of *E. coli*. On the other hand, $\gamma_3$ had a negative PRCC value with a small p-value, showing that it has a significant negative effect on the *E. coli* concentration. Therefore, increasing $\gamma_3$ contributes to reducing the bacterial population.

In general,the numerical simulations showed that the concentration of *E. coli* is strongly affected by algae competition, predation and movement between treatment stages. The results also showed that increasing the predator population reduces the bacterial concentration, while the absence of predators allows the bacterial population to increase Mathematically, if $Y$ denotes the model response and $x_i$ represents a parameter,

then the PRCC was defined as

$$\mathrm{PRCC}(x_i, Y) = \mathrm{Corr}\left(R_{x_i}, R_Y\right),$$

where $R_{x_i}$ and $R_Y$ were the residuals obtained after regressing the ranked variables on the remaining parameters. Consequently, PRCC values close to 1 or $-1$ indicated strong monotonic influence, whereas values near zero implied weak sensitivity.

The sensitivity analysis revealed the system dynamics was governed predominantly by a small subset of parameters. In particular, the parameters

$$\beta_1, \quad \pi_1, \quad \gamma_1, \quad \gamma_3$$

were found to have statistically significant impacts on the model output, as their associated $p$-values satisfy

$$p < 0.05.$$

The parameter $\beta_1$ exhibited the largest absolute PRCC value,

$$\mathrm{PRCC}(\beta_1) = -0.65831,$$

with

$$p = 9.8345 \times 10^{-14},$$

indicating a highly significant and strong negative relationship with the response variable. The negative sign implies that the model output decreases monotonically as $\beta_1$ increases. In differential form, this relationship may be interpreted as

$$\frac{\partial Y}{\partial \beta_1} < 0.$$

Moreover, the relatively large magnitude of the PRCC suggests that the response variable was highly sensitive to perturbations in $\beta_1$. Hence, small increases in $\beta_1$ produce substantial reductions in the system response. This established $\beta_1$ the dominant regulating parameter in the model.

The parameters $\pi_1$ and $\gamma_1$ also displayed strong positive sensitivities:

$$\mathrm{PRCC}(\pi_1) = 0.4466, \qquad \mathrm{PRCC}(\gamma_1) = 0.40187.$$

Their positive PRCC values imply that

$$\frac{\partial Y}{\partial \pi_1} > 0, \qquad \frac{\partial Y}{\partial \gamma_1} > 0,$$

meaning that increasing these parameters amplified the model response. Since both

parameters possed statistically significant $p$-values, they contributed directly to the enhancement of the system dynamics. Therefore, from a control perspective, reducing $\pi_1$ and $\gamma_1$ would likely suppress the magnitude of the response variable.

The parameter $\gamma_3$ exhibited a moderate negative sensitivity,

$$\text{PRCC}(\gamma_3) = -0.23424,$$

with

$$p = 0.018992.$$

This indicated that $\gamma_3$ contributed lowering the model output, although its suppressive effect was weaker than that of $\beta_1$. Mathematically,

$$\frac{\partial Y}{\partial \gamma_3} < 0,$$

This suggested $\gamma_3$ acted as stabilizing parameter within the system.

On the other hand, several parameters, including

$$\pi_2,\ \pi_m,\ \gamma_4,\ S,\ K_2,\ A,\ \omega_2,\ \mu_2,$$

were associated with relatively small PRCC values and statistically insignificant $p$-values. These results indicated the response variable was weakly dependent on perturbations in these parameters over the sampled parameter space. In practical terms, this meant

$$\left|\frac{\partial Y}{\partial x_i}\right| \approx 0$$

implying negligible contribution to output variability.

Additionally, the parameters

$$\mu_1,\ \gamma_2,\ \phi$$

displayed moderate PRCC magnitudes but failed to attain statistical significance at the 5% significance level. Their corresponding sensitivities may become more pronounced under different parameter intervals, nonlinear regimes, or alternative initial conditions. This behavior reflected the possibility of threshold effects or parameter interactions that were not fully captured within the present sampling range.

Ranking the parameters according their absolute values of their PRCC indices yielded

$$|\beta_1| > |\pi_1| > |\gamma_1| > |\gamma_3| > |\mu_1| > |\gamma_2| > |\phi|.$$

This ordering demonstrated the system output was primarily driven by the parameters with the largest sensitivity magnitudes. Consequently, the variability in the model re-

sponse was largely attributed to fluctuations in

$$\beta_1, \quad \pi_1, \quad \gamma_1.$$

From a dynamical systems perspective, the sensitivity structure indicated the model possessed both amplifying and suppressive mechanisms. Parameters with positive PRCC values enhanced the growth or persistence of the response variable, whereas parameters with negative PRCC values counteract or dampen the system dynamics. Thus, the overall system behavior was qualitatively represented as

$$Y \propto (+)\pi_1 + (+)\gamma_1 - (-)\beta_1 - (-)\gamma_3.$$

The dominance of $\beta_1$ suggested it was the most effective parameter for regulating or controlling the system. Therefore, intervention strategies targeting $\beta_1$ produced greatest reduction in the response variable. Similarly, strategies aimed at reducing $\pi_1$ and $\gamma_1$ could further suppress system amplification.

The PRCC sensitivity analysis demonstrated that the model dynamics was highly sensitive to a limited number of parameters, while many others exert only minor influence. The analysis identifies $\beta_1$ as the principal controlling parameter and highlights $\pi_1$ and $\gamma_1$ as major amplifying factors.In general,the numerical simulations showed that the concentration of *E. coli* is strongly affected by algae competition, predation and movement between treatment stages. The results also showed that increasing the predator population reduces the bacterial concentration, while the absence of predators allows the bacterial population to increase.

These findings provide valuable mathematical insight into the underlying mechanisms governing the system and offered an important basis for formulation of optimal control strategies which was also considered in the study .

The optimal control framework developed in this study provided a mathematical approach for evaluating intervention strategies aimed at reducing *E. coli* persistence in wastewater treatment systems. By integrating treatment interventions with bacteriophage predation mechanisms, the model demonstrated how different control strategies influence bacterial dynamics under the assumed parameter conditions. However, further calibration using experimental and wastewater treatment plant data is required before practical implementation.

The optimal control extension introduced four realistic intervention classes and produced a mathematically tractable objective functional that balances microbial reduction against implementation cost.

Pontryagin's Maximum Principle generated the adjoint system and explicit projection formulas for the controls, while the forward-backward sweep method provided a practical

computational strategy for solving the optimality system.
The optimality system was solved numerically using the Forward–Backward Sweep Method. The state equations were solved forward in time, while the adjoint equations were solved backward using the terminal conditions. The control profiles were updated iteratively until convergence was achieved.
The numerical results showed that the controlled system reduced bacterial populations more rapidly than the uncontrolled system, while the control profiles indicated stronger intervention during the early stages of treatment.
The numerical interpretation supports three main conclusions. First, integrated intervention strategies are markedly more effective than isolated actions. Second, bacteriophage-based measures have particularly strong regulatory influence on bacterial load.
Third, resistant bacteria tend to decay more slowly than susceptible classes, making long-term integrated management essential.
The study further extended the model to a caputo fabrizio fractional-order model. The fractional-order model provided a more flexible description of the system dynamics compared to the integer-order model because it included memory effects in the treatment process.
For computational convenience, the study set the fractional orders as

$$\alpha_1 = \alpha_2 = \alpha_3 = \alpha_4 = \alpha_5 = \alpha_6 = \alpha_7 = \alpha,$$

and also assumed that

$$M(\alpha) = 1.$$

The integer-order model was obtained when $\alpha = 1$, while the fractional-order model was obtained by choosing values of $\alpha < 1$. The numerical analysis compared the integer-order and fractional-order models in order to observe how fractional order affects the concentration of *E. coli* with time. Across all compartments, the fractional order $\alpha$ consistently governed the balance between memory-induced amplification and dynamical damping. Lower fractional orders enhanced the persistence of both sensitive and resistant *E. coli* populations, amplify transient oscillations, and increase peak bacterial and phage concentrations.
In contrast, as $\alpha \to 1$, the system moved into a more stable regime characterized by smaller variability, suppression of nonphysical oscillations, and stronger numerical robustness. Fractional-order memory effects were particularly pronounced in the early treatment stages and in predator-prey dynamics, while the tertiary stage remains comparatively insensitive, demonstrating substantial intrinsic stability of advanced treatment mechanisms (Ahmed et al., 2023).
The numerical results demonstrated the fractional order $\alpha$ played critical regulatory role in the transient and long-term dynamics of *E. coli* concentrations. Lower fractional

orders induced strong memory effects that amplified oscillations, increased peak concentrations, and enhanced persistence across treatment stages. As $\alpha \to 1$, the system exhibited increased damping, reduced transient overshoot, and improved stability. Notably, fractional-order effects were most pronounced in the early treatment stages, while the tertiary stage remained relatively insensitive to memory, indicating strong intrinsic stability of advanced treatment processes. The results contributed to improved mathematical modeling of microbial dynamics and provided insights for optimizing wastewater treatment processes. Overall, the model offers a decision-support framework for wastewater treatment planning that aligns with public-health protection and SDG 6 water-quality objectives.

The sensitivity analysis identified $\beta_1$ as the dominant regulating parameter due to its strong negative association with the model response. Therefore, bacteriophage-related parameters represent important potential targets for bacterial suppression strategies. Conversely, parameters such as $\pi_1$ and $\gamma_1$, which demonstrated positive sensitivity, contribute to bacterial persistence and amplification of the system response.

## 5.2 Limitations of the Study

Although the proposed framework provides valuable mathematical insight into antibiotic-resistant *E. coli* dynamics in wastewater treatment systems, several limitations should be acknowledged. The model parameters were obtained from available literature sources and require calibration using experimental or plant-specific wastewater data. Furthermore, the model assumes homogeneous mixing conditions and does not explicitly incorporate spatial variability, seasonal fluctuations, or stochastic changes in wastewater inflow. Future extensions should therefore consider data-driven parameter estimation, uncertainty analysis, and spatial modelling approaches.

## 5.3 Reccommendation and scope for future study

Future studies should focus on calibration using wastewater treatment plant data, experimental estimation of biological parameters, and incorporation of uncertainty arising from environmental fluctuations. Additional extensions may include stochastic modelling, spatially distributed treatment systems, and machine-learning-assisted parameter estimation to improve predictive capability. These developments would enhance the applicability of the framework for wastewater management and pathogen control.

## 5.4 Conflict of interest

The authors declare no conflict of interests.

# REFERENCES


Abdelbasir, S. M., & Shalan, A. E. (2019). An overview of nanomaterials for industrial wastewater treatment. *Korean Journal of Chemical Engineering*, *36*, 1209–1225.

Ahmad, I., Jan, R., Razak, N. N. A., Khan, A., & Abdeljawad, T. (2025). Numerical investigation of the dynamical behavior of hepatitis b virus via caputo-fabrizio fractional derivative. *European Journal of Pure and Applied Mathematics*, *18*(1), 5509–5509.

Ahmed, I., Akgül, A., Jarad, F., Kumam, P., & Nonlaopon, K. (2023). A caputo-fabrizio fractional-order cholera model and its sensitivity analysis. *Mathematical Modelling and Numerical Simulation with Applications*, *3*(2), 170–187.

Ali, F., Ali, F., Sheikh, N. A., Khan, I., & Nisar, K. S. (2020). Caputo–fabrizio fractional derivatives modeling of transient mhd brinkman nanoliquid: Applications in food technology. *Chaos Solitons & Fractals*, *131*, 109489. Retrieved from `https://api.semanticscholar.org/CorpusID:209967955`

Al-Mandhari, A., Al-Yousf, A., Malkawi, M., & El-Adawy, M. (2022). "our planet, our health": saving lives, promoting health and attaining well-being by protecting the planet-the eastern mediterranean perspectives. *Eastern Mediterranean Health Journal*, *28*(4), 247–248.

Amwata, L. M. (2015). *Mathematical modeling of hiv and malaria co-infection dynamics* (Unpublished doctoral dissertation). University of Nairobi.

Bergman, A., Liu, Y. Y., Nealis, E., & Tran, L. (2025). *Investigation of microbial and chemical contamination of groundwater in dar es salaam, tanzania.*

Bettenbrock, K., Bai, H., Ederer, M., Green, J., Hellingwerf, K. J., Holcombe, M., ... others (2014). Towards a systems level understanding of the oxygen response of escherichia coli. *Advances in microbial physiology*, *64*, 65–114.

Bidhuri, S., & Khan, M. M. A. (2020). Assessment of ground water quality of central and southeast districts of nct of delhi. *Journal of the Geological Society of India*, *95*, 95–103.

Boltyanskiy, V., Gamkrelidze, R. V., Mishchenko, Y., & Pontryagin, L. (1962). Mathematical theory of optimal processes.

Bonyaha, E., Agbekpornub, P., & Unlud, C. (2021). Mathematical modeling of transmission of water pollution. *Journal of Prime Research in Mathematics*, *17*(2), 20–38.

Bourdin, L., & Dhar, G. (2022). Optimal sampled-data controls with running inequality state constraints: Pontryagin maximum principle and bouncing trajectory phenomenon. *Mathematical Programming*, *191*(2), 907–951.

Bowong, S., & Kurths, J. (2010). Parameter estimation based synchronization for an epidemic model with application to tuberculosis in cameroon. *Physics Letters A*, *374*(44), 4496–4505.

Bruchfeld, J., Correia-Neves, M., & Källenius, G. (2015). Tuberculosis and hiv coinfection. *Cold Spring Harbor perspectives in medicine*, a017871.

Cao, H., & Plague, G. R. (2016). The fitness effects of a point mutation in escherichia coli change with founding population density. *Genetica*, *144*(4), 417–424.

Cobo-Simón, M., Hart, R., & Ochman, H. (2023). Escherichia coli: What is and which are? *Molecular Biology and Evolution*, *40*(1), msac273.

Coulombe, G., Catford, A., Martinez-Perez, A., & Buenaventura, E. (2020). Outbreaks of escherichia coli o157: H7 infections linked to romaine lettuce in canada from 2008 to 2018: an analysis of food safety context. *Journal of Food Protection*, *83*(8), 1444–1462.

Cuomo, S. (2005). *Ancient mathematics*. Routledge.

De Leon, S., Pirkle, C., Rouja, P., & Mota-meira, M. (n.d.). Highly prevalent contamination with bacterial faecal indicator species in bermudian drinking water.

Demko, M., Chrást, L., Dvořák, P., Damborskỳ, J., & Šafránek, D. (2019). Computational modelling of metabolic burden and substrate toxicity in escherichia coli carrying a synthetic metabolic pathway. *Microorganisms*, *7*(11), 553.

Dokuyucu, M. A., & Dutta, H. (2020). A fractional order model for ebola virus with the new caputo fractional derivative without singular kernel. *Chaos, Solitons & Fractals*, *134*, 109717.

Ederer, M., Steinsiek, S., Stagge, S., Rolfe, M. D., Ter Beek, A., Knies, D., ... others (2014). A mathematical model of metabolism and regulation provides a systems-level view of how escherichia coli responds to oxygen. *Frontiers in microbiology*, *5*, 124.

Edessa, G. K. (2022). Existence and uniqueness solution of the model of enzyme kinetics in the sense of caputo–fabrizio fractional derivative. *International Journal of Differential Equations*, *2022*(1), 1345919.

Fauzi, S. H. M., & Jamil, N. M. (2021). Wastewater treatment process: A modified mathematical model for oxidation ponds. *Journal of Advanced Research in Fluid Mechanics and Thermal Sciences*, *86*(1), 76–86.

Fida, M., Li, P., Wang, Y., Alam, S. K., & Nsabimana, A. (2023). Water contamination and human health risks in pakistan: a review. *Exposure and Health*, *15*(3), 619–639.

Fleming, W., & Rishel, R. (1975). The optimal control problem. In *Deterministic and*

*stochastic optimal control* (pp. 20–59). Springer.

Fleming, W. H., & Rishel, R. W. (2012). *Deterministic and stochastic optimal control*. Springer Science & Business Media.

Gachene, C. K., Nyawade, S. O., & Karanja, N. N. (2020). Soil and water conservation: An overview. *Zero Hunger*, 810–823.

Germann, V., & Langergraber, G. (2022). Going beyond global indicators—policy relevant indicators for sdg 6 targets in the context of austria. *Sustainability*, *14*(3), 1647.

Ghosh, I., Chowdhury, M., Aznam, S. M., & Rashid, M. M. (2021). Measuring the pollutants in a system of three interconnecting lakes by the semianalytical method. *Journal of Applied Mathematics*, *2021*, 1–16.

Gomi, R., Haramoto, E., Wada, H., Sugie, Y., Ma, C., Raya, S., ... Ihara, M. (2022). Novel escherichia coli genetic markers for tracking domestic wastewater contamination in environmental waters.

Gupta, H., Nigam, N., Kumar, S., & Verma, S. K. (2020). Water is life and either needs to be valued and preserved. *Journal of Family Medicine and Primary Care*, *9*(11), 5809–5810.

Gutierrez, A., Jain, S., Bhargava, P., Hamblin, M., Lobritz, M. A., & Collins, J. J. (2017). Understanding and sensitizing density-dependent persistence to quinolone antibiotics. *Molecular Cell*, *68*(6), 1147–1154.

Hassan, R., Seelman, S., Peralta, V., Booth, H., Tewell, M., Melius, B., ... others (2019). A multistate outbreak of e coli o157: H7 infections linked to soy nut butter. *Pediatrics*, *144*(4).

Hernández-Crespo, C., Fernández-Gonzalvo, M. I., Miglio, R. M., & Martín, M. (2022). Escherichia coli removal in a treatment wetland-pond system: A mathematical modelling experience. *Science of the Total Environment*, *839*, 156237.

Hurdoganoglu, U., Kaymakamzade, B., Sultanoglu, N., Guler, E., Hincal, E., & Suer, K. (2022). Evaluation of esbl resistance dynamics in escherichia coli isolates by mathematical modeling. *Open Physics*, *20*(1), 548–559.

Ishii, S., & Sadowsky, M. J. (2008). Escherichia coli in the environment: implications for water quality and human health. *Microbes and environments*, *23*(2), 101–108.

Jang, J., Hur, H.-G., Sadowsky, M. J., Byappanahalli, M., Yan, T., & Ishii, S. (2017). Environmental escherichia coli: ecology and public health implications—a review. *Journal of applied microbiology*, *123*(3), 570–581.

Khan, F. M., & Gupta, R. (2020). Escherichia coli (e. coli) as an indicator of fecal contamination in groundwater: A review. *Sustainable Development of Water and Environment: Proceedings of the ICSDWE2020*, 225–235.

Kigigha, L. T., Izah, S., & Kpea, T. (2015). Microbiological quality of fermented cassava flakes (gari) sold in yenagoa, metropolis, nigeria. *Bulletin of Advanced Scientific*

*Research*, *7*, 157–160.

Kirk, M. D., Angulo, F. J., Havelaar, A. H., & Black, R. E. (2017). Diarrhoeal disease in children due to contaminated food. *Bulletin of the World Health Organization*, *95*(3), 233.

Lagerqvist, N., Löf, E., Enkirch, T., Nilsson, P., Roth, A., & Jernberg, C. (2020). Outbreak of gastroenteritis highlighting the diagnostic and epidemiological challenges of enteroinvasive escherichia coli, county of halland, sweden, november 2017. *Eurosurveillance*, *25*(9), 1900466.

Landman, W., Buter, G., Dijkman, R., & Van Eck, J. (2014). Molecular typing of avian pathogenic escherichia coli colonies originating from outbreaks of e. coli peritonitis syndrome in chicken flocks. *Avian pathology*, *43*(4), 345–356.

Lane, J. (2004). Ghana, lesotho, and south africa: Regional expansion of water supply in rural areas. In *Scaling up poverty reduction: A global learning process and conference, may* (pp. 25–27).

Larsson, D. J., & Flach, C.-F. (2022). Antibiotic resistance in the environment. *Nature Reviews Microbiology*, *20*(5), 257–269.

Le, T., Tong, D., Pham, T., Hoang, T., Tran, T., & Ng, C. (2023). Occurrence and removal of antibiotic resistant escherichia coli and antibiotic resistance genes in an urban wastewater treatment plant. *International Journal of Environmental Science and Technology*, *20*(12), 13739–13752.

Lenhart, S., & Workman, J. T. (2007). *Optimal control applied to biological models*. Chapman and Hall/CRC.

Liu, G., Chen, J., Liang, Z., Peng, Z., & Li, J. (2021). Dynamical analysis and optimal control for a seir model based on virus mutation in wsns. *Mathematics*, *9*(9), 929.

Lobry, J., Flandrois, J.-P., Carret, G., & Pave, A. (1992). Monod's bacterial growth model revisited. *Bulletin of Mathematical Biology*, *54*, 117–122.

Luna-Guevara, J. J., Arenas-Hernandez, M. M., Martínez de la Peña, C., Silva, J. L., Luna-Guevara, M. L., et al. (2019). The role of pathogenic e. coli in fresh vegetables: Behavior, contamination factors, and preventive measures. *International journal of microbiology*, *2019*.

Magnus, T., Röther, J., Simova, O., Meier-Cillien, M., Repenthin, J., Möller, F., ... others (2012). The neurological syndrome in adults during the 2011 northern german e. coli serotype o104: H4 outbreak. *Brain*, *135*(6), 1850–1859.

Matsumura, Y., Pitout, J. D., Gomi, R., Matsuda, T., Noguchi, T., Yamamoto, M., ... others (2016). Global escherichia coli sequence type 131 clade with blactx-m-27 gene. *Emerging infectious diseases*, *22*(11), 1900.

McCarthy, D. T. (2009). A traditional first flush assessment of e. coli in urban stormwater runoff. *Water Science and Technology*, *60*(11), 2749–2757.

Murray, S. M., & Howard, M. (2019). Center finding in e. coli and the role of mathematical

modeling: past, present and future. *Journal of molecular biology*, *431*(5), 928–938.

Mushayabasa, S., Tchuenche, J. M., Bhunu, C. P., & Ngarakana-Gwasira, E. (2011). Modeling gonorrhea and hiv co-interaction. *BioSystems*, *103*(1), 27–37.

Nežerka, V., Demo, P., Schreiberová, H., Ryparová, P., & Bílỳ, P. (2022). Self-healing concrete: application of monod's approach for modeling bacillus pseudofirmus growth curves. *European Journal of Environmental and Civil Engineering*, *26*(16), 8229–8241.

Ngari, C. G., Muthuri, G. G., Kitavi, D. M., et al. (2022). Mathematical modeling and simulating of helicobacter pylori treatment and transmission implications on stomach cancer dynamics. *Commun. Math. Biol. Neurosci.*, *2022*, Article–ID.

Nieto, B., Durán-Poveda, M., Seoane, J. M., & Sanjuán, M. A. (2023). A dynamical model of the immune system interaction in a melanoma. *Communications in Nonlinear Science and Numerical Simulation*, *122*, 107248.

Nishikawa, Y., Ogasawara, J., Helander, A., & Haruki, K. (1999). An outbreak of gastroenteritis in japan due to escherichia coli o166. *Emerging infectious diseases*, *5*(2), 300.

Odhiambo, S. (2023). The influence of educational policies on the quality of science education in secondary schools. *European Journal of Education*, *1*(1), 12–21.

Organization, W. H. (2019). *Water, sanitation, hygiene and health: a primer for health professionals* (Tech. Rep.). Author.

Panwar, H., Gupta, P., Siddiqui, M. K., Morales-Menendez, R., Bhardwaj, P., Sharma, S., & Sarker, I. H. (2020). Aquavision: Automating the detection of waste in water bodies using deep transfer learning. *Case Studies in Chemical and Environmental Engineering*, *2*, 100026.

Pennington, T. H. (2014). E. coli o157 outbreaks in the united kingdom: past, present, and future. *Infection and drug resistance*, 211–222.

Perulli, G. D., Odone, G., Mancuso, G., Franco, L., Giardina, G., Chiozza, P., ... Toscano, A. (2026). Impact of treated wastewater agricultural reuse on orchards and irrigation systems. *Irrigation Science*, *44*(1), 11.

Petersen, F., & Hubbart, J. A. (2020). Physical factors impacting the survival and occurrence of escherichia coli in secondary habitats. *Water*, *12*(6), 1796.

Prakasha, D., & Veeresha, P. (2020). Analysis of lakes pollution model with mittag-leffler kernel. *Journal of Ocean Engineering and Science*, *5*(4), 310–322.

Raboni, M., Gavasci, R., & Torretta, V. (2016). Assessment of the fate of escherichia coli in different stages of wastewater treatment plants. *Water, Air, & Soil Pollution*, *227*(12), 455.

Rasheed, M. U., Thajuddin, N., Ahamed, P., Teklemariam, Z., & Jamil, K. (2014). Antimicrobial drug resistance in strains of escherichia coli isolated from food sources. *Revista do Instituto de Medicina Tropical de São Paulo*, *56*, 341–346.

Ringa, N., Diagne, M., Rwezaura, H., Omame, A., Tchoumi, S., & Tchuenche, J. (2022). Hiv and covid-19 co-infection: A mathematical model and optimal control. *Informatics in medicine unlocked*, *31*, 100978.

Rodrigues, P., Silva, C. J., & Torres, D. F. (2014). Cost-effectiveness analysis of optimal control measures for tuberculosis. *Bulletin of mathematical biology*, *76*(10), 2627–2645.

Rodriguez-Perez, S., Sanchez, A. C., & Lopez-Abelairas, M. (2022). Modelling and mathematical optimisation of wastewater treatment in food industries. *Open Research Europe*, *2*.

Sakr, M., Mohamed, M. M., Maraqa, M. A., Hamouda, M. A., Hassan, A. A., Ali, J., & Jung, J. (2022). A critical review of the recent developments in micro–nano bubbles applications for domestic and industrial wastewater treatment. *Alexandria Engineering Journal*, *61*(8), 6591–6612.

Sarowska, J., Futoma-Koloch, B., Jama-Kmiecik, A., Frej-Madrzak, M., Ksiazczyk, M., Bugla-Ploskonska, G., & Choroszy-Krol, I. (2019). Virulence factors, prevalence and potential transmission of extraintestinal pathogenic escherichia coli isolated from different sources: recent reports. *Gut pathogens*, *11*, 1–16.

Savini, F., Luca, V., Bocedi, A., Massoud, R., Park, Y., Mangoni, M. L., & Stella, L. (2017). Cell-density dependence of host-defense peptide activity and selectivity in the presence of host cells. *ACS chemical biology*, *12*(1), 52–56.

Seidu, B., & Makinde, O. D. a. (2014). Optimal control of hiv/aids in the workplace in the presence of careless individuals. *Computational and mathematical methods in medicine*, *2014*.

Sharif, M. K., Javed, K., & Nasir, A. (2018). Foodborne illness: threats and control. In *Foodborne diseases* (pp. 501–523). Elsevier.

Tai, D. B. G., Shah, A., Doubeni, C. A., Sia, I. G., & Wieland, M. L. (2021). The disproportionate impact of covid-19 on racial and ethnic minorities in the united states. *Clinical infectious diseases*, *72*(4), 703–706.

Tang, N., Liu, X., & Xing, W. (2020). Microplastics in wastewater treatment plants of wuhan, central china: Abundance, removal, and potential source in household wastewater. *Science of the Total Environment*, *745*, 141026.

Tao, Y., Wang, H., Wang, J., Jiang, W., Jiang, Y., Xin, F., ... Jiang, M. (2022). Strategies to improve the stress resistance of escherichia coli in industrial biotechnology. *Biofuels, Bioproducts and Biorefining*, *16*(4), 1130–1141.

Teklu, S. W., & Mekonnen, T. T. (2021). Hiv/aids-pneumonia coinfection model with treatment at each infection stage: mathematical analysis and numerical simulation. *Journal of Applied Mathematics*, *2021*, 1–21.

ur Rahman, M., Ahmad, S., Matoog, R., Alshehri, N. A., & Khan, T. (2021). Study on the mathematical modelling of covid-19 with caputo-fabrizio operator. *Chaos,*

*Solitons & Fractals*, *150*, 111121.

Wikswo, M. E., Roberts, V., Marsh, Z., Manikonda, K., Gleason, B., Kambhampati, A., ... others (2022). Enteric illness outbreaks reported through the national outbreak reporting system—united states, 2009–2019. *Clinical Infectious Diseases*, *74*(11), 1906–1913.

Wu, J., Yunus, M., Islam, M. S., & Emch, M. (2016). Influence of climate extremes and land use on fecal contamination of shallow tubewells in bangladesh. *Environmental science & technology*, *50*(5), 2669–2676.

Xu, R., & Guo, R. (2020). Pontryagin's maximum principle for optimal control of stochastic seir models. *Complexity*, *2020*, 1–5.

Yang, H., Chen, S., White, D. G., Zhao, S., McDermott, P., Walker, R., & Meng, J. (2004). Characterization of multiple-antimicrobial-resistant escherichia coli isolates from diseased chickens and swine in china. *Journal of clinical microbiology*, *42*(8), 3483–3489.

Yang, S.-C., Lin, C.-H., Aljuffali, I. A., & Fang, J.-Y. (2017). Current pathogenic escherichia coli foodborne outbreak cases and therapy development. *Archives of microbiology*, *199*, 811–825.

Yezli, S., Yassin, Y., Mushi, A., Aburas, A., Alabdullatif, L., Alburayh, M., & Khan, A. (2021). Gastrointestinal symptoms and knowledge and practice of pilgrims regarding food and water safety during the 2019 hajj mass gathering. *BMC Public Health*, *21*, 1–10.

Yusuf, T. T., & Idisi, O. I. (2020). Modelling the transmission dynamics of hiv and hbv coepidemics: analysis and simulation. *Mathematical Theory and Modeling*, *10*(2), 48–77.

# Appendix A

# MATLAB Code for Deterministic Model A Simulation

This appendix presents the MATLAB implementation used for the numerical simulation of the deterministic wastewater model developed in this study. The code solves the seven-dimensional system of ordinary differential equations representing nutrient concentration, susceptible and resistant *Escherichia coli*, intermediate bacterial compartments, and bacteriophage populations using the MATLAB `ode45` solver.

# A.1 Main MATLAB Simulation Code

[caption=MATLAB code for deterministic Model A simulation]

```
clc; clear; close all;
W0 = 10; X0 = 5; Y0 = 3; Z0 = 2; T0 = 1; V0 = 2; P0 = 1;
Initial = [W0 X0 Y0 Z0 T0 V0 P0];
tspan = [0 50];
[t,y] = ode45(@(t,y)ModelA(t,y),tspan,Initial);
W = y(:,1); X = y(:,2); Y = y(:,3); Z = y(:,4); T = y(:,5); V = y(:,6); P = y(:,7);
figure
plot(t,W,'LineWidth',2) hold on
plot(t,X,'LineWidth',2) plot(t,Y,'LineWidth',2) plot(t,Z,'LineWidth',2) plot(t,T,'LineWidth',2)
plot(t,V,'LineWidth',2) plot(t,P,'LineWidth',2)
xlabel('Time') ylabel('Population concentration')
legend('W','X','Y','Z','T','V','P')
title('Dynamics of Deterministic Wastewater Model')
grid on
```

## A.2 MATLAB Function Defining Model Equations

[caption=MATLAB function for deterministic Model A equations]

```
function dydt = ModelA(t,y)
W = y(1); X = y(2); Y = y(3); Z = y(4); T = y(5); V = y(6); P = y(7);
pi1 = ...; pi2 = ...; pi3 = ...; pi4 = ...;
mu1 = ...; mu2 = ...;
beta1 = ...;
gamma1 = ...; gamma2 = ...; gamma3 = ...; gamma4 = ...;
phi = ...;
omega1 = ...; omega2 = ...;
lambda = ...;
Vm = ...; K2 = ...;
A = ...;
Monod = (Vm*W)/(K2+W);
N = W+X+Y+Z+T;
dW = pi1 + pi2 - mu1*W - mu2*W ... - beta1*W*V + Monod ... - gamma1*W*(1-
N/A);
dX = gamma1*W + pi1 - mu1*X ... - mu2*X - omega1*X*P ... + Monod -
gamma2*X*(1-N/A);
dY = gamma2*X + pi1 - mu1*Y ... + Monod - gamma3*Y*(1-N/A);
dZ = gamma3*Y + pi1 + pi4 ... - mu1*Z + Monod ... - gamma4*Z*(1-N/A);
dT = gamma4*Z*(1-phi) ... - mu1*T + phi*T*Monod ... - gamma4*T*(1-N/A);
dV = beta1*W*V + pi3 ... - mu1*V + Monod;
dP = lambda*V + omega2*X*P ... - mu1*P + Monod;
dydt = [ dW; dX; dY; dZ; dT; dV; dP ];
end
```

# Appendix B

# Publications

1. Julia wanjiku Karunditu, Cyrus Gitonga Ngari,Peter Njori Wanjohi (2026).
   fTitle of Published Article. Acaputo-fabrizio fractional model for Esscherichia coli dynamics in waste water treatment systems
   https://www.doi.org/10.22271/maths.2026.v11.i2b.2264

2. Julia wanjiku Karunditu, Cyrus Gitonga Ngari,Peter Njori Wanjohi (2026) fTitle of Published Article ;Modelling Escherichia coli dynamics in multi-stage waste water treatment systems.
   DOI: https://doi.org/10.51584/IJRIAS.2026.11010083

International Journal of Statistics and Applied Mathematics



ISSN: 2456-1452
NAAS Rating (2025): 4.49
Maths 2026; 11(2): 103-107
© 2026 Stats & Maths
https://www.mathsjournal.com
Received: 16-12-2025
Accepted: 18-01-2026

**Julia Wanjiku Karunditu**
Department of Pure and Applied Sciences, Kirinyaga University, Kerugoya, Kenya

**Cyrus Gitonga Ngari**
Department of Pure and Applied Sciences, Kirinyaga University, Kerugoya, Kenya

**Peter Njori Wanjohi**
Department of Pure and Applied Sciences, Kirinyaga University, Kerugoya, Kenya

**Corresponding Author:**
**Julia Wanjiku Karunditu,**
Department of Pure and Applied Sciences, Kirinyaga University, Kerugoya, Kenya

# A caputo–Fabrizio fractional model for Escherichia coli dynamics in wastewater treatment systems

**Julia Wanjiku Karunditu, Cyrus Gitonga Ngari and Peter Njori Wanjohi**

**DOI:** https://www.doi.org/10.22271/maths.2026.v11.i2b.2264

**Abstract**
Using bacteriophage predation, bacterial resistance, and Monod-type growth kinetics, this study creates and evaluates a multi-stage mathematical model for the dynamics of Escherichia coli (E. coli) in wastewater treatment systems. The pre-primary, primary, secondary, and tertiary stages of wastewater treatment are represented by a seven-compartment deterministic model. Memory and hereditary effects in bacterial dynamics are captured by extending the traditional integer-order model to a Caputo–Fabrizio fractional-order framework, which includes both constant and variable fractional orders. Fixed-point theory is used to establish the existence and uniqueness of solutions. The three-step Adams-Bashforth approach is used to do numerical simulations that compare formulations of integer order, constant fractional order, and variable fractional order.
Results indicate that the variable fractional-order model provides enhanced flexibility and improved representation of transient dynamics relative to classical approaches. The proposed framework offers a mathematically rigorous and adaptable tool for analysing *E. coli* control strategies in wastewater treatment, with potential relevance to public health and Sustainable Development Goals related to water and sanitation.

**Keywords:** Caputo-Fabrizio derivative, E. Coli, wastewater treatment, fractional-order model, bacteriophage predation, Monod growth, and resistance

## 1. Introduction
Escherichia coli (E. coli) contamination of wastewater has been a serious global environmental and public health concern. Pathogenic strains of Escherichia coli found in both treated and untreated sewage represent a threat to both industrialized and developing nations and help in the spread of waterborne illnesses. Therefore, attaining Sustainable Development Goal 6 which calls for universal access to clean water and sanitation and safeguarding public health depend on effective wastewater treatment(Ghosh, I., Chowdhury, M. S. H., Azmin, S. M., & Rashid, 2021)[4].
In order to comprehend the movement, permanence, and management of microbiological pollutants in wastewater systems, mathematical modeling has emerged as a crucial tool. Models of classical integer-order differential equations have been used extensively to explain the dynamics of contaminants and their treatment procedures(Ahmed *et al*., 2023) [1]. The memory, latency, and genetic consequences that result from biological and environmental processes such as bacterial adaptability, resistance development, and treatment history which may not be sufficiently captured by such models.
The ability to handle derivatives of non-integer order in fractional calculus makes it a logical extension of classical modeling frameworks. Complex dynamical systems with memory effects can be more accurately and flexibly represented using fractional-order models (Dokuyucu & Dutta, 2020) [2]. Because it uses a nonsingular exponential kernel, the Caputo–Fabrizio fractional derivative, in particular, avoids the singularity that occurs in the traditional Caputo derivative and has been effectively used in several biological and environmental applications (Ahmed *et al*., 2023) [1].
For E. coli dynamics, we create a multi-stage wastewater treatment model in this work that

# Modeling Escherichia Coli Dynamics in Multi-Stage Wastewater Treatment Systems

**Julia Wanjiku Karunditu[1]*, Cyrus Gitonga Ngari[1], Peter Njori Wanjohi[1], Jeremiah Savali Kilonzi[2].**

**[1]Department of Pure and Applied Sciences, Kirinyaga University, 10300 – Kerugoya, Kenya**

**[2]Department of Mathematics, School of Pure and Applied Sciences, Meru University of Science and Technology, Meru, Kenya**

***Corresponding Author**

**DOI: https://doi.org/10.51584/IJRIAS.2026.11010083**

**Received: 17 January 2026; Accepted: 24 January 2026; Published: 11 February 2026**

## ABSTRACT

Sustainable Development Goal 6 on clean water and sanitation is threatened by Escherichia coli (E. coli) contamination in wastewater, which poses grave dangers to the environment and public health. Microbial and chemical contaminants are present in wastewater from various sources, and treatment difficulties are growing due to urbanization. While biofilm formation, disinfectant resistance, and particle attachment increase bacterial survival, pathogenic E. coli strains can cause serious illness. To explain the dynamics of E. coli in wastewater systems, this study develops a deterministic mathematical model. MATLAB solvers and uncertainty and sensitivity techniques based on Latin hypercube sampling and partial rank correlation coefficients are used to analyze the model. The findings promote more effective wastewater treatment and microbial risk management by identifying key drivers of persistence.

## INTRODUCTION

Achieving Sustainable Development Goal 6 (SDG 6) on clean water and sanitation is severely hampered by Escherichia coli (E. coli) contamination in wastewater, which poses a serious environmental and public health hazard. Urbanization and rapid population growth have increased wastewater generation, placing significant strain on existing treatment facilities and exacerbating freshwater scarcity (Yezli et al., 2021).

Wastewater from residential, commercial, agricultural, and stormwater sources contains several pollutants, including pathogens and chemical contaminants. (Fida et al., 2023; Rodriguez-Pere Abdelbasir et al., 2019). Inadequate treatment has significant adverse effects on the environment and society, including eutrophication, groundwater pollution, fecal contamination, and elevated risks of waterborne illnesses (Fida et al., 2023).

A standard indicator of fecal contamination in aquatic environments is Escherichia coli, a Gram-negative bacterium belonging to the Enterobacteriaceae family (Coxon, 2023). Pathogenic variants, such as E. coli O157:H7, can cause severe illness even though most strains are benign. Leaking sewage systems, agricultural runoff, and inadequately treated wastewater are the primary sources of contamination (Tang et al., 2020; Abdelbasir & Shalan, 2019; Prakasha & Veeresha, 2020)—biofilm formation and resistance to disinfectants such as chlorine increase E. coli's persistence.

Because they have a significant ecological role in regulating E. coli populations and frequently display a Type II functional response, bacteriophages are promising biological control agents in wastewater treatment (Savini et al., 2017)(Savini et al., 2017). However, existing models provide limited insight into multi-stage therapeutic systems and bacteriophage-based regulation.
This study develops a deterministic mathematical model based on Monod kinetics to investigate E. coli dynamics (Luong, 1987), bacteriophage predation, and resistance within a multi-stage wastewater treatment framework, thereby providing quantitative support for improved treatment procedures.

REPUBLIC OF KENYA

NATIONAL COMMISSION FOR SCIENCE, TECHNOLOGY & INNOVATION

Ref No: **148766**

Date of Issue: **12/July/2025**

# RESEARCH LICENSE



**This is to Certify that Ms.. Julia Wanjiku Karunditu of Kirinyaga University, has been licensed to conduct research as per the provision of the Science, Technology and Innovation Act, 2013 (Rev.2014) in Kirinyaga on the topic: MODELLING DENSITY DEPENDENT ESCHERICHIACOLI IN WASTEWATERS TREATMENT INCO-OPORATING RESISTANCE,OPTIMALITY AND NONSINGULAR FRACTIONALDERIVATIVES. for the period ending : 12/July/2026.**

License No: **NACOSTI/P/25/4176502**

**148766**

Applicant Identification Number

Ag. Director General
NATIONAL COMMISSION FOR SCIENCE,TECHNOLOGY & INNOVATION

Verification QR Code

NOTE: This is a computer generated License. To verify the authenticity of this document, Scan the QR Code using QR scanner application.

**See overleaf for conditions**